Department of Civil and Environmental Engineering
The University of South Florida

Seal Slab/Pile Interface Bond

Gray Mullins, Ruben Sosa and Rajan Sen
Department of Civil and Environmental Engineering

June 2000

DISCLAIMER

The opinions, findings and conclusions expressed in this publication are those of the authors and not necessarily those of the State of Florida Department of Transportation.

CONVERSION FACTORS, US CUSTOMARY TO METRIC UNITS

Multiply	by	to obtain
inch	25.4	mm
foot	0.3048	meter
square inches	645	square mm
cubic yard	0.765	cubic meter
pound (lb)	4.448	newtons
kip (1000 lb)	4.448	kilo newton (kN)
newton	0.2248	pound
kip/ft	14.59	kN/meter
pound/in^2	0.0069	MPa
kip/in^2	6.895	MPa
MPa	0.145	ksi
ft-kip	1.356	kN-m
in-kip	0.113	kN-m
kN-m	0.7375	ft-kip

PREFACE

EXECUTIVE SUMMARY

This report presents results from a two-year experimental study to evaluate the interface bond between a cast-in-place seal slab and prestressed concrete or steel piles. Both scale model and full-scale tests were conducted and several cofferdam conditions were simulated. These were (1) marine environment (2) fresh water conditions and (3) drilling fluid condition. Normal pile surfaces were investigated. Additionally, the situation of "soil-caked" piles was also investigated.

In the model tests, a total of 36 one-third scale specimens were tested - twenty eight prestressed concrete and eight steel. Bonded embedment depth in the seal slab was varied between d to 2d where d was the size of the pile. The results of these tests indicated that shear stress variation was non-uniform leading to larger computed bond stresses with shallower embedment. Values were least for drilling fluid. Concrete piles had better bond with the seal concrete than steel piles. "Soil-caked" condition was found to be relevant for the drilling fluid situation only. In other cases, it was washed away from the pile surface.

In the full-scale tests, a total of 32 specimens were tested divided equally between steel and concrete. The prestressed piles were 14 in. square and the steel piles were 14 in. deep wide flange sections. Embedment depth, D, was varied between 0.5d to 2d, i.e. 7 to 28 in. with the larger depth reserved for the drilling fluid condition. Four of the sixteen prestressed piles were cast with embedded gages located at the top, middle and bottom of the interface region. The results of the full-scale tests were similar to those from the one-third scale tests. The most important findings were (1) loads were transferred over a distance equal to the depth d of the pile (2) scale effects were present - the average calculated bond stresses were lower for the full-scale tests than from the corresponding scale model tests (3) prestressed piles cracked prior to bond failure and (4) the seal slab cracked prior to bond failure.

Based on the test results it is proposed that the interface bond between piles and the seal slab be restricted to an effective area in contact with the cast in place seal slab. The effective area is calculated using the actual embedment depth (D) or the size of the pile (d) whichever is smaller. The average bond stress over this region is limited to 300 psi for concrete piles and 150 psi for steel piles. These values are reduced by a third (i.e. 100 psi and 50 psi respectively) in cases where drilling fluid is used. Application of the proposed values to the conditions related to the full-scale tests led to average factors of safety in excess of two for both the prestressed and steel piles. However, tension loads taken by the piles should not lead to cracking (concrete) or exceed the allowable tension load (steel) of the piles. Nor should the seal slab crack.

TABLE OF CONTENTS

LIST OF TABLES

LIST OF FIGURES

LIST OF FIGURES (Contd.)

LIST OF FIGURES (Contd.)

LIST OF FIGURES (Contd).

CHAPTER 1

INTRODUCTION

1.1   Introduction

Bridge superstructures are commonly supported on pile foundations. In this case, superstructure loads are transferred to a reinforced concrete pile cap that ties the supporting individual piles into a complete structural unit. The piles themselves may be made of reinforced concrete, prestressed concrete or steel.

When the required elevation of the pile cap is below the existing water table, i.e. excavations or over-water bridges, de-watering of the foundation area must occur to allow accurate placement of the reinforcing steel as well as pouring of the concrete. If global de-watering is not possible due to induced adverse ground settlement or is impractical due to the proximity of a body of water, a cofferdam must be employed.

A cofferdam is a temporary structure usually constructed of thin sheet piles that interconnect to form a water-tight perimeter. Typically, the cofferdam sheet piles are installed first. Then, using a template which locates the pile positions, the piles are driven. Both of the processes are conducted in the saturated or submerged conditions. At this stage of the construction, a cast-in-place concrete (CIP) seal slab is poured at the bottom of the

cofferdam with the use of a tremie. This seals the bottom of the cofferdam preventing the seepage of water and completes the coffer cell. By design, the top elevation of the seal slab is the base elevation for the structural pile cap. The sheet piles and the seal slab provide the formwork for the reinforced concrete pile cap.

1.2   Objectives

As the function of the seal slab is primarily to provide a dry working surface, its design is relatively unsophisticated. Under current design guidelines it is an unreinforced concrete slab with its depth selected so that its weight largely offsets maximum uplift forces *(for the maximum safe elevation of water outside the cofferdam when completely dewatered)*. Allowance for interface bond between the seal slab and the piles is minimal - allowable interface bond is 40 psi for concrete piles and 5 psi for steel piles [1].

The interface bond stresses permitted in the Structural Design Guidelines are not based on any tests results. In view of this, in 1997 the Florida Department of Transportation issued a request for proposals (RFP) to assess this bond from full-scale tests. The University of South Florida were selected to conduct this study.

In January 1998, the University of South Florida commenced a two-year research program to investigate this problem. In the study, a limited number of full-scale tests were conducted to assess the interface seal slab/pile bond characteristics for prestressed concrete and steel piles and to recommend suitable values for design. The complete results from this study are presented in this report.

2

Although the goal of the study was to evaluate bond on the basis of full-scale tests, a 1/3rd scale pilot study was initially carried out to evaluate critical parameters and to develop an efficient method of testing. This was particularly important because of the need to complete the testing in a timely manner. This phase of the study was completed in the first year. Full-scale testing was carried out in the second year once a suitable outdoor site was found. The University of South Florida is indebted to Hayward Baker Inc. Tampa, FL for providing such a site and more importantly, access to plant and heavy equipment required to carry out the full-scale tests.

1.3   Organization of Report

The pilot study was carried out on 1/3 scale specimens at a site located in the University of South Florida campus. A complete description of the experimental program developed following discussions with the Florida Department of Transportation is presented in Chapter 2. An analysis of the pilot test results and the principal findings are summarized in Chapter 3. A description of the test program and details of the full-scale testing are described in Chapter 4. As for the pilot study, results of the full-scale tests are presented in the following chapter, Chapter 5. Analysis of all the results is included in Chapter 6 with the conclusions and recommendations summarized in Chapter 7. In addition to the six chapters, two appendices I and II provide load vs displacement plots from all the pilot and full-scale tests respectively.

For convenience, all references are listed at the end of the respective chapters.

References

1. Structural Design Guidelines (1998). Florida Department of Transportation, Section 4.18, Topic No: 625-020-150-c, July. p 4-12, Tallahassee, FL.

4

CHAPTER 2

PILOT STUDY

2.1   Introduction

This chapter provides details of the pilot study carried out. An analysis of the test results is presented in the next chapter. A description of the test program is contained in Section 2.2. Materials used are described in Section 2.3 and fabrication of the pile specimens is covered in Section 2.4. Preparation of the pile surface to simulate field conditions is summarized in Section 2.5. The construction of the coffer dams is discussed in Section 2.6. The equipment designed to carry out the tests is described in Section 2.7 while details on the test procedure and instrumentation may be found in Section 2.8.

2.2   Test Program

The aim of the pilot study was to simulate three different seal slab placement conditions involving (1) salt water (2) fresh water and (3) drilling fluid. These results were compared against the controls where no fluid had to be displaced by the concrete. One-third

scale was selected for the study to limit costs. Both prestressed concrete and steel piles were tested and two different surface conditions - natural and soil-caked were investigated.

Based on results of a preliminary study [1] the maximum interface bond between two concrete surfaces was estimated to be about 250 psi. This value was used to estimate the maximum embedment depth that would not lead to material failure of the prestressed pile in tension. As a result, three different embedment depths d, 1.5 and 2d (d is the side of the pile) were investigated. Table 2.1 presents the laboratory-scale test matrix.

Table 2.1 Test Matrix for Pilot Study.

Construction Condition	Embedment Depth (in)		Concrete Specimens		Steel Specimens
			Natural Surface	Soil-Caked Surface	
Control	d	6	2	-	-
	1.5d	9	2	-	1
	2d	12	2	1	1
Salt Water	d	6	2	-	-
	1.5d	9	2	-	1
	2d	12	2	1	1
Fresh Water	d	6	2	-	-
	1.5d	9	2	-	1
	2d	12	2	1	1
Bentonite	d	6	2	-	-
	1.5d	9	2	-	1
	2d	12	2	1	1

6

A total of thirty-six (36) pile specimens were tested. Of these, twenty eight were prestressed piles and eight were steel H piles. As the focus of the study was more on prestressed concrete than steel, fewer steel piles were investigated.

Inspection of Table 2.1 shows that for prestressed piles two specimens were tested for each construction condition and the natural surface. For the soil caked case, only one specimen was tested. In case of steel, greater embedment depths of 1.5d and 2d were tested because its bond with concrete was poorer.

2.3 Materials

2.3.1 Concrete Mix

The concrete used in the preparation of the concrete specimens was the Florida Department of Transportation (FDOT) specification Class V Special, typically used for prestressed piles. The specified 28-day strength was 6000 lbf/in^2 (41 MPa). The concrete was purchased from Florida Rock Industries, Inc., Tampa, Florida (FDOT Plant No 15-303, Mix No 07-0002). The mix design details are summarized in Table 2.2.

Table 2.2 Mix Design for Prestressed Piles.

Item	Quantity per m³	Quantity per yd³
Cement (Type II)	321 kg	702 lbf
Coarse Aggregate (#57 Crushed Limestone)	784 kg	1730 lbf
Fine Aggregate (Silica Sand)	465.7 kg	1027 lbf
Water	117 L	30.9 gal
Water	117 kg	258 lbf
Fly Ash (Class F)	69 kg	150 lbf
Air Entrainment Admixture (Darex)	0.296 L	10.0 oz
Water Reducing Agent (WRDA 19)	2.51 L	85.0 oz
Water/Cementitious Ratio	0.3	0.3
Slump Range	127 to 203 mm	5 to 8 in
Air Content	2%	2%
Unit Weight	2254 kg/m³	143.2 lbf/ft³

2.3.2 Spiral Ties

Spiral ties were provided as in actual piles using #5 gage steel wire. The spirals were fabricated by Wire Products Inc. The material properties of the spirals as provided by their fabricator are summarized in Table 2.3.

Table 2.3 Steel Spiral Tie Properties.

Property	Standard	Metric
Diameter	0.208 in	5.28 mm
Actual Area	0.034 in²	21.9 mm²
Average Tensile Strength	109.6 ksi	755.9 MPa
Average Yield Strength	97.1 ksi	669.7 MPa

2.3.3 Prestressing Strands

The concrete specimens were prestressed using 5/16 inch (7.9 mm) diameter, seven wire, Grade 250, low relaxation steel strands. The strands were donated by Florida Wire and Cable Company, Jacksonville, Florida. The properties of the strands as provided by the manufacturer are summarized in Table 2.4.

Table 2.4 Steel Strand Properties.

Property	Standard	Metric
Ultimate Breaking Strength	15,959 lbf	71.0 kN
Load at 1% Extension	14,740 lbf	65.6 kN
Ultimate Elongation in 24 in., in/in.	5.5%	5.5%
Modulus of Elasticity	29.3×10^6 psi	202 GPa
Nominal Cross-Sectional Area	0.058 in^2	37.42 mm^2

2.3.4 Dywidag Rods

Threaded rods were incorporated into the reinforcement design to supply a convenient point of attachment for the hydraulic pullout frame and to increase the specimen tensional capacity. The threaded rods were purchased from Dywidag Systems International, Inc., Fairfield, New Jersey. The properties of the rods are tabulated in Table 2.5.

Table 2.5 Dywidag Steel Rod Properties.

Property	Standard	Metric
Diameter	1.25 in	32 mm
Area	1.25 in^2	806 mm^2
Ultimate Strength	187.5 kip	834 kN
Ultimate Stress	150 ksi	1030 MPa

2.3.5 Structural Steel

The steel pile specimens were fabricated using a W 6 x 15 beam section made from A36 structural steel. This had the same 6 in. depth as the prestressed pile. The beams were purchased from Tampa Steel and Supply, Inc., Tampa, Florida. Properties summarized in Table 2.6 are according to the specifications found in the American Institute of Steel Construction's Manual of Steel Construction [2].

Table 2.6 Structural Steel Pile Properties.

Property	Standard	Metric
Beam Depth	5.99 in	152 mm
Flange Width	5.99 in	152 mm
Cross-Sectional Area	4.43 in^2	2857 mm^2
Yield Stress	36 ksi	248 MPa
Ultimate Stress	58 ksi	400 MPa

2.4   Fabrication

The concrete specimens were cast and prestressed at Henderson Prestress, Tarpon Springs, Florida. The steel specimens were prepared for testing at University of South Florida College of Engineering machine shop.
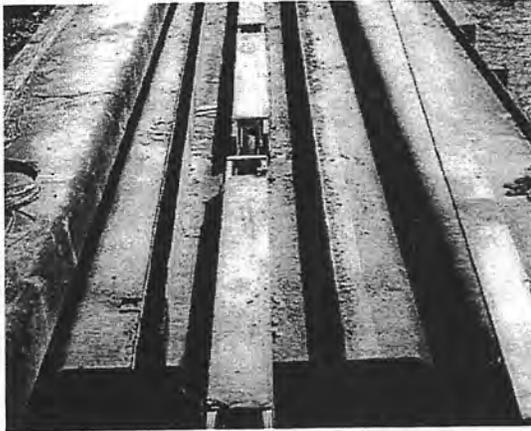
Figure 2.1 Prestressing Bed.
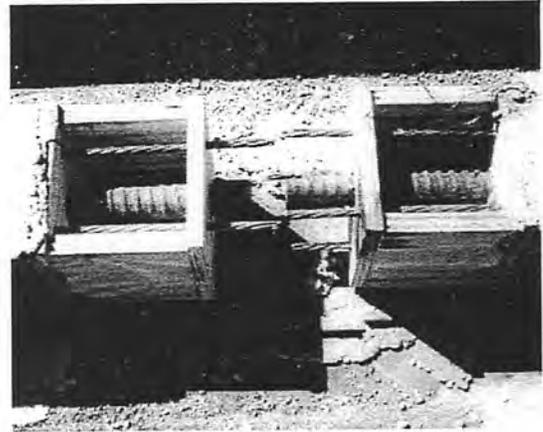
Figure 2.2 Header Sections.

2.4.1   Prestressed Piles

The prestressed concrete specimens were six inches (152.4 mm) square in cross-section and four feet (1.2 m) long. The formwork consisted of two welded lengths of a 5/16 inch (7.9 mm) thick steel angle section with legs 6 inches (152.4 mm) by 4 inches (101.6 mm) long. The angles were welded to a steel base which was part of an existing 220 ft long industrial double-tee concrete form (Fig. 2.1). The long length of the bed allowed all the specimens to be cast at once. Wooden header blocks were placed between adjacent specimens to facilitate separation (Fig. 2.2).

11

The specimens were prestressed by four 5/16 inch (7.9 mm) prestressing strands. Spiral ties made from #5 gage steel were spaced at 4.5 in. (Fig. 2.3). A 1.25 in. Dywidag rod was embedded centroidally to provide a point of attachment for pullout testing and to increase the tensional capacity.

Each strand was loaded to about 10 kips (44 kN). With minimal loss, the average transferred force approximately equaled the initial tensile force of 40 kips (176 kN) or approximately 1100 psi (7.6 MPa). After placement, the concrete was allowed to cure for 24 hours before the strands were severed.

The force in the strands was monitored using load cells. A total of eight load cells were used. Four were positioned at the live (pulling) end and the remaining four at the dead (restrained only) end. The prestressing data was collected using a Megadac data acquisition computer system manufactured by Optim Electronics Corporation.
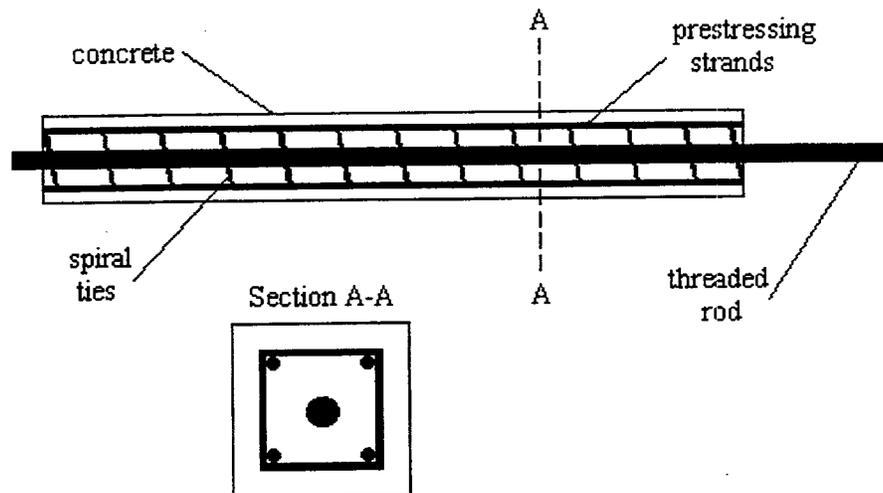
Figure 2.3 Prestressed Pile Details.

12

2.4.2 Steel Piles

The W 6 x 15 sections used for the steel piles were purchased and machined in the University of South Florida College of Engineering shop. Each steel pile was fabricated to 36 inches (914.4 mm) in length. A line of three, 15/16 inch (23.8 mm) diameter holes were drilled into each flange. These holes were specified according to the bolted connection design for the pullout testing apparatus. Several of the pile specimens are shown in Fig. 2.4.
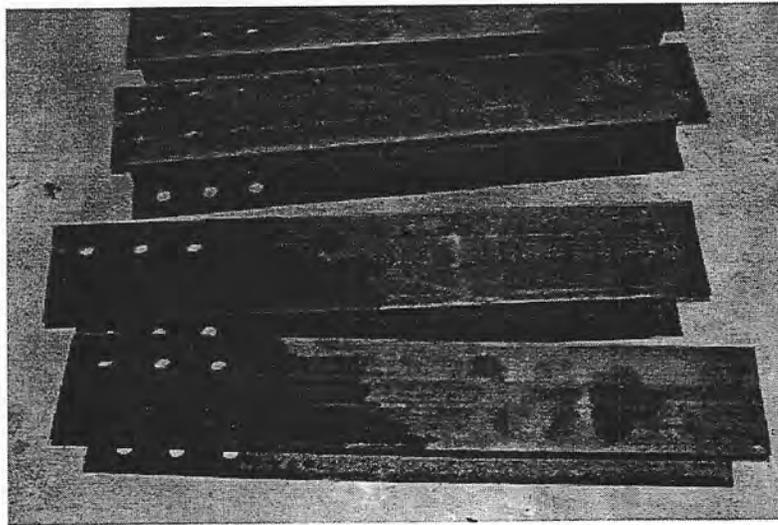
Figure 2.4   Steel Pile Specimens.

2.4.3 Surface Condition

As the embedment depth varied between d to 2d (Table 2.1) it was necessary to incorporate a debonded region to the fabricated pile specimens. A "soil caked" secondary surface condition was also incorporated. This condition modeled the possible adherence of soil particles to the pile surfaces after excavation.

2.4.3.1   Bonded Surface

The surfaces of the pile specimens were delineated according to the desired bond areas. The areas expected to bond to the CIP concrete slab were not modified. In the case of the concrete specimens, this was the naturally cured concrete surface. In the case of the steel specimens, the natural surface was a slightly corroded one. Although the corrosion was expected to have an influence on the bond characteristics, it was allowed to remain because it simulated actual construction conditions.

2.4.3.2   De-Bonded Surface

The surfaces exposed to the CIP slab but outside of the desired bond area were covered with different separating layers to negate any significant bonding. The separating layers used depended on pile specimen type.

The de-bonded layers of the pre-stressed concrete specimens were first covered with a layer of roofing tar (Fig. 2.5). Bituminous coatings are often applied to piles to decrease friction from possible downdrag caused by consolidating soil layers [3]. A similar bond breaking effect was theorized to occur in this application. To further de-bond the two concrete surfaces, a layer of 12 lbf (0.05 kN) felt paper was applied (Fig. 2.6). This physically separated the surfaces over a significant distance. As a final treatment, the felt paper was covered with a layer of duct tape. The extremely smooth surface was expected to further inhibit bond and also served as a method for fixing the position of the paper.

14
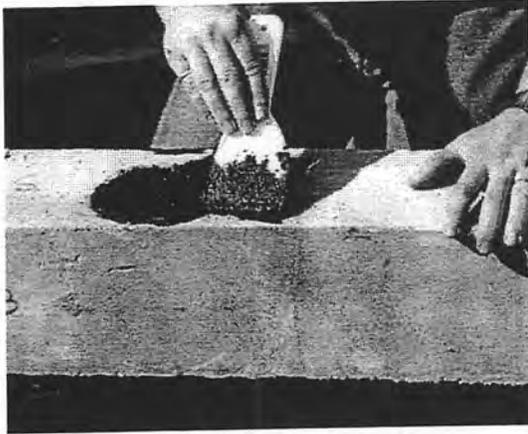
Figure 2.5 Applying Tar.

Figure 2.6 Placing Felt Paper.

The steel pile specimens received a reduced form of the procedure used for the de-bonding of the concrete specimens. Due to the irregularity of the steel surfaces and difficulty molding the felt paper to these surfaces, only a tar layer was applied to the steel. The tar had excellent adhesive characteristics which allowed it to conform to the contour of the beam section and, once applied, remained only on the de-bonded areas. Laboratory investigations revealed that this treatment led to minimal bond stresses ranging between 2-15 psi [4].

2.4.3.3 Soil-Caked Surface

This surface condition may exist if the bonding pile surfaces are not properly inspected and cleaned prior to bonding to the CIP concrete seal slab. It was expected that this would have a detrimental effect upon the bond capacity. As a worst case scenario, clay was used for the surface treatment. Clay has the greatest cohesive and adhesive properties among all soil types. Consequently, without proper surface preparation, clay could exist as a possible de-

15

bonding soil layer. For the pilot study, a clay paste was applied to the bonding surface of selected prestressed concrete specimens and allowed to dry. The paste consisted of a viscous mixture of the clay mineral Kaolinite and water that was applied with a trowel. There was some difficulty with the clay soil flaking off of the specimen surface as it dried (Fig. 2.7). Subsequently, the clay was kept damp until placement of the pile inside the cofferdam formwork.
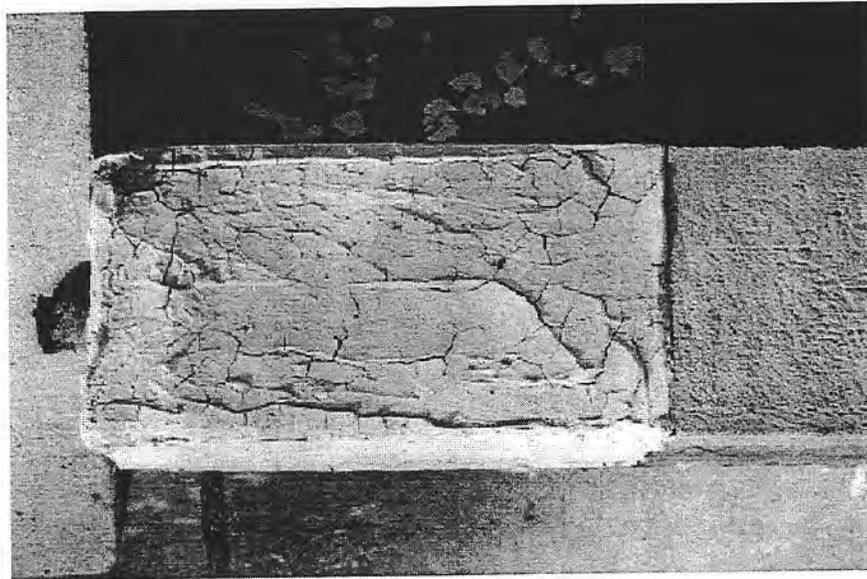
Figure 2.7 Soil-Caked Concrete Specimen.

2.5   Seal Slab Preparation

2.5.1   Cofferdam Formwork

The preparation for the cast-in-place seal slab first required the construction of the sides of the cofferdam. Since it was not practical to use actual sheet piles due to expense and the bracing required above ground, wood box forms were used instead. As the piles were not to be actually driven into the ground, the test specimens were also required to be supported

16

in these forms. In addition, the forms needed to be impermeable to the various types of construction fluids to be placed in the cofferdams depending on the modeled condition.

2.5.2 Box Forms

The cofferdam simulated formwork was constructed using wood box forms. The forms were fashioned using a two-by-four framework faced with 3/4 inch (19 mm) plywood (Figs 2.8-2.9). The box forms were arranged such that the inside dimensions were 54 inches (1372 mm) square and attached to a concrete base. Their positions were fixed using powder-activated concrete nails forced into the base with the use of a Remington Power Fastener (Figs 2.10-2.11). Once the specimens were placed, the tops of the forms were secured by tying them with a wooden framework that also served as the pile template. Additionally, each cofferdam was lined with 6 mil plastic sheeting. This allowed the forms to be water-tight, preventing the loss of any construction fluid, e.g. water, bentonite-slurry.

Figure 2.8 Box Frame.
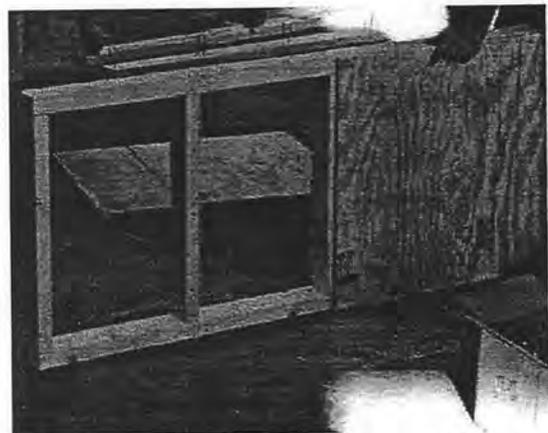
Figure 2.9 Attaching Plywood Face.

Figure 2.10 Securing Base.

Figure 2.11 Remington Fastener.

2.5.3 Specimen Support

Once the cast-in-place seal slab formwork was completed, the specimens were positioned. To support the specimens, a wooden template was constructed (Fig. 2.12). A sheet of plywood was cut with holes for exposed threaded rods which matched the locations of the concrete specimens. Templates for both the top and bottom of each form were constructed.

First, a bottom template, supported on attached wooden blocks, was placed upon the plastic sheeting at the bottom of each cofferdam. But before each concrete specimen was positioned, a silicone seal was placed between the template and the specimen to prevent any seal concrete from migrating under the specimens. Then, another template was placed on top of the concrete specimens. This effectively locked all the concrete specimens together as one unit. The unit was then laterally supported by reinforcing some of the concrete specimens against movement using lengths of two-by-fours nailed to the tops of the concrete forms (Figs 2.13-2.15).

18
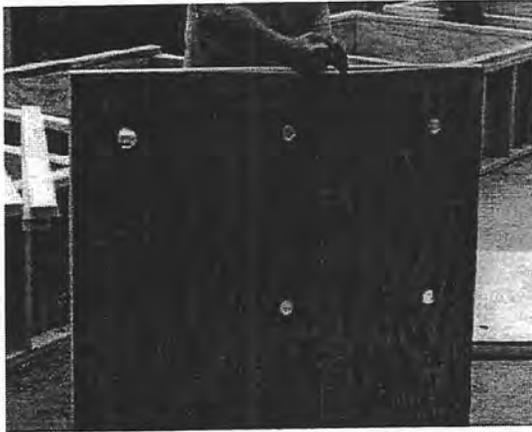
Figure 2.12 Specimen Template.
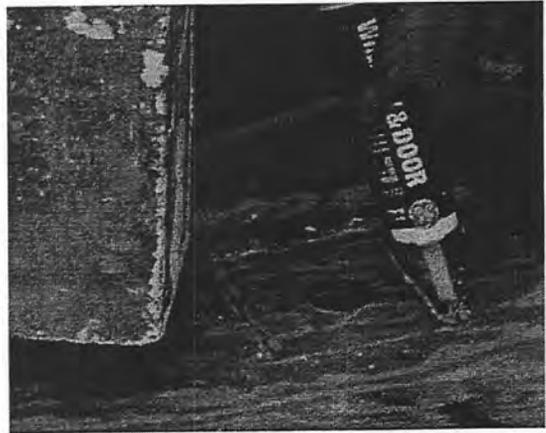
Figure 2.13 Applying Silicone Seal.

Figure 2.14 Installing Specimen.
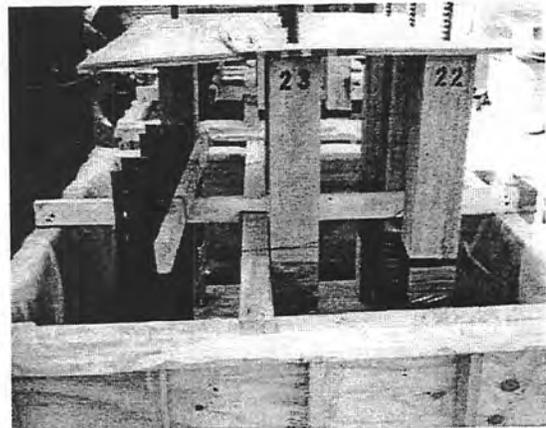
Figure 2.15 Fully-supported Specimens.

As shown in Fig. 2.15, the steel specimens were not supported the same way as the concrete ones. This was due to a lack of a vertical fixation point such as the threaded rods in the concrete specimens. The steel piles were simply placed upon the bottom template and secured using steel tie wire. A silicone pad was not used at the steel specimen/template interface because the contact area was minimal.

2.5.4 Materials

2.5.4.1   Concrete Mix

The concrete used in the preparation of the cast-in-place seal slab was the Florida Department of Transportation specification Class III Seal, specified for use as a hydraulic seal in cofferdam construction. The specified 28-day strength was 3000 lbf/in^2 (21 MPa). The concrete was purchased from Ewell Industries, Inc., Tampa, Florida (FDOT Plant No 10-012, Mix No. 63018). Mix details are summarized in Table 2.7.

Table 2.7 Seal Slab Mix Design.

Item	Quantity per m^3	Quantity per yd^3
Cement (Type II)	254 kg	560 lbf
Coarse Aggregate (Crushed Limestone, 3/8 in)	657 kg	1450 lbf
Fine Aggregate (Silica Sand)	477.5 kg	1054 lbf
Water	167 L	44 gal
Water	166 kg	367 lbf
Fly Ash (Class F)	70.2 kg	155 lbf
Air Entrainment Admixture (MBAE-90)	0.21 L	7.0 oz
Water Reducing Agent (MBL-80)	1.9 L	64.35 oz
Water/Cementitious Ratio	0.3	0.51
Slump	178 to 229 mm	7 to 9 in
Air Content	1 to 6 %	1 to 6 %
Unit Weight	2090 kg/m^3	132.8 lbf/ft^3

2.5.4.2   Fresh Water

The fresh water used was obtained from the University of South Florida's main potable water supply (Figs 2.16-2.17). This water originates from ground water sources.
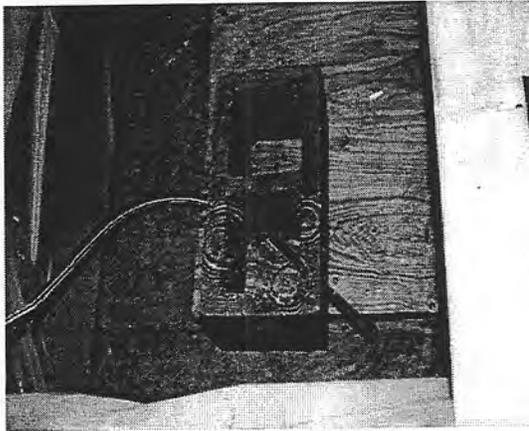
Figure 2.16   Filling Cofferdam.
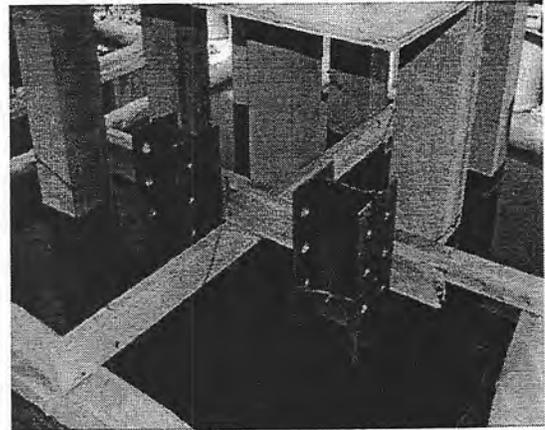
Figure 2.17   Water-filled Bed.

Through the use of this source, construction conditions in which the ground water table is encountered was effectively modeled.

2.5.4.3   Salt Water

The salt water was produced by combining fresh water and salt crystals typically used in water softeners. The mixing process involved filtering the fresh water into a perforated plastic refuse container which was filled with the salt crystals until a satisfactory density was achieved. At the time of the concrete pour, the salt water had a specific gravity of 1.026 and a temperature of $71.6°$ F ($22°$ C).

21

2.5.4.4   Bentonite Slurry

The bentonite slurry was made by mixing dry, high yield bentonite and fresh water. The mixing was accomplished by circulating the water/soil mixture between the simulated cofferdam and an external tank using a 1 inch (25.4 mm), gasoline-powered centrifugal pump (Figs 2.18-2.19). The mixture was circulated between the two reservoirs until a uniform consistency was reached. Enough bentonite clay was added to achieve slurry properties

Figure 2.18 Mixing Bentonite Slurry.   **Figure 2.19** Bentonite-filled Bed.
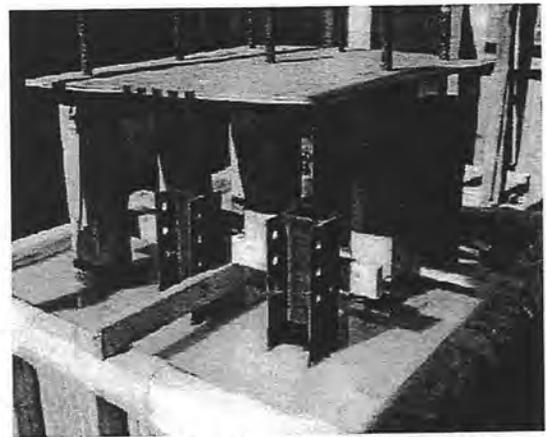
similar to FDOT specifications [3]. The final density achieved was 64 lbf/ft^3 (1025 kg/m^3) with a viscosity of 37 seconds (Marsh Cone method) and a pH of 8.

2.6   Seal Slab Placement

As stated before, the conditions under which the cast-in-place seal slab was poured were varied to model concrete bonding under various possible construction conditions. During actual construction, a tremie, which is essentially a large funnel, is used to place the seal slab. The concrete is tremied from the bottom of the excavation up to the required

22

elevation of seal slab. As the concrete is poured, the tip of the tremie is kept below the surface of the concrete to maintain concrete quality. This prevents the segregation of aggregate and the loss of cement which would occur if the concrete were allowed to drop down through any liquid that may be present (water, drilling fluid, etc.).

In the pilot study, the concrete was placed using a concrete pump. The concrete was pumped through a 3 inch (76 mm) diameter hose. The concrete was placed from the bottom upwards keeping the hose tip below the rising level of concrete. This is similar in placement and identical in effect to the tremie method (Figs 2.20-2.23).

Figure 2.20 Concrete Pump.
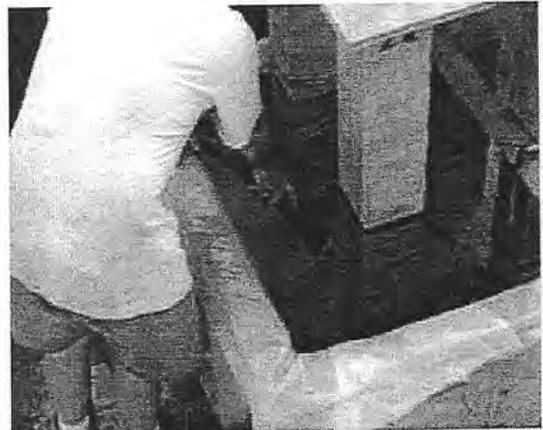
Figure 2.21 Filling Control Bed.
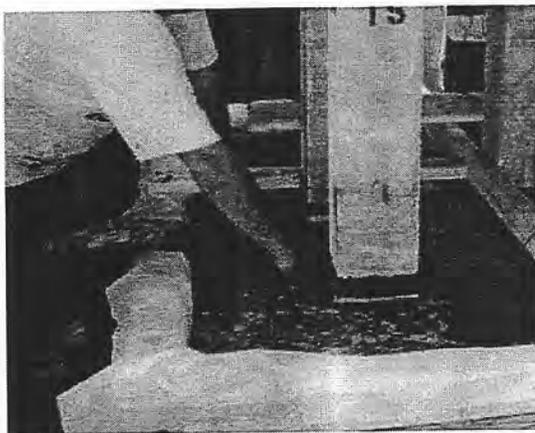
Figure 2.22 Filling Fresh Water Bed.
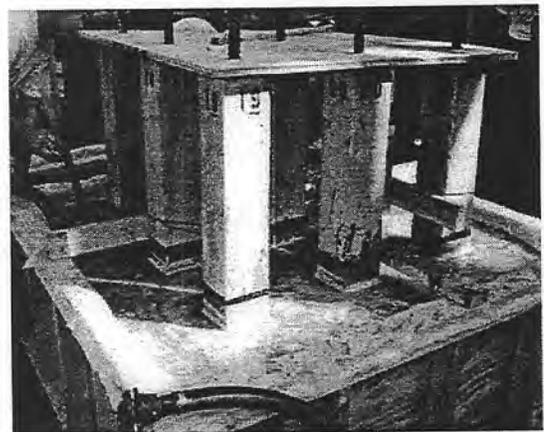
Figure 2.23 Filled Salt Water Bed.

23

2.7   Testing Apparatus

A mechanism to measure bond capacity, while maintaining the same field load transfer mechanics was required. Since it was difficult to load the slab from below due to inaccessibility, it was decided that the most practical loading scheme was one in which a uniformly distributed load was applied to the top of the seal slab. In addition, the pile would also be loaded at the top. This exactly models the field loading conditions except that the orientation is rotated 180 degrees (Fig. 2.24). In the field, the uniformly distributed load is located at the bottom of the seal slab due to uplift pressure and the pile resistance comes from pile/soil interface bond.

field loading   experimental loading
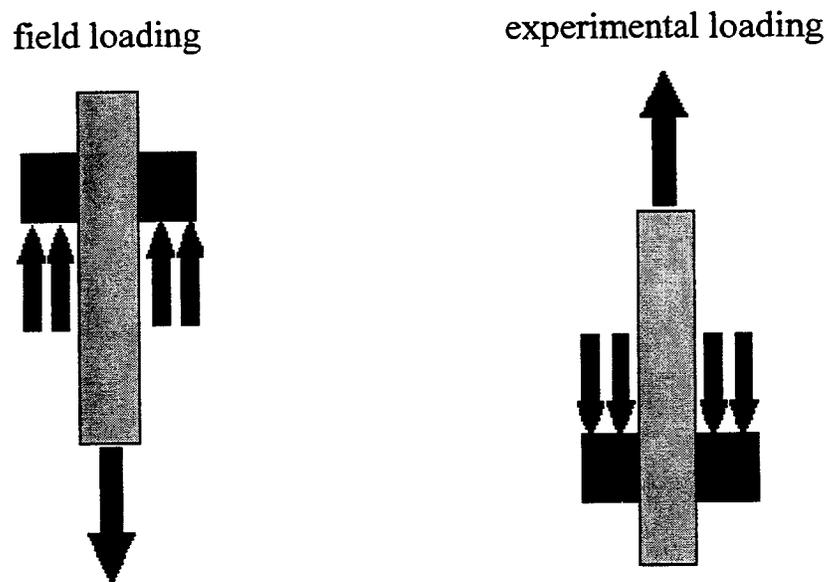
Figure 2.24   Equivalence of Field/Simulated Conditions.

24

2.7.1 Design Requirements

The apparatus to test bond capacity needed to provide the expected loading capacity while being portable enough so it could be easily moved to each pile location. A flexible design was also required to accommodate the differing connections to both the steel and concrete pile specimens.

It was decided to design a steel testing frame that would take advantage of an available single-acting, 50 ton (445 kN) hydraulic jack. The jack would be operated with a 10 ksi (69 MPa) hydraulic pump system. The frame required connection designs for both specimen types. Additionally, the frame needed to be integrated with electronic devices to measure loads and displacements.

2.7.2 Design Methodology

The Load and Resistance Factor Design (LRFD) specification of the American Institute of Steel Construction, Inc. (AISC) was used for the design of the hydraulic test frame [4]. The anticipated load on the frame was 100 kips (445 kN).

2.7.3 Initial Design

The frame design (Fig. 2.25) consisted of two main sections: a tension assembly (Fig. 2.26) and a compression assembly (Fig. 2.27).

25
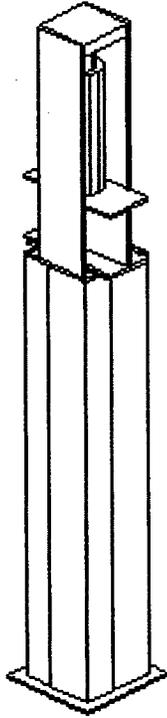
Figure 2.25
Frame
Isometric
Pictorial.
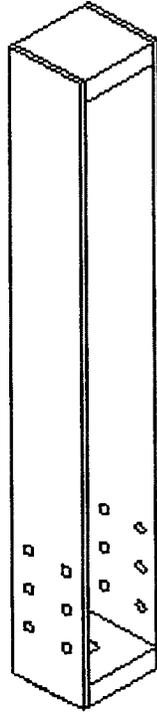
Figure 2.26
Frame
Tension
Assembly.
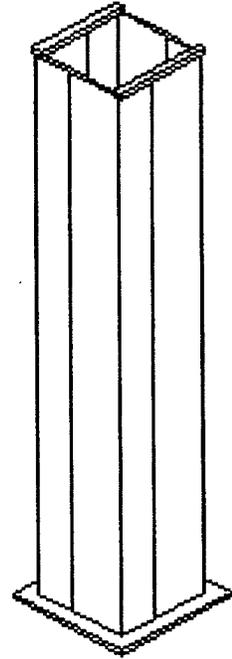
Figure 2.27 Frame
Compression Assembly.

2.7.3.1   Compression Assembly

The 6 x 4 x 5/16 in. steel angle sections were salvaged from the specimen fabrication phase of the pilot study and incorporated into the steel frame design. The angles were welded into a built-up box section 10 in. (254 mm) square and 50 in. (1270 mm) long with a wall thickness of 5/16 in. (7.9 mm). The box section was more than sufficient for transferring the compression load to the seal slab. Two ½ in. (12.7 mm) thick bearing plates were attached to the top of the section to accommodate the load transfer from a short beam section on which

26

the hydraulic jack was placed. A ½ inch (12.7 mm) thick load bearing plate was placed under the bottom of the box section to serve as an interface between the seal slab and the frame. A 7 in. (177.8 mm) square cut-out was incorporated into the plate to accommodate the pile specimens. The pile specimens would slip through the body of the compression assembly and would be attached to the tension assembly using a threaded rod coupling nut (concrete specimens) or a bolted connection (steel specimens).

2.7.3.2 Tension Assembly

The tension assembly consisted of two square plates and two long rectangular plates. The square plates were 7 in. (177.8 mm) across and 2 in. (50.8 mm) thick. The rectangular plates were 57 in. (1447.8 mm) long and ½ in. (12.7 mm) thick. The two thicker plates were placed on each end with the two long plates welded between them. The bottom 2 in. (50.8 mm) plate had a 1.5 in. (38.1 mm) hole drilled in its center to accommodate the threaded rod from the prestressed concrete specimens. The long plates had 15/16 in. (23.8 mm) diameter bolt holes drilled into them for the bolted connection used for the steel specimens.

2.7.4 Final Modified Design

After the first pullout test, it was apparent that the initial design capacity of the hydraulic jack was insufficient. A modification of the frame and the hydraulic load system was required to successfully complete the test program.

27

Two short "pancake" hydraulic jacks were used instead of the single hydraulic jack (Fig. 2.28). Each smaller jack had a capacity of 100 kips giving a total possible tensile capacity of 200 kips. According to calculations, the tension and the compression assembly designs were adequate for the increased load but the center beam section (Fig. 2.25) had to be further stiffened. To incorporate the two jacks and maintain the frame geometric tolerances, an additional beam section, along with small steel plate shims, were required.
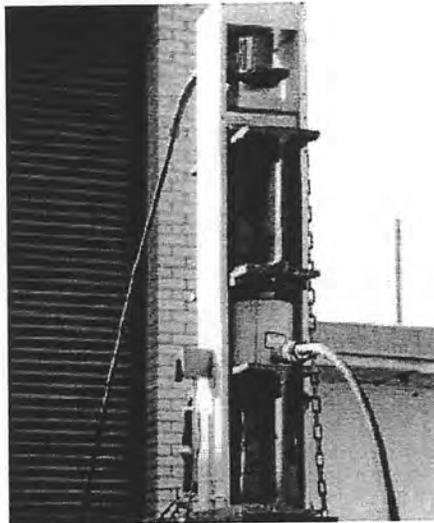
Figure 2.28 Modified Frame.

2.8 Pull-Out Testing

2.8.1 Test Set-Up

After the seal slabs were allowed to cure for the allowable minimum of 72 hours, the pull-out testing of the specimens was performed. To conduct the testing, several steps

28

were undertaken: placement of a grout pad, assembly and connection of the hydraulic testing apparatus, attachment of the data acquisition system, and application of loading until failure.

2.8.1.1   Leveling Grout Pad

Since concrete vibration is not used in seal slab construction due to possible aggregate segregation in the submerged environment, various degrees of surface roughness developed according to the pour condition. The bentonite pour condition had the greatest degree of evenness and the control the least. To perform the vertical tension load application as specified in the test program, the uneven surfaces needed to be compensated for. To this end, a grout pad was poured around each individual pile specimen.

First, a dam of sandy soil was placed around the pile specimen to prevent migration
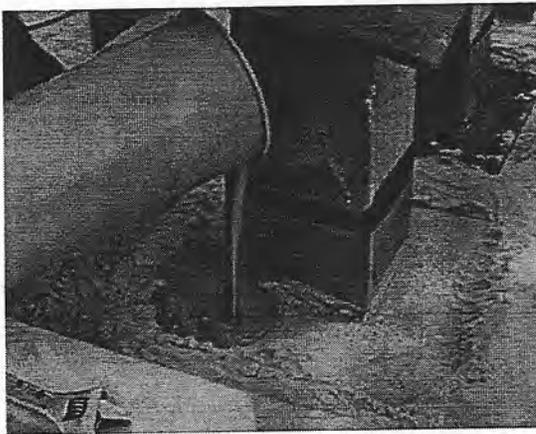
Figure 2.29 Pouring High Strength Grout.
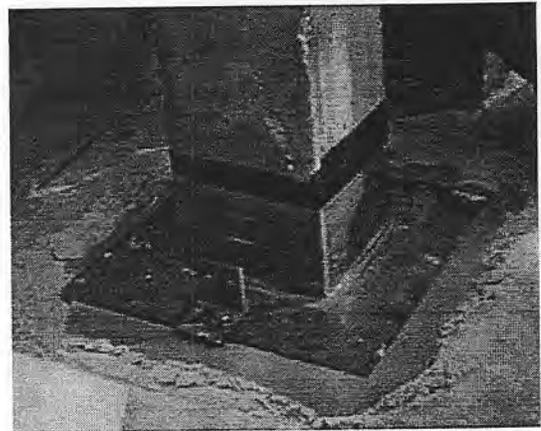
Figure 2.30   Installing Bearing Plate.

of the curing grout (Fig. 2.29). Then, a high strength, fast curing grout pad was poured. The grout was prepared with a water content such that it was *self-leveling*. To further assist in the leveling process, the steel concrete bearing plate was placed (Fig. 2.30) upon the grout

immediately after pouring. Once the grout had time to cure (about 15 minutes), the pull-out

frame could be assembled and fixed to the pile specimen.

2.8.1.2 Frame Assembly

First, the tension assembly was connected to the pile specimen. This was

accomplished by holding the compression assembly aloft with an external lifting frame.

While the frame was held, the bottom of the tension assembly was exposed which allowed

connection to the specimen. The type of connection depended on specimen type. In the case

of the prestressed concrete specimens, the threaded rod was inserted through the 1.25 inch (32

mm) diameter hole in the lower plate of the tension assembly and a coupling nut was installed

(Fig. 2.31). With the steel specimens, extension plates were attached to the tension straps

using 7/8 inch (22 mm) diameter bolts. The plates were then used to connect the frame to

pile specimen (Fig. 2.32). Once the tension assembly was connected, the compression section
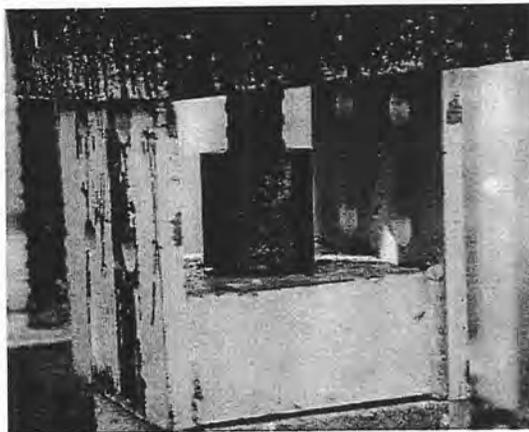
Figure 2.31 Concrete Specimen.
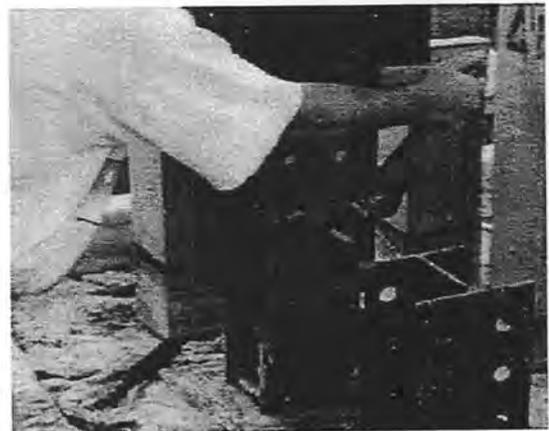
Figure 2.32 Connecting Steel.

was then lowered completely while the tension assembly was supported by the top of the pile

specimen. The two beam sections, along with the hydraulic jacks and the steel plate shims,

30

were positioned within the loop formed by the tension assembly. The jacks were extended so that the compression assembly now supported the entire frame.

2.8.2 Data Acquisition

The Megadac data acquisition system by Optim Electronics Corporation was used for collecting and recording the test data generated by the pull-out testing. Along with the Megadac, a load cell and two LVDTs were used to monitor movement. The load cell had a capacity of 200 kips (890 kN). The LVDTs had a 2 in. (50.8 mm) range. One of the LVDTs was magnetically attached to the compression assembly and positioned to record displacement with respect to an external reference beam. This registered any possible seal slab surface crushing or settlement that may occur during testing. The other LVDT was attached to the tension assembly and referenced to the top of the compression assembly. This accounted for specimen movement, along with elastic deformation of the frame which was later accounted for in the data reduction (Figs. 2.33-2.34).
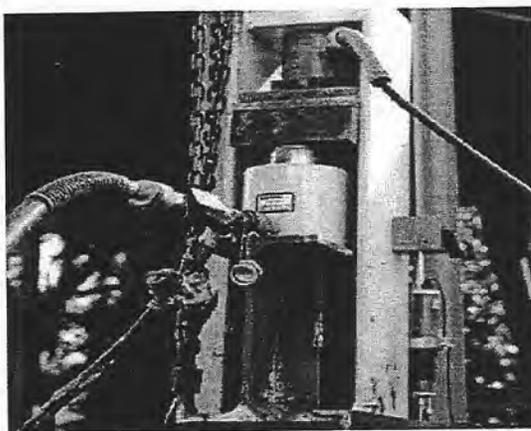
Figure 2.33 LVDT And Load Cell.

Figure 2.34 Lower LVDT.

31

2.8.3   Test Procedure

Once the set-up procedure was completed, the pull-out testing could be conducted. The tensile load was increased slowly using a manually operated toggle switch which intermittently engaged the power to the hydraulic pump (Fig. 2.35). The load was increased

Figure 2.35   Applying Load.
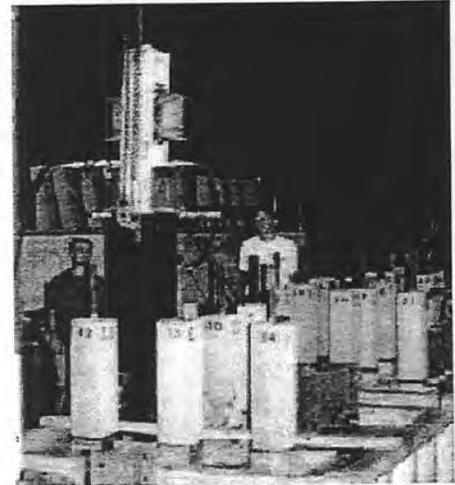
Figure 2.36   Testing Specimen.

slowly to reduce any possible dynamic stiffening of the system. Each specimen was displaced upward at least one inch (25.4 mm) (Fig. 2.36).

References

1. Fischer, J. (1999).   Strength of Repaired Piles.   MSCE Thesis submitted to Department of Civil and Environmental Engineering, USF, December.

2. American Institute of Steel Construction (1994). Manual of Steel Construction Load and Resistance Factor Design. Second Edition, Chicago, IL.

3. Bowles, J. (1996). Foundation Analysis and Design. Fifth Edition, Mc-Graw-Hill, New York, NY.

4. Sosa, R. (1999). Bond Capacity of Pile/Seal Slab Interfaces. MSCE Thesis submitted to Department of Civil and Environmental Engineering, USF, December.

CHAPTER 3

PILOT STUDY RESULTS

3.1   Introduction

The results of the laboratory-scale investigation are summarized in this chapter.
Section 3.2 contains results for the prestressed pile specimens for the four different
cofferdam conditions. Section 3.3 provides the corresponding results for the steel specimens.
The principal conclusions are summarized in Section 3.4.

3.2   Concrete Specimens

The results are grouped for the different simulated cofferdam conditions that were
outlined in the previous chapter. The same format is used throughout. All results are
presented in two ways: in tabular form and also as bar diagrams. Each table contains
information from the test relating to the specimen number, the average concrete strength, the
measured area of the pile in contact with the seal slab and the maximum recorded load. The
corresponding bond stress and average bond stress are also included. For conditions other
than the control, average bond stress values are normalized with respect to those for the

control for the same embedment depth. The bar diagrams contain information only on the maximum load and the average bond stresses. Load vs displacement plots may be found in Appendix I.

A detailed description of each of the conditions is presented in succeeding sub-sections.

3.2.1 Control Condition

Table 3.1 presents the test results for the concrete control specimens. The maximum load varied between 80.5 kips to 142.2 kips. The computed bond stresses ranged between 479 to 628 psi. The results suggest that the bond stress variation is non-uniform with embedment depths above 1.5d ineffective. The average bond stresses were highest for the 1.5d embedment and lowest for the 2d embedment.

Figs. 3.1-3.2 present in the same information in the form of a bar diagram.

Table 3.1 Summary for Control Concrete Specimens.

Specimen	f'c (psi)	Bond Length	Bond Area (in^2)	Max Load (kip)	Bond Stress (psi)	Average (psi)
C22	3930	1d	149.0	84.7	568	556
C23	3930	1d	147.9	80.5	544	
C24	3930	1.5d	225.3	137.1	609	618
C25	3930	1.5d	226.4	142.2	628	
C26	3930	2d	295.9	141.7	479	479
C27	3930	2d	292.9	140.6	480	
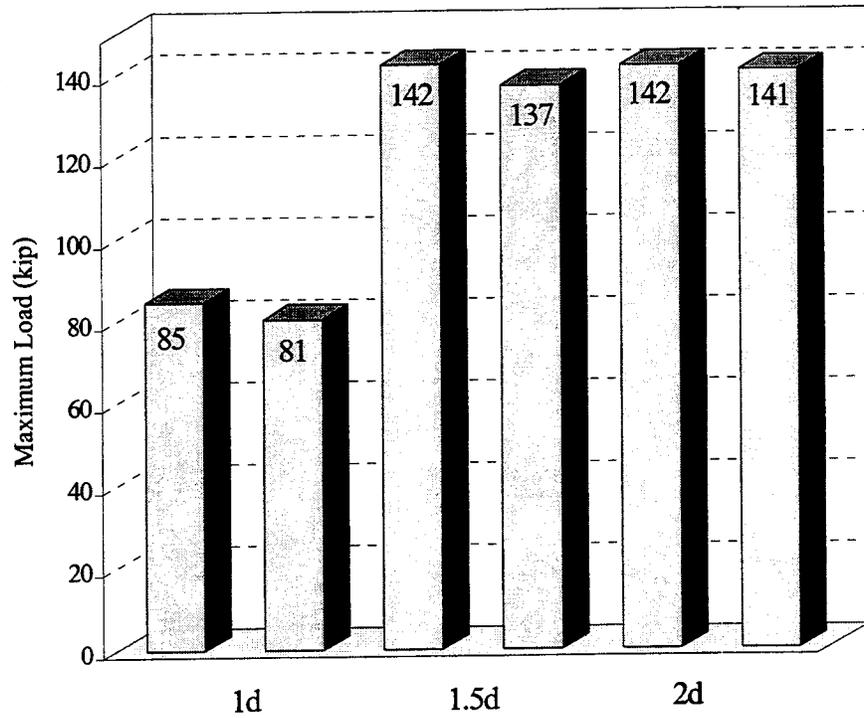
Figure 3.1 Force Summary for Pilot Control Concrete Specimens.
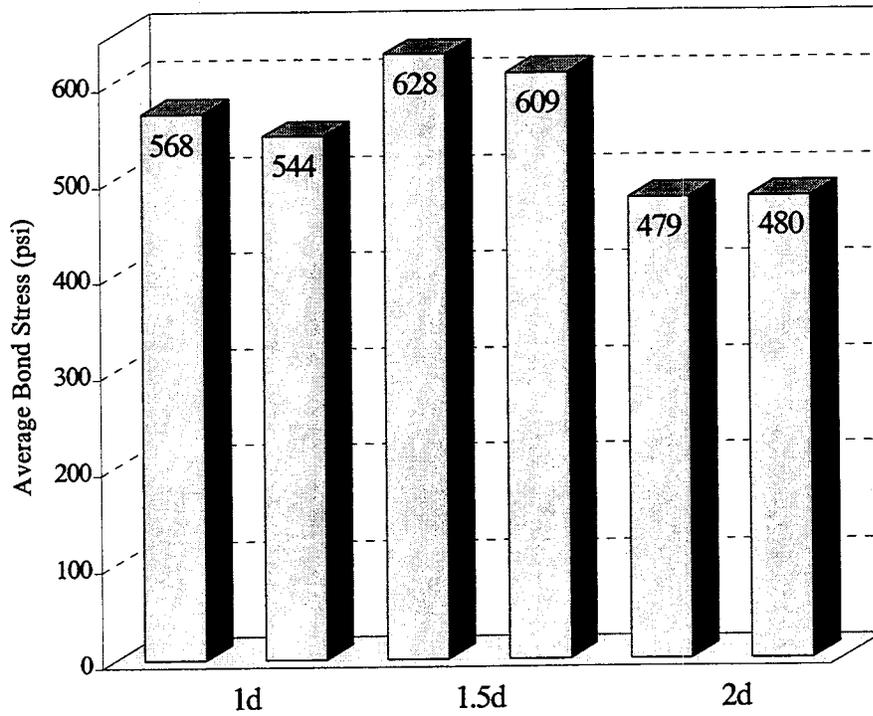
Figure 3.2 Average Bond Stress For Control Concrete Specimens.

35

3.2.2 Salt Water Condition

Table 3.2 presents the test results for the salt water control specimens. Compared to the controls, the maximum pullout loads (and computed bond stresses) tend to be higher. This may be because the concrete strength was higher (4270 vs 3930) due to the accelerating effect of chlorides. The maximum load ranged between 85 -155 kips. The computed bond stress ranged between 480-634 psi. As with the control concrete specimens, there was a decrease in average bond stress from 1.5d to 2d although the maximum load for 2d was somewhat larger (than 1.5d). These results are presented in bar diagrams in Figs. 3.3-3.4.

Table 3.2 Summary for Salt Water Concrete Specimens.

Specimen	f'c (psi)	Bond Length	Bond Area (in²)	Max Load (kip)	Bond Stress (psi)	Average (psi)	Percent of Control
C8	4270	1d	150.9	89.4	592	592	106
C9	4270	1d	144.1	85.1	591		
C10	4270	1.5d	223.9	141.9	634	614	99
C11	4270	1.5d	223.9	132.9	594		
C12	4270	2d	304.5	146.3	480	498	104
C13	4270	2d	300.8	154.8	515		
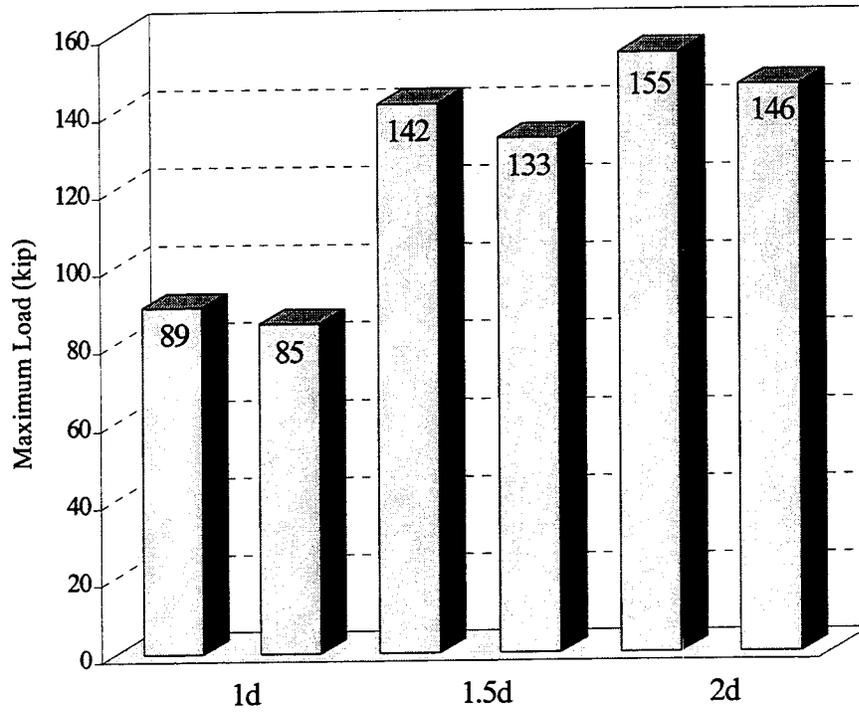
Figure 3.3 Force Summary for Salt Water Concrete Specimens.
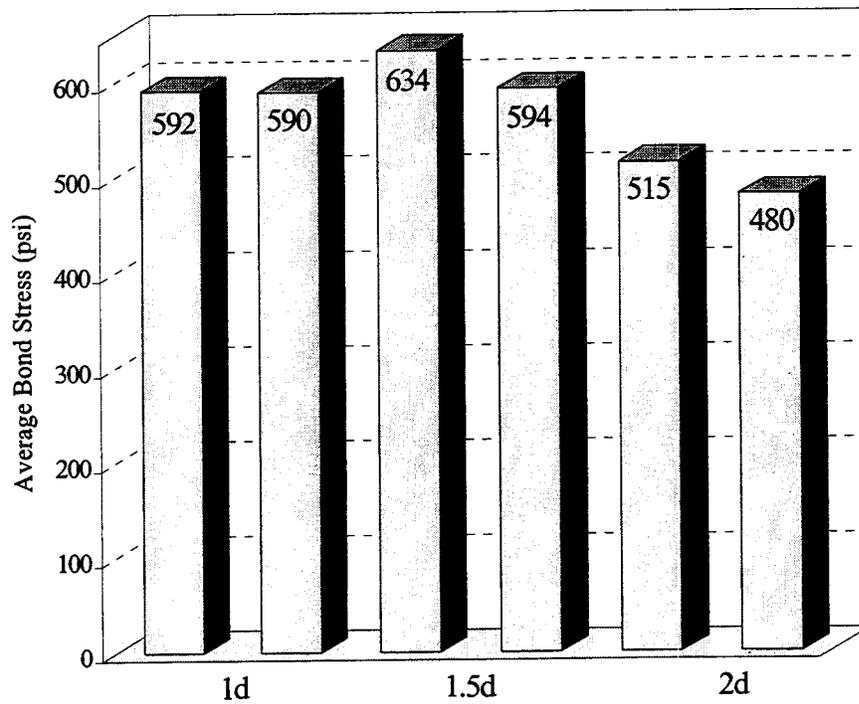
Figure 3.4 Average Bond Stress For Salt Water Concrete Specimens.

3.2.3 Fresh Water Condition

Table 3.3 presents the test results for the concrete fresh water specimens. Additionally, Figs 3.5 and 3.6 graphically depict these results. The pattern of the results is similar to those for the two previous sets. The maximum load ranges between 79-139 kips. Bond stresses range between 423-622 psi with the highest load corresponding to an embedment depth of 2d. As before, depths above 1.5d appear to be largely ineffective signifying a non-uniform variation in bond stress. Note also that the average bond stress values were larger than the control for an embedment depth of d but were smaller (varying between 93-96%) for the other two cases. This is probably due to the higher concrete strength.

Table 3.3 Summary for Fresh Water Concrete Specimens.

Specimen	f'c (psi)	Bond Length	Bond Area (in²)	Max Load (kip)	Bond Stress (psi)	Average (psi)	Percent of Control
C15	4270	1d	148.3	79.5	536	579	104
C16	4270	1d	150.9	93.8	622		
C17	4270	1.5d	225.6	139.3	617	595	96
C18	4270	1.5d	225.0	128.7	572		
C19	4270	2d	297.8	125.9	423	445	93
C20	4270	2d	299.3	139.8	467		
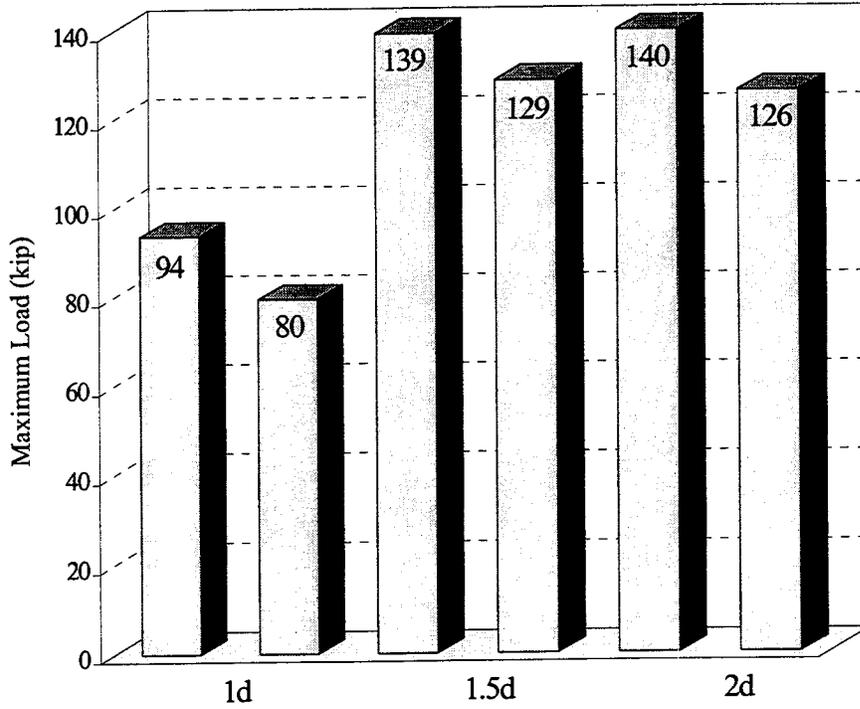
Figure 3.5 Force Summary For Concrete Fresh Water Specimens.
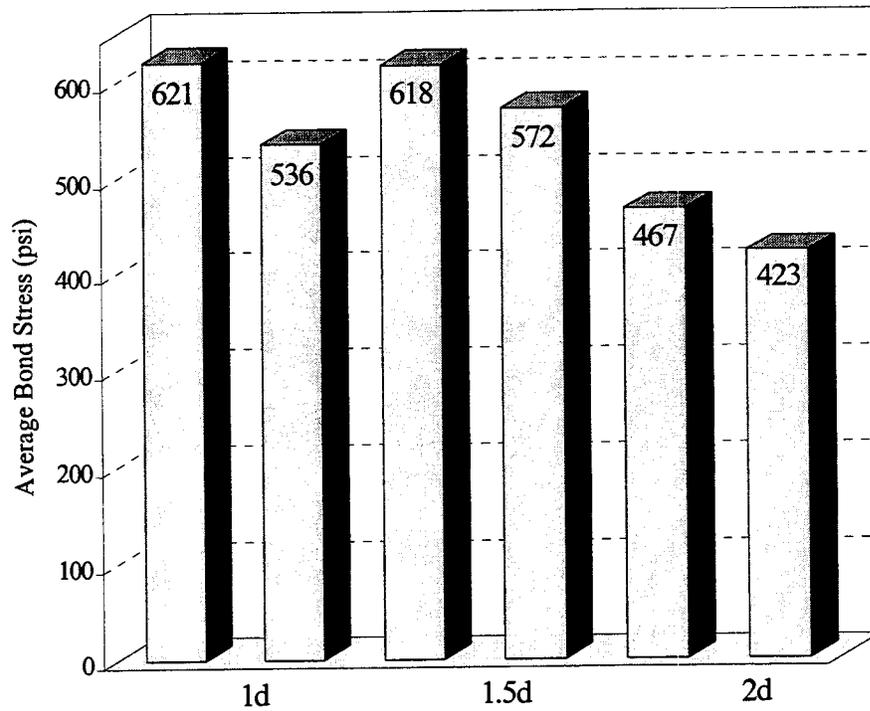
Figure 3.6   Average Bond Stress For Fresh Water Concrete Specimens.

3.2.4 Bentonite Slurry Condition

Table 3.4 presents the test results for the concrete bentonite slurry specimens. Additionally, Figs 3.7 and 3.8 graphically depict the same results. Note that Specimens C3 and C6 were not used for the average pull-out force calculation because they are considered non-representative. Specimens C3 and C6 had maximum pull-out resistances that were not in good agreement with the other bentonite specimens. These pile specimens were probably scoured free of bentonite during the placement of the CIP seal slab concrete. Therefore, they are testing at capacities consistent with the fresh water condition. Disregarding the probable non-representative test specimens, the trend of decreased average bond stress at 2d is in evidence. The maximum load varied between 31-125 kips and corresponding bond stresses between 154-238 psi. These were approximately one-third of that of the controls.

Table 3.4   Summary for Bentonite Specimens.

Specimen	f'c (psi)	Bond Length	Bond Area (in²)	Max Load (kip)	Bond Stress (psi)	Average (psi)	Percent of Control
C1	4270	1d	148.1	31.7	214	219	39
C2	4270	1d	149.3	33.4	224		
C3	4270	1.5d	223.3	125.3*	561	238	38
C4	4270	1.5d	224.4	53.3	238		
C5	4270	2d	299.6	46.2	154	154	32
C6	4270	2d	295.9	122.0*	412		

*not used for average calculation
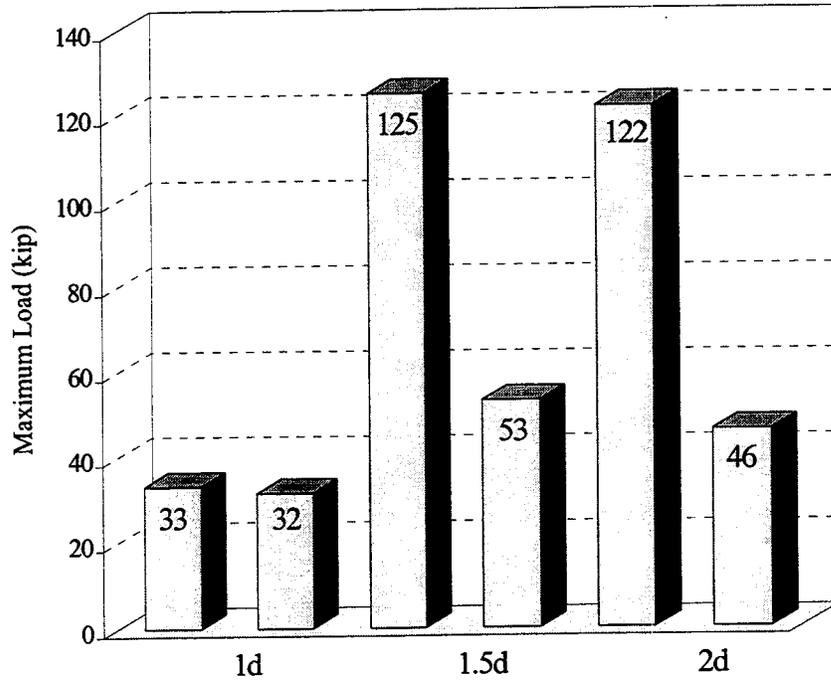
Figure 3.7 Force Summary For Bentonite Slurry Concrete Specimens.
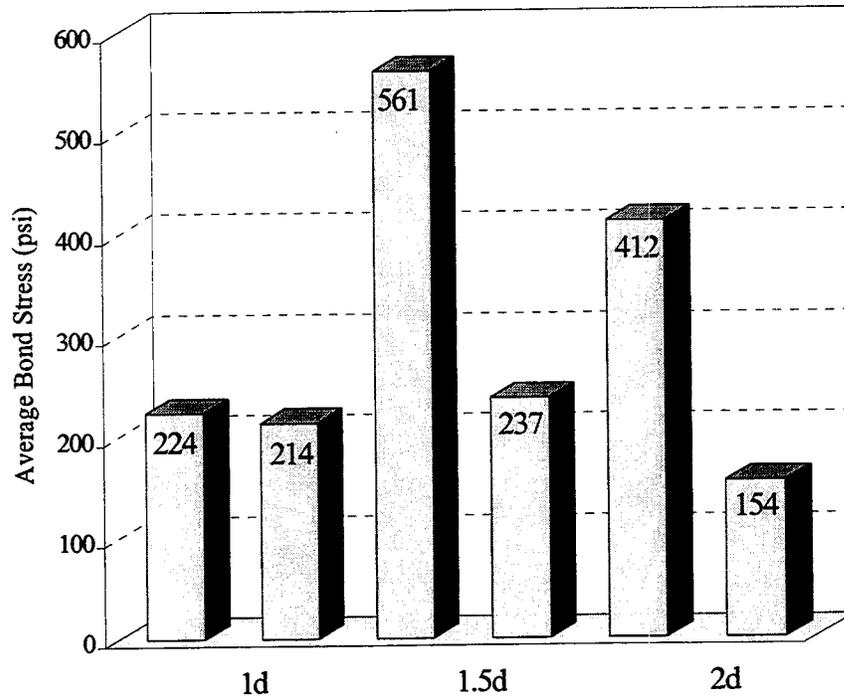
Figure 3.8 Average Bond Stress For Bentonite Slurry Concrete Specimens.

41

3.2.5 Soil-Caked Condition

Table 3.4 presents the test results for the concrete soil-caked specimens. Additionally, Figs 3.7 and 3.8 graphically depict the experimental results. Note that specimens C14 and C21 are considered non-representative of soil-caked conditions.

Inspection of Table 3.5 shows a wide variation in results. The maximum pull-out load ranges from 8-117 kips with the corresponding stresses varying between 29-398 psi. These represent between 6-83% of that of the control. Due to the cofferdam condition environments (salt water and fresh water), the applied soil migrated off the bond surface before the CIP concrete could be placed. This suggests that soil-caked piles may adversely affect bond only in situations where it is used in conjunction with bentonite.

Table 3.5 Summary for Soil-Caked Specimens.

Specimen	Pour Condition	f'c (psi)	Bond Length	Bond Area (in²)	Max Load (kip)	Bond Stress (psi)	Percent of Control
C28	control	3930	2d	300.4	8.8	29	6
C14	salt water	4460	2d	294.8	117.2	398	83
C21	fresh water	4460	2d	300.0	89.2	297	62
C7	bentonite	4460	2d	293.3	10.9	37	8
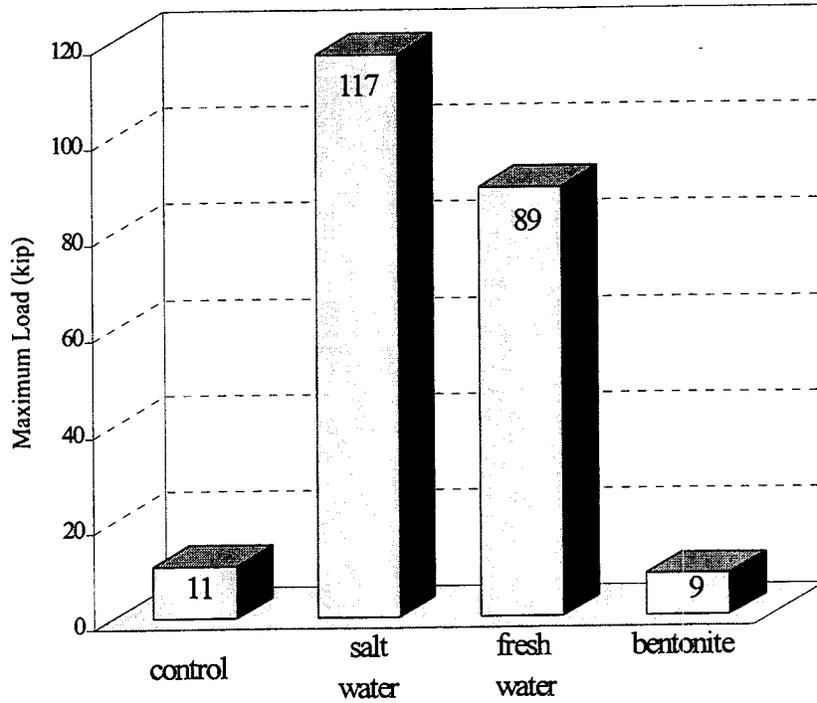
Figure 3.9 Force Summary For Soil-Caked Concrete Specimens.
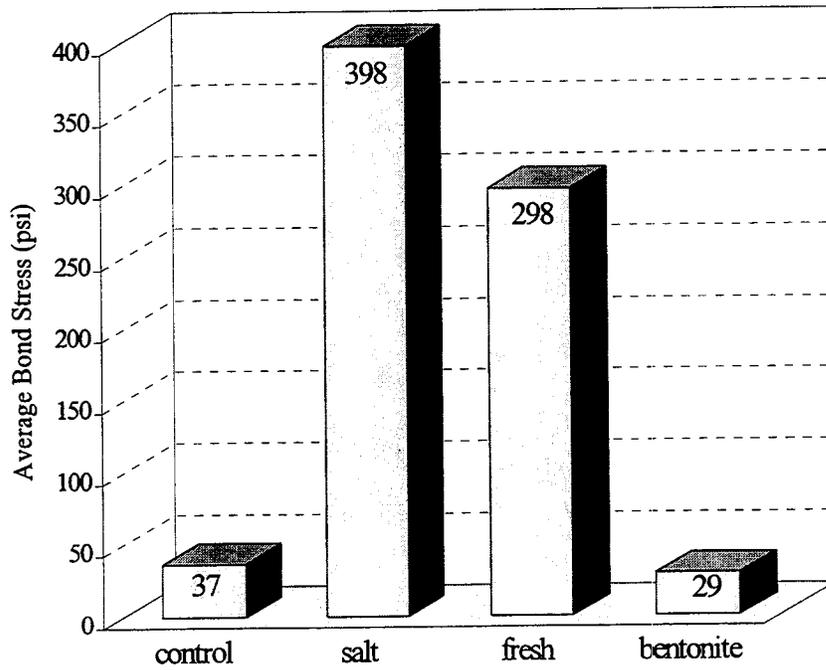
Figure 3.10 Average Bond Stress For Soil-Caked Concrete Specimens.

43

3.3   Steel Specimens

3.3.1   Control Condition

Table 3.6 presents the test results for the steel control specimens. Additionally, Figs 3.11 and 3.12 graphically depict the experimental results. Fig 3.11 shows the maximum pull-out force for each specimen. Fig. 3.12 is a graphical presentation of the average stress along the bond interface. This was calculated by dividing the maximum pull-out force by the bonded surface area. The maximum load varied between 137-161 kips and the corresponding bond stress between 380-431 psi.

The decrease from 1.5d to 2d exhibited with the concrete specimens is also apparent with the control steel specimens. The overall magnitude of the average bond stress for the steel specimens was significantly less then the concrete specimens.

Table 3.6   Summary for Control Steel Specimens.

Specimen	f'c (psi)	Bond Length	Bond Area (in^2)	Max Load (kip)	Average Bond Stress (psi)
H41	4460	1.5d	319.3	137.5	431
H42	4460	2d	425.8	161.9	380
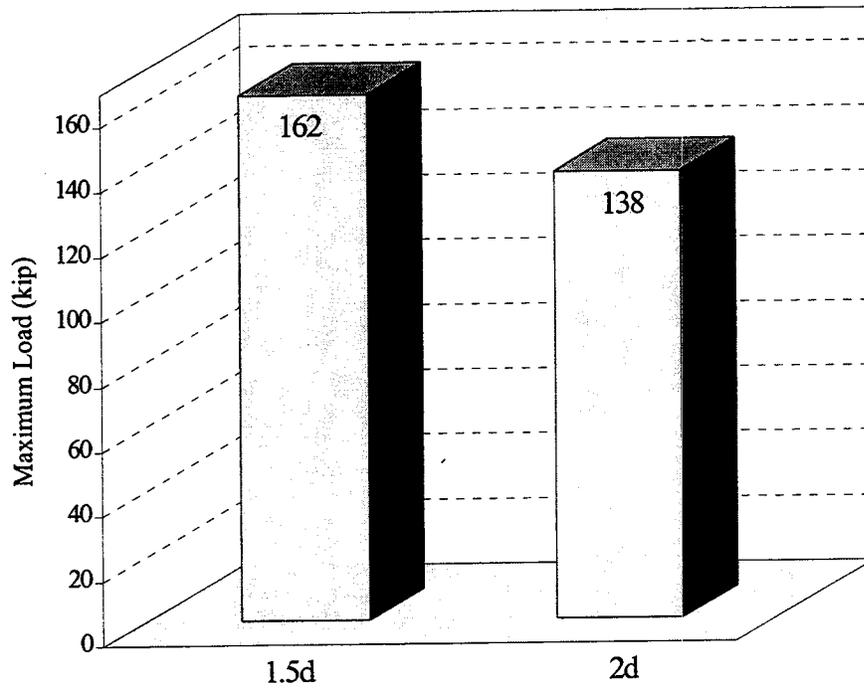
Figure 3.11 Force Summary For Control Steel Specimens.
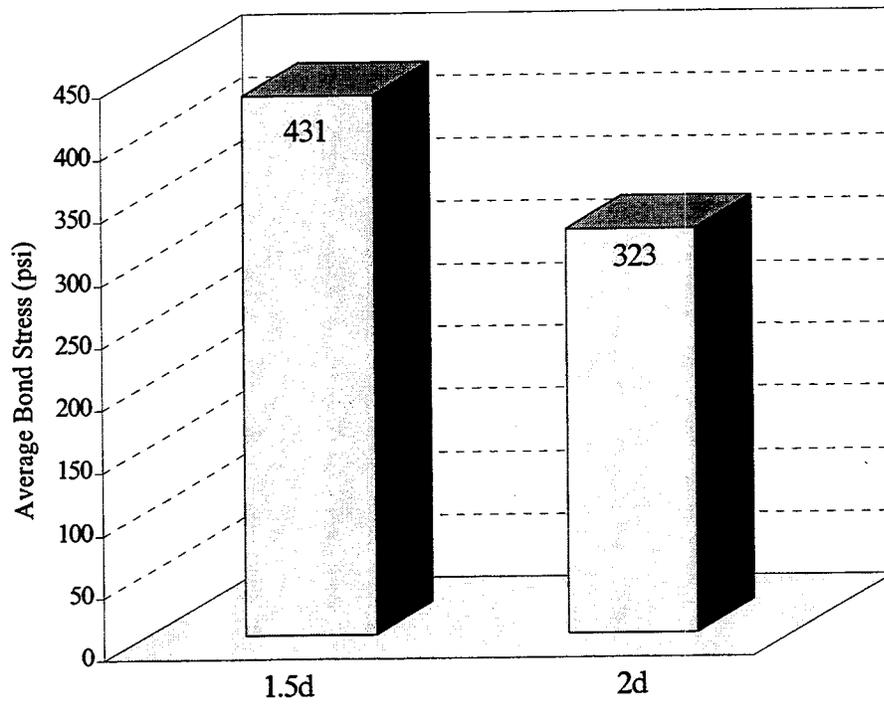
Figure 3.12 Average Bond Stress For Control Steel Specimens.

3.3.2   Salt Water Condition

Table 3.7 presents the test results for the concrete salt water specimens. Additionally, Figs 3.13 and 3.14 graphically depict the experimental results. Fig. 3.13 shows the maximum pull-out force for each specimen. Fig. 3.14 is a graphical presentation of the average stress along the bond interface. This was calculated by dividing the maximum pull-out force by the bonded surface area. The maximum load varied between 126-167 kips and the maximum bond stress between 297-524 psi.

Even though the strength of the seal slab concrete was the same for both the control and the salt water pour condition, the average bond stress for the 1.5d salt water specimen was greater than that control (122%). This may be an indication of scatter in the experimental data.

Table 3.7   Summary for Salt Water Steel Specimens.

Specimen	f'c (psi)	Bond Length	Bond Area (in^2)	Max Load (kip)	Bond Stress (psi)	Percent of Control
H21	4460	1.5d	319.3	167.4	524	122
H22	4460	2d	425.8	126.6	297	78
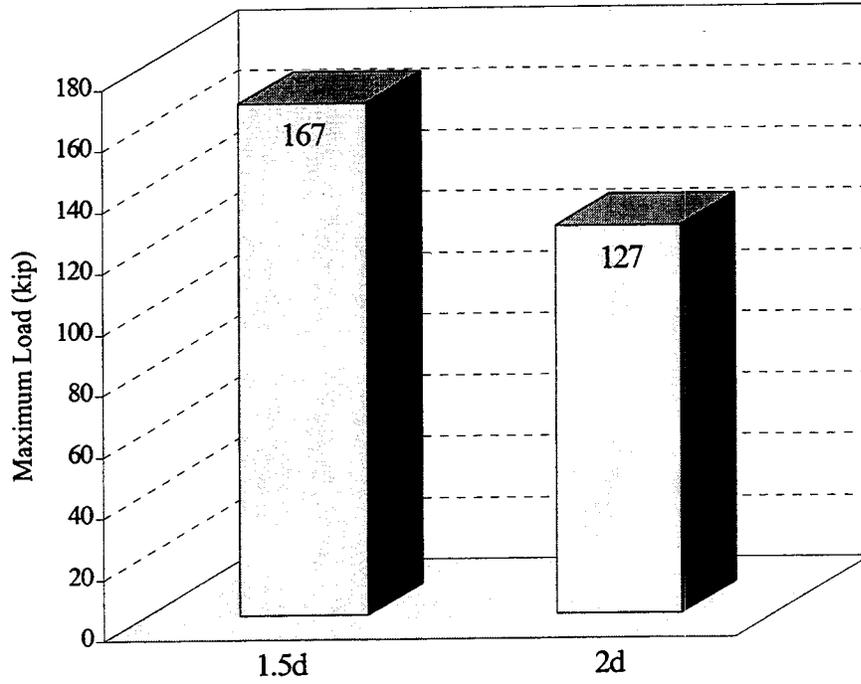
Figure 3.13 Force Summary For Salt Water Steel Specimens.
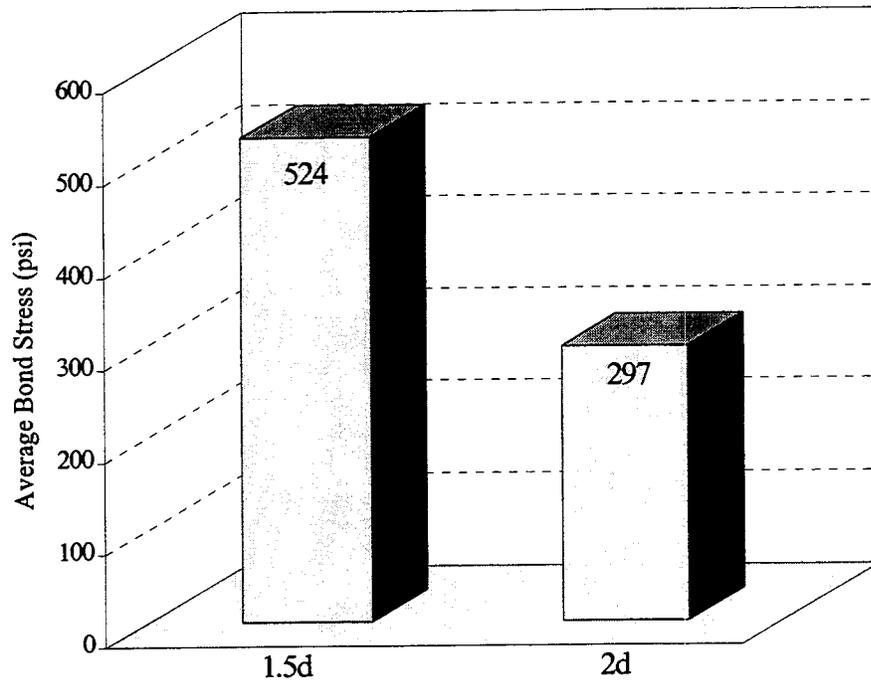
Figure 3.14 Average Bond Stress For Salt Water Steel Specimens.

47

3.3.3 Fresh Water Condition

Table 3.8 presents the test results for the steel fresh water specimens. Additionally, Figs 3.15 and 3.16 graphically depict the experimental results. Fig. 3.15 shows the maximum pull-out force for each specimen. Fig. 3.16 is a graphical presentation of the average stress along the bond interface. This was calculated by dividing the maximum pull-out force by the bonded surface area. The maximum load varied between 75-139 kips and the corresponding bond stress between 237-328 psi.

The experimental data for the fresh water steel specimens does not agree with the trends exhibited by the other specimens. Specifically, the trend for a decrease of average bond stress at 2d is not mirrored by the fresh water specimens. Without further data, there is no explanation for this anomaly.

Table 3.8   Summary of Fresh Water Steel Specimens.

Specimen	f'c (psi)	Bond Length	Bond Area (in²)	Max Load (kip)	Bond Stress (psi)	Percent of Control
H31	4460	1.5d	319.3	75.6	237	55
H32	4460	2d	425.8	139.6	328	86
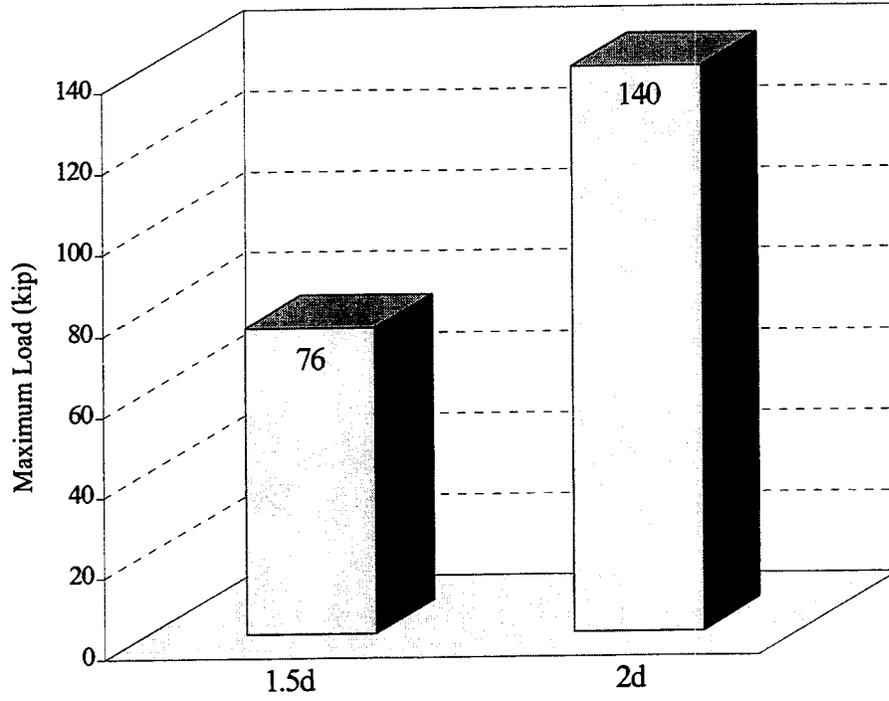
Figure 3.15 Force Summary For Fresh Water Steel Specimens.
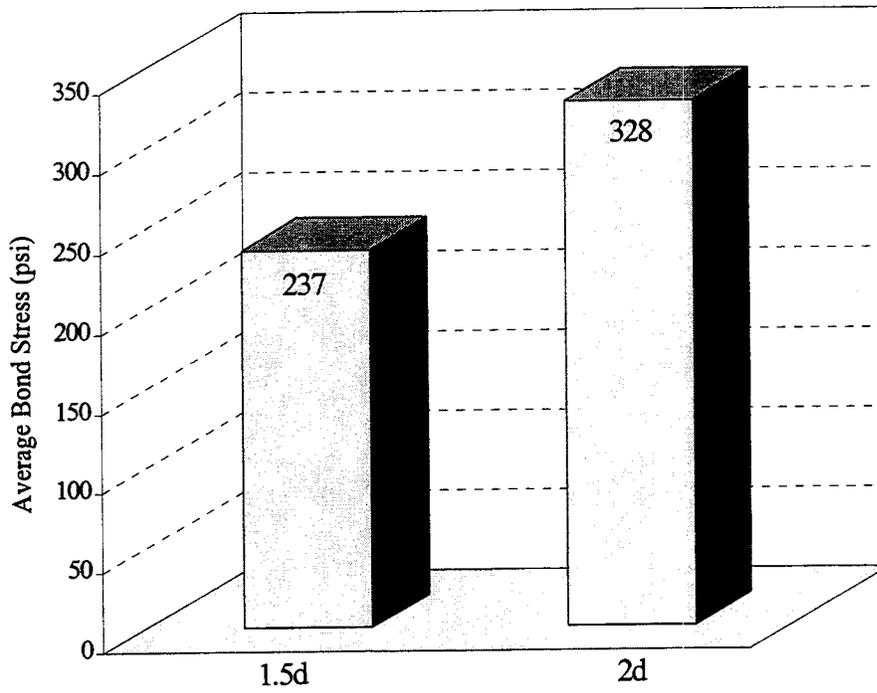
Figure 3.16 Average Bond Stress For Fresh Water Steel Specimens.

3.3.4 Bentonite Slurry Condition

Table 3.9 presents the test results for the concrete bentonite slurry specimens. Additionally, Figs 3.17 and 3.18 graphically depict the experimental results. Fig. 3.17 shows the maximum pull-out force for each specimen. Fig. 3.18 is a graphical presentation of the average stress along the bond interface. This was calculated by dividing the maximum pull-out force by the bonded surface area. The maximum load varied between 71-77 kips and the corresponding bond stress between 182-225 psi.

As in the concrete specimens, there is a decrease in average bond stress for embedment exceeding 1.5d. Again, the magnitudes of the bond stress were significantly lower for the steel specimens than the concrete.

Table 3.9   Summary for Bentonite Steel Specimens.

Specimen	f'c (psi)	Bond Length	Bond Area (in²)	Max Load (kip)	Bond Stress (psi)	Percent of Control
H11	4460	1.5d	319.3	71.9	225	52
H12	4460	2d	425.8	77.3	182	48
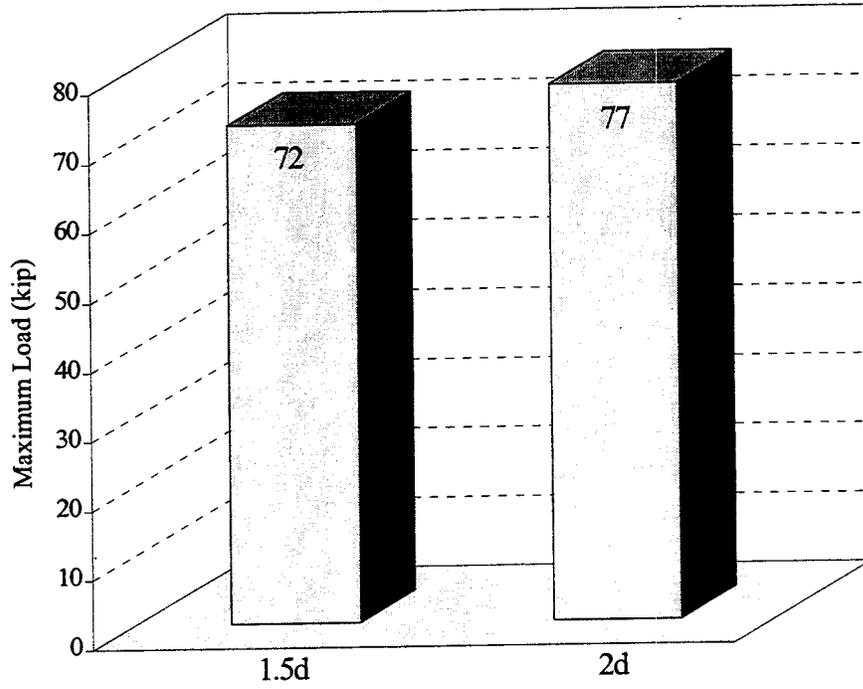
Figure 3.17   Force Summary For Bentonite Slurry Steel Specimens.
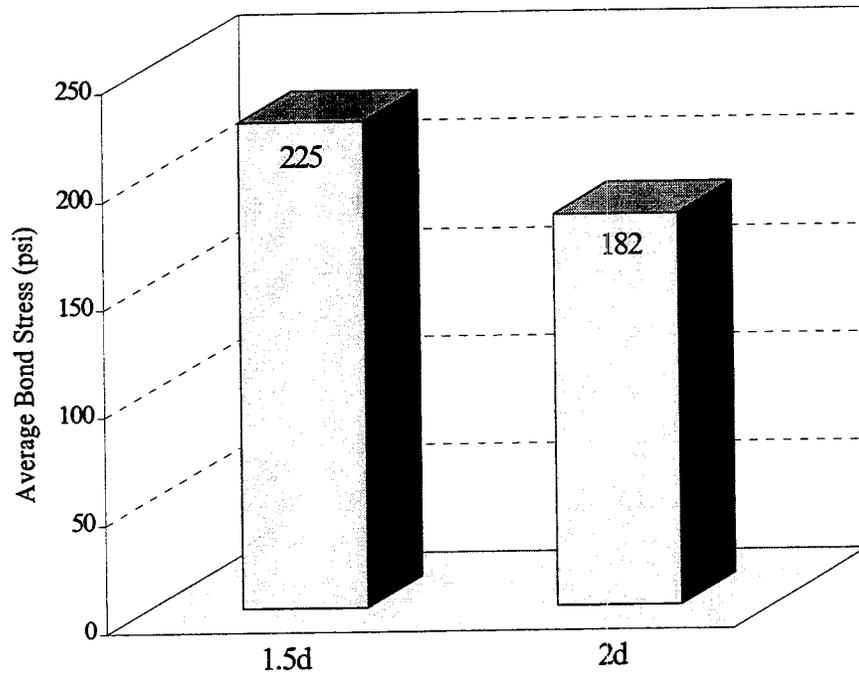
Figure 3.18 Average Bond Stress For Bentonite Slurry Steel Specimens.

51

3.4   Conclusions

The goal of the pilot study was to identify critical parameters that would facilitate full-scale testing. On the basis of the results presented and additional plots and photos included in this section, the following observations may be made:

(1)   Significant bond stresses developed for both the concrete (Tables 3.1-3.5) and steel specimens (see Tables 3.6-3.9).   Average bond stresses were consistently higher for concrete.

(2)   The results of tests on both concrete and steel piles showed that embedment depths above 1.5d were largely ineffective. This suggests that the bond stress distribution is non-uniform and instrumentation will be required to gain an understanding on the stress distribution.

(3)   For concrete specimens, the salt water and fresh water cofferdam conditions were not shown to differ significantly (percentages of control at 1.5d were 96% for the fresh water and 99% for the salt water shown in Fig. 3.19). This was not the case for the limited number of steel specimens tested (Fig. 3.20). There may be no special advantage in testing the salt water cofferdam condition in the full-scale tests.

(4)   For the larger embedment depths, the prestressed concrete specimens cracked (see Figs. 3.21-3.22- separation photos for concrete and steel are shown in Figs. 3.23-3.24). This suggests that depths in excess of 1.5d may be inappropriate for the full-scale tests.

52
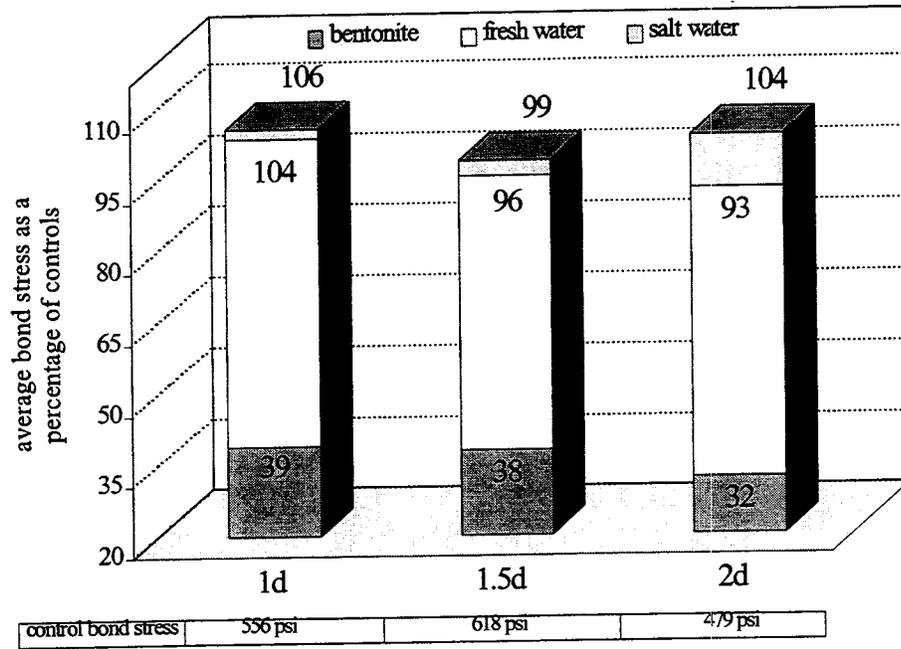
Figure 3.19 Bond Stress Results for Concrete Specimens.
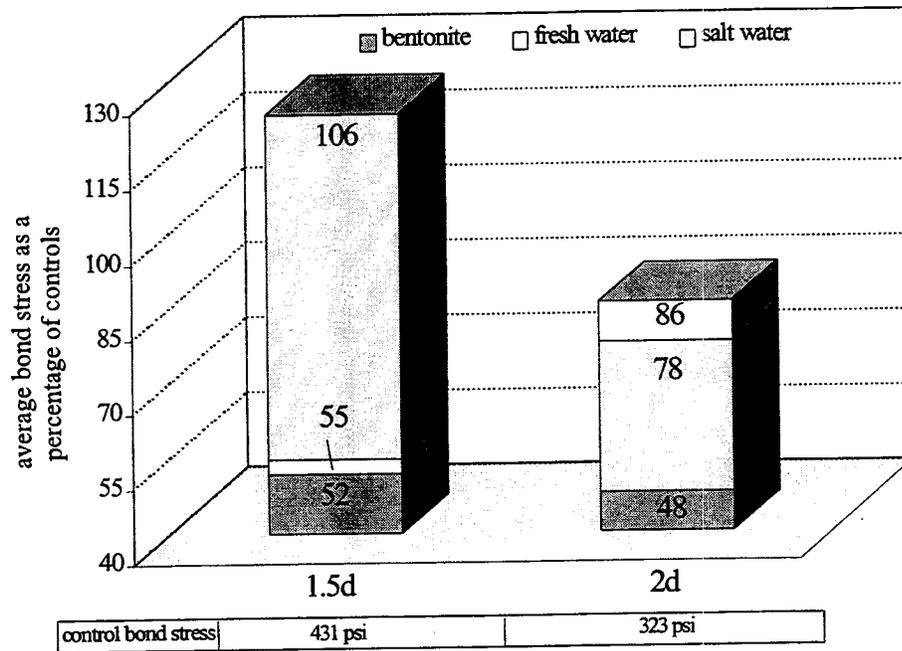
Figure 3.20 Bond Stress Results for Steel Specimens.

53
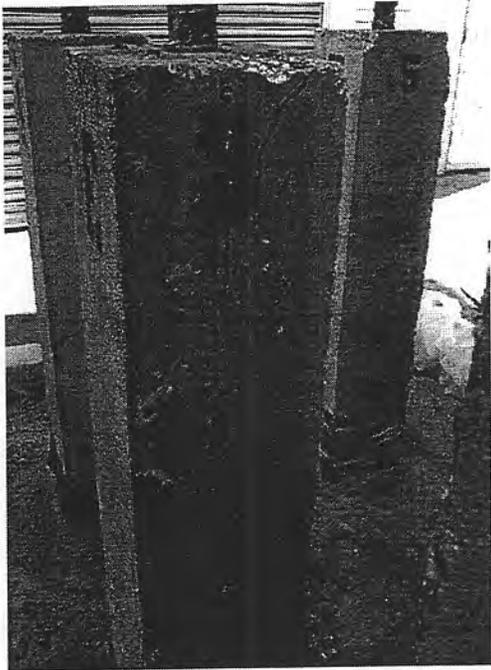
Figure 3.21 Longitudinal Cracks.
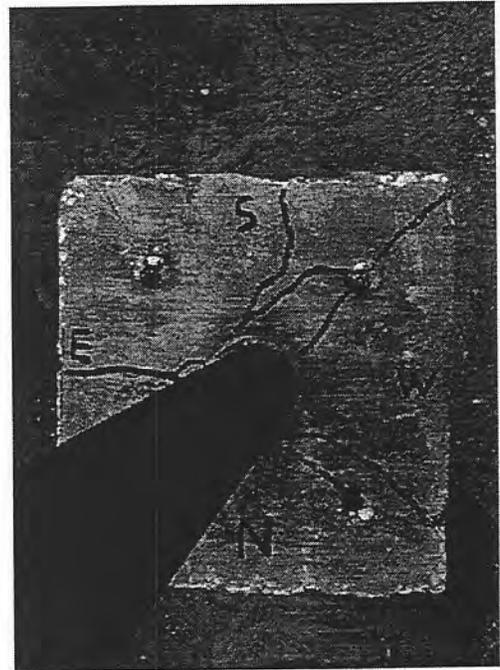
Figure 3.22 Radial Cracking.
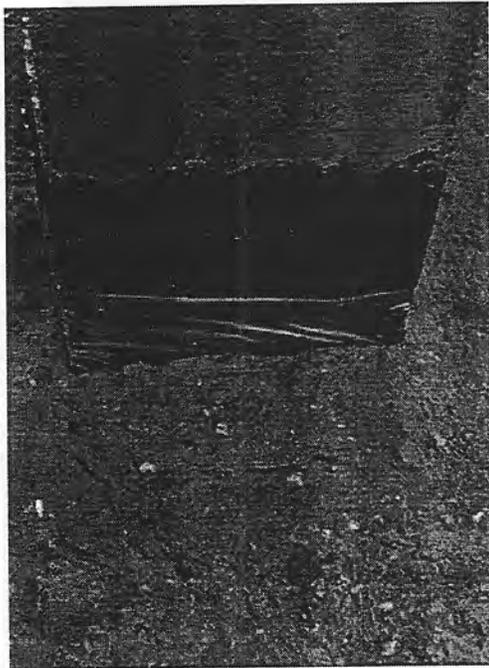
Figure 3.23 Separation of the pile/seal slab interface after failure for a concrete specimen.
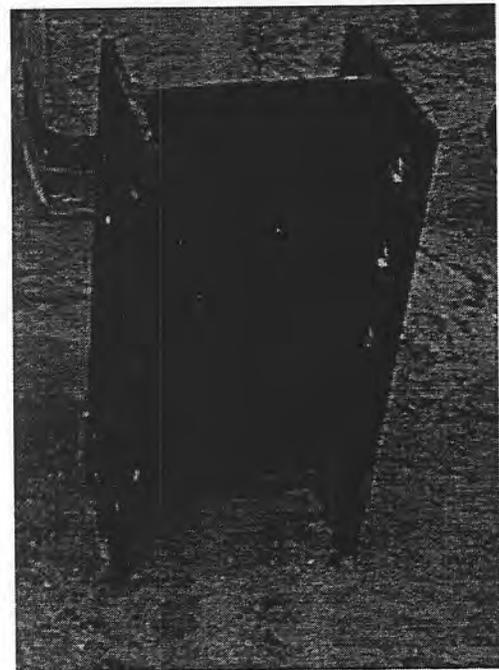
Figure 3.24 Separation of the pile/seal slab interface after failure for a steel specimen.

54

(5)   The soil-caked condition did not affect interface bond except in the case of

        bentonite slurry. In salt water or fresh water conditions, the caked soil was

        washed off the piles prior to the installation of the seal slab.

(6)   Due to the significant scatter of the steel specimen data, the number of steel

        specimens will need to be increased in the full-scale investigation to better

        identify the nature of steel pile to CIP seal slab bonding.

CHAPTER 4

FULL-SCALE STUDY

4.1   Introduction

This chapter provides details of the full-scale study carried out. An analysis of the test results is presented in the next chapter. A description of the test program is contained in Section 4.2. Materials used are described in Section 4.3 and fabrication of the pile specimens is covered in Section 4.4. Preparation of the pile surface to simulate field conditions is summarized in Section 4.5. The construction of the coffer dams is discussed in Section 4.6. The equipment designed to carry out the tests is described in Section 4.7 while details on the test procedure and instrumentation may be found in Section 4.8.

4.2   Test Program

The results of the pilot study were used to develop the test program for the full-scale tests. The principal changes were (1) elimination of the salt water condition (2) increase in the number of steel specimens (3) reduction in the embedment depth to 1.5d (4) restriction of the soil-caked surface to bentonite slurry (5) instrumentation of selected specimens.

As a result of these adjustments, a total of 32 specimens - equally divided between steel and concrete - were tested. The prestressed pile size was selected to be 14 in. Wide flange sections with the same depth were selected as steel piles.

Because of the very large bond stresses that developed, an additional case for 0.5d embedment was tested for the control and fresh water conditions. However, only one such specimen was tested. In all other cases, two specimens were tested. Table 4.1 summarizes the test matrix.

Table 4.1 Test Matrix.

Construction Condition	Embedment Length (d=14 in)	Concrete Specimens		Steel Specimens	
		Natural Surface	Soil-Caked Surface	Natural Surface	Soil-Caked Surface
control	0.5d	1	-	1	-
	1d	2	-	2	-
	1.5d	2	-	2	-
fresh water	0.5d	1	-	1	-
	1d	2	-	2	-
	1.5d	2	-	2	-
bentonite	1d	2	2	2	2
	2d	2	-	2	-

Fig. 4.1 shows the layout for the three conditions. Each of the simulated cofferdams were aligned to allow movement of equipment between them. All center-to-center pile spacings were kept at 3d (42 in.) [2]. To maintain the same spacing for the exterior piles, the edge of the cofferdam extended a distance 2d (28 in.) from these piles.

Control
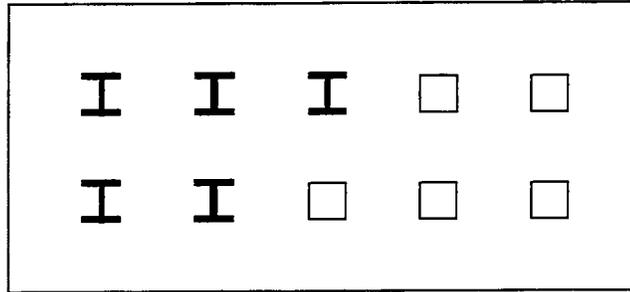
Fresh Water
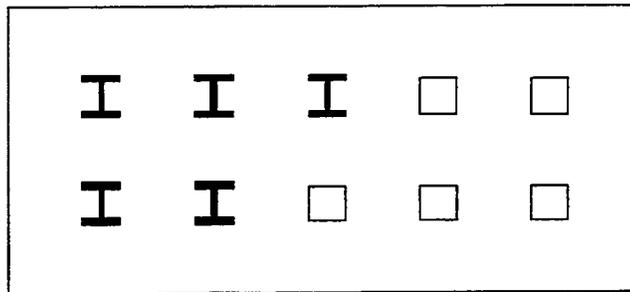
Bentonite Slurry
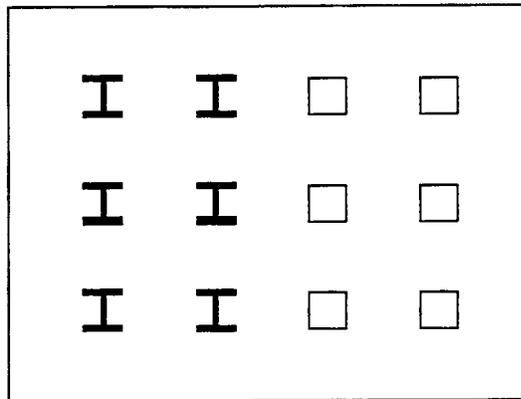
Figure 4.1 Full-Scale Study Cofferdam Layout

58

4.3   Materials

4.3.1   Concrete Mix

The concrete used in the preparation of the concrete specimens was the Florida Department of Transportation (FDOT) specification Class V Special, typically used for prestressed piles. The specified 28-day strength was 6000 lbf/in^2 (41 MPa). The concrete was purchased from Florida Rock Industries, Inc., Tampa, Florida (FDOT Plant No 15-303, Mix No 07-0002). The mix design details are summarized in Table 4.2.

Table 4.2 Mix Design for Prestressed Piles.

Item	Quantity per m^3	Quantity per yd^3
Cement (Type II)	344 kg	752 lbf
Coarse Aggregate (#57 Crushed Limestone)	777 kg	1700 lbf
Fine Aggregate (Silica Sand)	530 kg	1159 lbf
Water	126 L	33.5 gal
Water	128 kg	280 lbf
Air Entrainment Admixture (Daracem 100)	1.77 L	60.0 oz
Water Reducing Agent (WRDA 64)	0.443 L	15.0 oz
Water/Cementitious Ratio	0.37	0.37
Slump Range	152 to 203 mm	6 to 8 in
Air Content	1.5%	1.5%
Unit Weight	2268 kg/m^3	144.1 lbf/ft^3

4.3.2 Spiral Ties

Spiral ties using #5 gage steel were spaced as in full sized piles. They were fabricated by Insteel Wire Products, Mount Airy, NC. Material properties as provided by the fabricators are summarized in Table 4.3.

Table 4.3 Steel Spiral Tie Properties.

Property	Standard	Metric
Diameter	0.208 in	5.28 mm
Actual Area	0.034 in²	21.9 mm²
Average Tensile Strength	96.7 ksi	666.7 MPa
Average Yield Strength	97.1 ksi	669.7 MPa

4.3.3 Prestressing Strands

To ensure adequate pulling capacity, 0.6 in. rather than 0.5 in. Grade 270 strands were used. They were purchased from Concrete Reinforcing Products, Fort Lauderdale, FL. The properties of the strands as provided by the manufacturer are presented in Table 4.4.

Table 4.4 Steel Strand Properties.

Property	Standard	Metric
Ultimate Breaking Strength	58,565 lbf	260.5 kN
Load at 1% Extension	52,703 lbf	243.4 kN
Ultimate Elongation in 24 in., in/in.	3.5%	3.5%
Modulus of Elasticity	28.5×10^6 psi	196.6 GPa
Nominal Cross-Sectional Area	0.283 in²	182 mm²

4.3.4 Structural Steel

The steel pile specimens were fabricated using a W 14 x 90 section made from A36 structural steel. This section was used because it had the same depth as the 14 in. prestressed pile. The steel sections were purchased from Tampa Bay Steel Corp., Tampa, Florida.

The properties of the cross-section are summarized in Table 4.5 according to the specifications found in the American Institute of Steel Construction's Manual of Steel Construction.

Table 4.5 Structural Steel Pile Properties.

Property	Standard	Metric
Beam Depth	14.02 in	356.1 mm
Flange Width	14.52 in	368.8 mm
Cross-Sectional Area	26.5 in^2	17096 mm^2
Yield Stress	36 ksi	248 MPa
Ultimate Stress	58 ksi	400 MPa

4.4   Fabrication

The concrete specimens were cast and prestressed at Henderson Prestress, Tarpon Springs, Florida. The steel specimens were prepared for testing by Daniel Welding, Lutz, Florida.

4.4.1 Concrete Pile Specimens

As stated previously, the prestressed concrete piles were purchased from Henderson Prestress, Tarpon Springs, Florida. Fig. 4.2 through Fig. 4.6 show the various stages of specimen fabrication. They were constructed according to industry standards and, in fact,
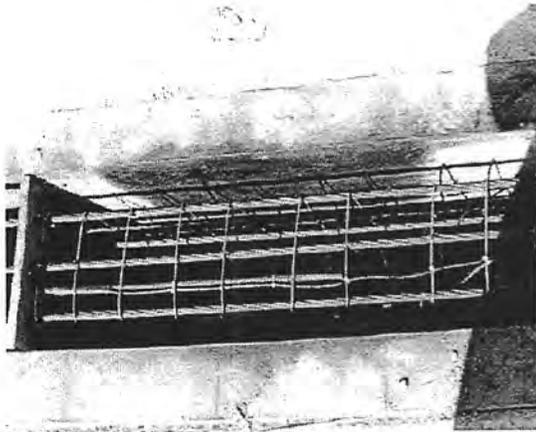

Figure 4.2 Instrumented Pile.
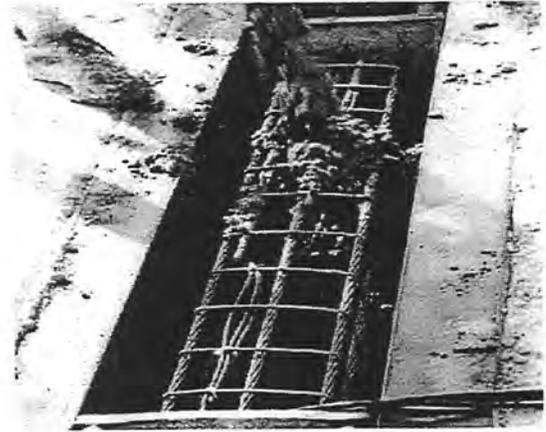
Figure 4.3 Concreting.

actual production piles were prestressed and cast along with the requested specimen. The concrete specimens were cast 14 in. (355.6 mm) square in cross-section and five feet (1.5 m) long. The longer length was used to accommodate the longer transfer length.

The prestressing steel consisted of eight 0.6 in. steel strands were tied to #5 gage spirals that were uniformly spaced at 6 in. A two ft length of the strand extended at the top of the specimen to serve as a connection point for the pull-out apparatus. Additionally, to allow the distribution of the bond stresses to be determined, four of the eighteen specimens cast were provided with embedded strain gages. These were located at the bottom, middle and top of the bonded length of 1d (three specimens) or 2d (1 specimen).
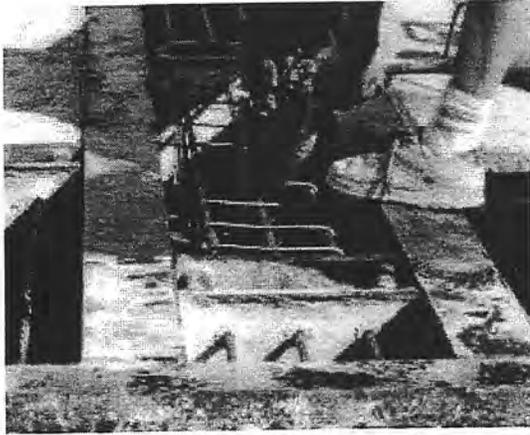
Figure 4.4 Vibrating Specimen.
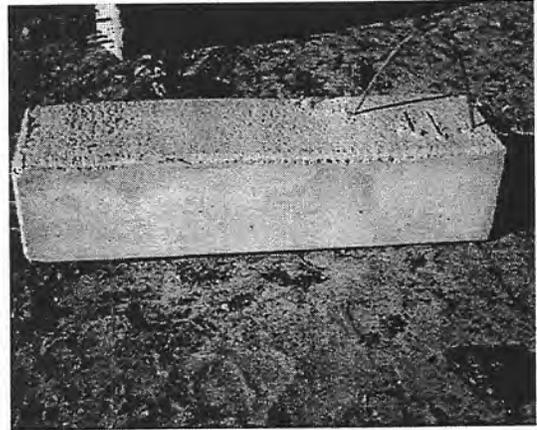
Figure 4.5 Completed Specimen.

4.4.2 Steel Pile Specimens

The W 14 x 90 steel beam section used for the steel pile specimens was purchased at Tampa Bay Steel Corp., Tampa, Florida. They were cut and machined at Daniel Welding, Lutz, Florida. Each specimen was 60 inches (1524 mm) in length. Holes for 1 1/8 inch (28.6 mm) diameter bolts were drilled in each flange to connect the pile specimens to the hydraulic pull-out frame (Fig. 4.6).

Figure 4.6 Fully Machined Steel Pile Specimen.

63

4.4.3 Surface Condition

As in the pilot study, two primary types of surfaces were required. A field-typical surface for exposure to the cast-in-place concrete seal slab and a de-bonded surface to which no significant bonding would occur. Again, a "soil caked" secondary surface condition was incorporated into the test program to simulate an adhered soil condition.

4.4.3.1   Bonded Surface

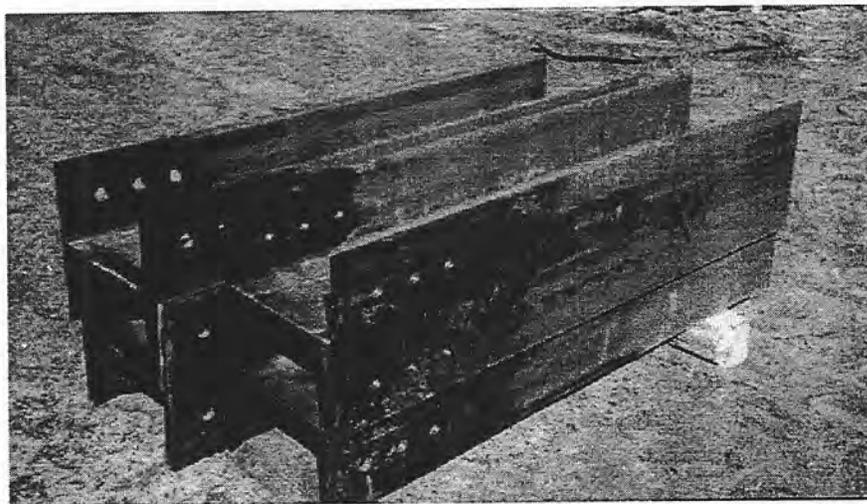Similar to the pilot study, the areas to be subjected to bond were not modified. The bonded concrete surfaces were left in their natural state. The steel specimens where cleaned of any hole drilling lubricant remaining from the fabrication process. As in the pilot study, the exposed steel surfaces were left slightly corroded to simulate actual steel piles.

4.4.3.2   De-Bonded Surface

The surfaces exposed to the CIP slab, but outside of the desired bond area, were covered with different separating layers to negate any significant bonding.

The de-bonded areas of the specimens were first covered with a layer of roofing tar (Fig. 4.7). Bituminous coatings are often applied to piles to decrease the friction from possible downdrag caused by consolidating soil layers. A similar bond breaking effect was theorized to occur in this application.

To further de-bond the two concrete surfaces, a layer of 12 lbf (0.05 kN) felt paper was applied. This physically separated the surfaces over a significant distance. As a final treatment, the felt paper was covered with a layer of duct tape (Fig. 4.8). The extremely smooth surface was reasoned to further inhibit bond and also served as a method for fixing the position of the paper.
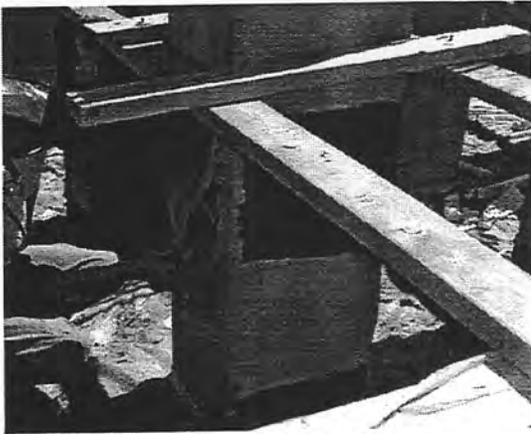

Figure 4.7 Applying Tar.
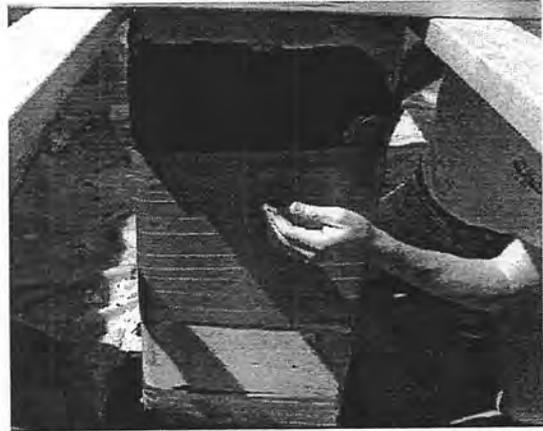
Figure 4.8 Securing Roofing Felt.

4.4.3.3 Soil-Caked Surface

As stated before, the soil-caked surface treatment was performed to simulate construction conditions in which un-removed soil particles have adhered to the pile surfaces (Fig. 4.9). In the full-scale investigation, an adhesive clay soil was utilized. The soil was purchased at an art supply store and is typically used for clay models. It was used because it was much more adhesive than the Kaolinite paste used in the pilot study. Based on the findings of the pilot study, the clay was only used in the bentonite pour condition.

The soil-caked condition was of limited value because of the possibility of the soil being washed away. Nonetheless, it offered the prospects of obtaining a lower limit on the soil-pile interface bond.

Figure 4.9 Applying Soil to Steel Specimen Surface.

4.5   Seal Slab Preparation

4.5.1   Simulated Cofferdam

The preparation for the cast-in-place seal slab first required the construction of the sides of the cofferdam. Since it was not practical to use actual sheet piles due to expense and the bracing required above ground, steel box forms were used instead. As the piles were not to be actually driven into the ground, the test specimens were also required to be supported in these

forms. In addition, the forms needed to be impermeable to the various types of construction fluids to be placed in the cofferdams depending on the modeled condition.

4.5.2 Box Forms

The cofferdam simulated formwork was constructed using rented steel reinforced plywood box forms from Symons Corporation, Des Plaines, IL. The forms (Fig. 4.10) were connected to form each cofferdam using wedge pins provided by the manufacturer (Fig. 4.11). They were also externally braced using wooden stakes and a two-by-four framework (Fig. 4.12). Additionally, each cofferdam was lined with 6 mil plastic sheeting (Fig. 4.13). This allowed for the forms to be water-tight, preventing the loss of any construction fluid (water, bentonite slurry).
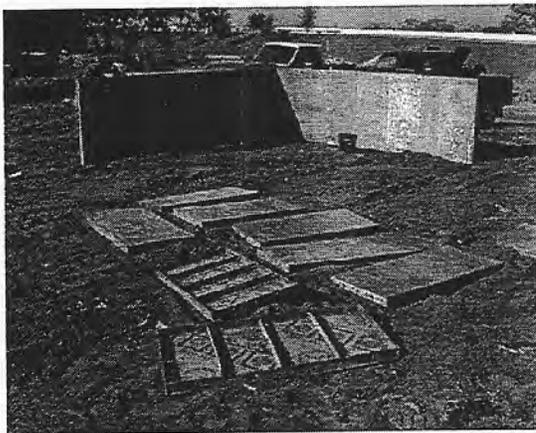
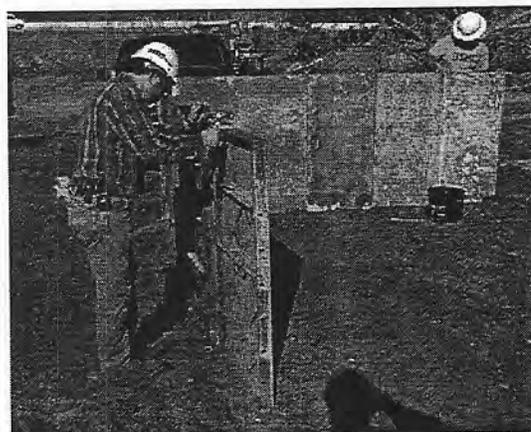

Figure 4.10 Steel Reinforced Forms.

Figure 4.11 Form Assembly.

Figure 4.12 Fully Braced.

Figure 4.13 Plastic Liner.

4.5.3 Specimen Support

Once the construction of CIP seal slab formwork was completed, the specimens were positioned (Figs 4.14 and 4.15). But before the specimens were placed, a plywood pad was first put under each pile to prevent piercing of the plastic lining (Fig. 4.16).
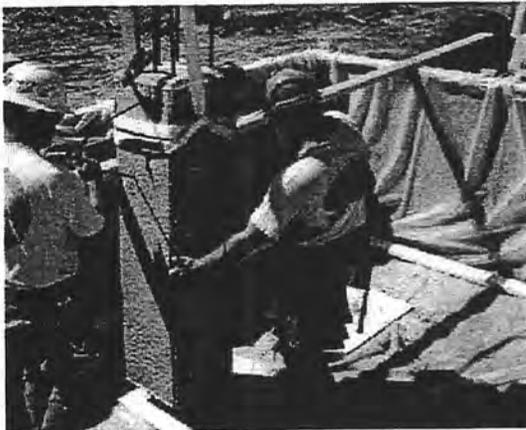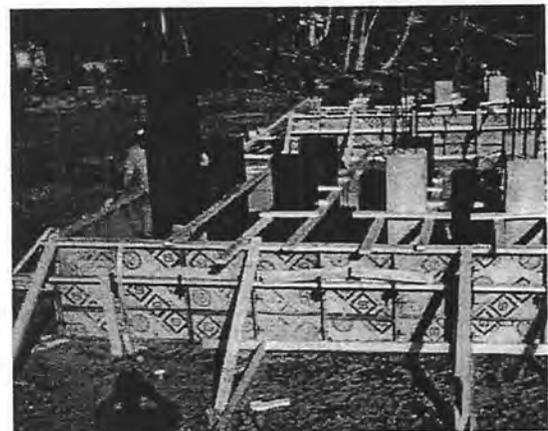

Figure 4.14 Placing Concrete Pile.
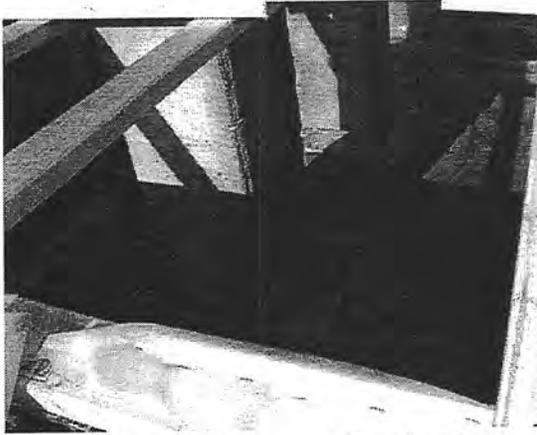

Figure 4.15 Placing Steel Pile.
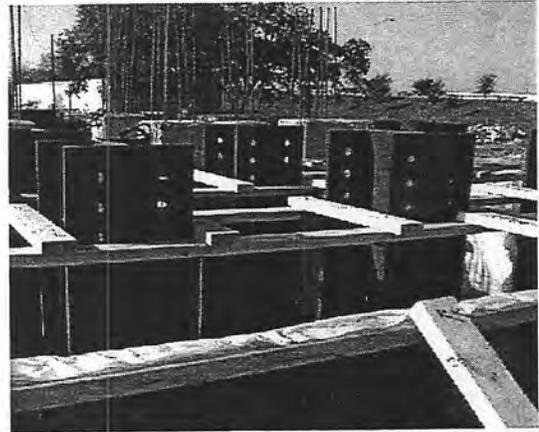
Figure 4.16 Plywood Bearing Pad.

Figure 4.17 Fully Supported Piles.

Additionally, a polystyrene seal was placed between each concrete pile specimen and the wooden pad. This prevented any possible bonding between the CIP concrete and the bottom of the pile. The polystyrene seal was not used with the steel specimens because it was reasoned that no significant bonding would occur to the relatively small exposed cross section. The specimens were vertically supported with a wooden two-by-four framework that was secured to the Symons forms (Fig. 4.17).

4.5.4 Materials

4.5.4.1 Concrete Mix

The concrete used in the preparation of the cast-in-place seal slab was the Florida Department of Transportation specification Class III Seal, specified for use as a hydraulic seal in cofferdam construction. The specified 28-day strength was 3000 lbf/in^2 (21 MPa). The

concrete was purchased from Ewell Industries, Inc., Tampa, Florida (FDOT Plant No 10-012, Mix No. 63018). Mix details are summarized in Table 4.6.

Table 4.6   Seal Slab Mix Design.

Item	Quantity per m^3	Quantity per yd^3
Cement (Type II)	254 kg	560 lbf
Coarse Aggregate (Crushed Limestone, 3/8 in)	657 kg	1450 lbf
Fine Aggregate (Silica Sand)	477.5 kg	1054 lbf
Water	167 L	44 gal
Water	166 kg	367 lbf
Fly Ash (Class F)	70.2 kg	155 lbf
Air Entrainment Admixture (MBAE-90)	0.21 L	7.0 oz
Water Reducing Agent (MBL-80)	1.9 L	64.35 oz
Water/Cementitious Ratio	0.3	0.51
Slump	178 to 229 mm	7 to 9 in
Air Content	1 to 6 %	1 to 6 %
Unit Weight	2090 kg/m^3	132.8 lbf/ft^3

4.5.4.2   Fresh Water

The fresh water used was obtained from a potable source located at the test site (Hayward Baker, Inc., Tampa, FL) (Fig. 4.18-4.19). The water primarily consists of ground water. Through the use of this source, construction conditions in which the ground water table is encountered was effectively modeled.
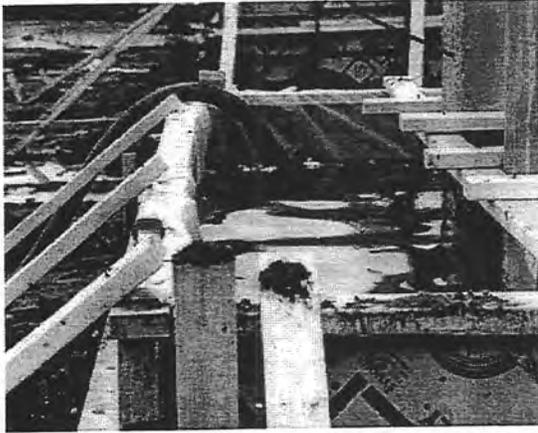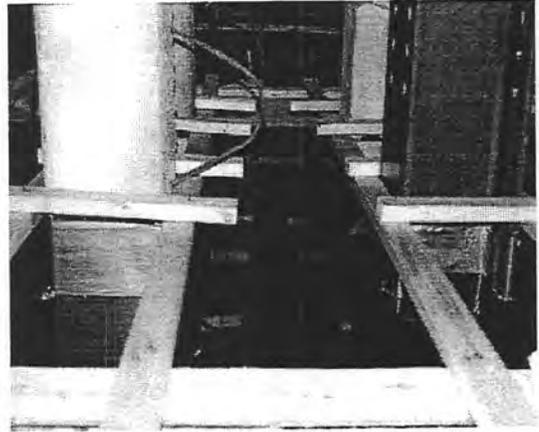
Figure 4.18 Filling Fresh Water Bed.

Figure 4.19 Fully Filled Water Bed.

4.5.4.3 **Bentonite Slurry**

The bentonite slurry was made by mixing dry, high yield bentonite and fresh water. The mixing was accomplished through the use of a shear pump (Figs 4.20 and 4.21) Enough bentonite clay was added to achieve slurry properties similar to FDOT specifications. The final density achieved was 65 lbf/ft^3 (1025 kg/m^3) with a viscosity of 40 seconds (Marsh Cone Method) and a pH of 8. Figs 4.22 and 4.23 depict the filling and completion of the bentonite slurry filled simulated cofferdam.

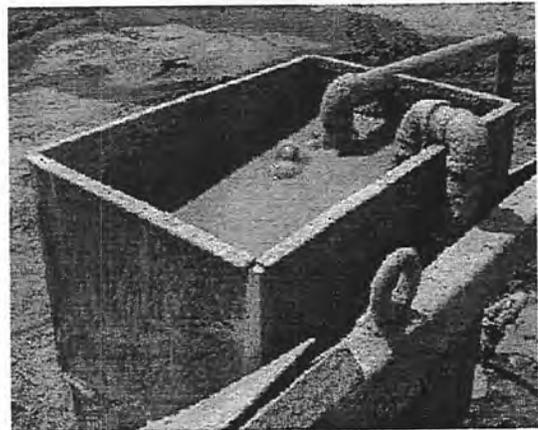
Figure 4.20 Shear Pump in Operation.

Figure 4.21 Shear pump reservoir filled with fully mixed bentonite slurry.

71

Figure 4.22 Filling Bentonite Bed.

Figure 4.23 Filled Bentonite Bed.

4.6   Seal Slab Placement

As stated before, the conditions under which the CIP seal slab was poured were varied to model concrete bonding under various possible construction conditions. During actual construction, a tremie, which is essentially a large funnel, is used to place the seal slab. The concrete is tremied from the bottom of the excavation up to the required elevation of seal slab. As the concrete is poured, the tip of the tremie is kept below the surface of the concrete to maintain the concrete quality. This prevents the segregation of aggregate and the loss of cement which would occur if the concrete was allowed to drop down through any liquid that may be present (water, drilling fluid, etc.).

In the full-scale study, the concrete was placed using a concrete pump truck (Fig. 4.24). The concrete was pumped through a 6 inch (152 mm) diameter hose. The concrete was placed from the bottom upwards keeping the hose tip below the rising level of concrete (Fig. 4.25). This is similar in placement and identical in effect to the tremie method.
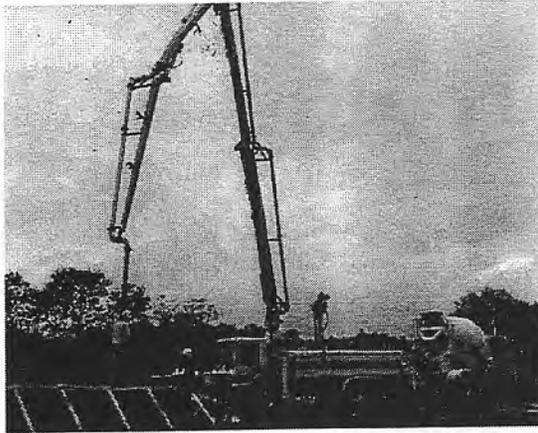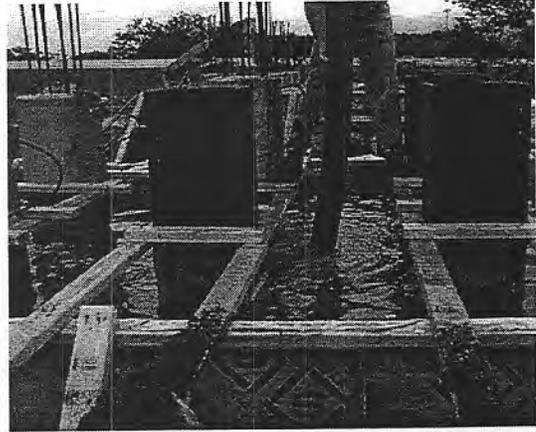
Figure 4.24 Concrete Pump Truck.

Figure 4.25 Placing CIP concrete in fresh water bed.

4.7 Testing Apparatus

As in the pilot study, a mechanism to measure the bond capacity, while maintaining the same field load transfer mechanics, was required. Since it was difficult to load the slab from below due to inaccessibility, it was decided that the most practical loading scheme was one in which a uniformly distributed load was applied to the top of the seal slab. In addition, the pile would also be loaded at the top. This exactly models the field loading conditions except that the orientation is rotated 180 degrees (see Fig. 2.24).

4.7.1 Design Requirements

The apparatus to test bond capacity needed to provide the expected loading capacity while being portable enough so it could be easily moved to each pile location. A flexible

design was also required to accommodate the differing connections to both the steel and concrete pile specimens.

It was decided to design a steel testing frame that would take advantage of an available double-acting, 300 ton (2670 kN) hydraulic jack. The jack would be operated with a 10 ksi (69 MPa) hydraulic pump system. The frame required connection designs for both the concrete and steel pile types. Additionally, the frame would need to be integrated with electronic devices to measure loads and displacements.

4.7.2 Design Methodology

The Load and Resistance Factor Design (LRFD) specification of the American Institute of Steel Construction, Inc. (AISC) was used for the design of the hydraulic test frame. Due to possible variations in bond capacity, the anticipated load on the frame was set to the maximum capacity of the hydraulic jack (300 tons).

4.7.3 Initial Design

Similar to the laboratory-scale hydraulic pullout frame, the full-scale hydraulic pullout frame consisted of two main sections: a tension assembly (Fig. 4.26) and a compression assembly (Fig. 4.27).
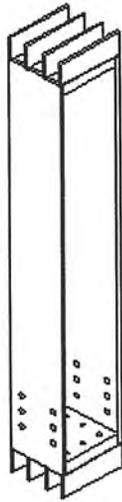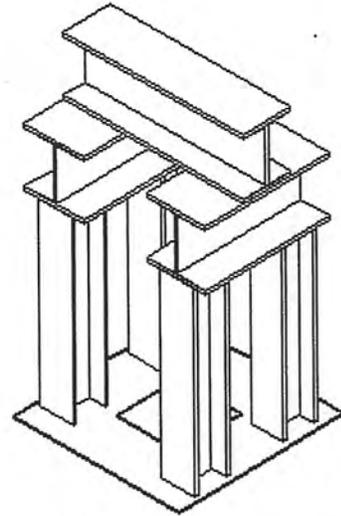
Figure 4.26 Tension Frame Assembly.

Figure 4.27 Compression Frame Assembly.
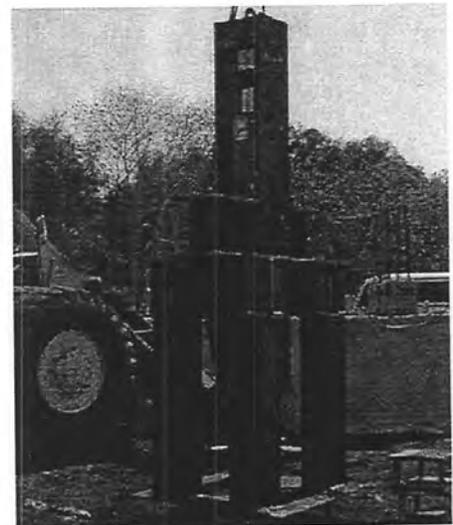

Figure 4.28 Hydraulic Pullout Frame.

Figure 4.29 Fully Assembled Pullout Frame.

4.7.3.1   Compression Assembly

The compression assembly consisted of four 44 inch vertical columns welded at the bottom to a 43 inch square, 3/4 inch thick steel bearing plate and connected at the top to two lengths of beam section. The columns were made from a W 8 x 58 structural steel section. The beams were all W 14 x 109 sections. The cross-beam which transferred loads to the other two beams had a 3/8 inch thick doubler plate plug welded to the web for added shear capacity. During testing, the hydraulic jack expanded to push the tension assembly upwards and to bear downwards onto the beam section which transferred to the top of the seal slab. Since the tension assembly was connected to the specimen, tensile force is applied to the pile.

4.7.3.2   Tension Assembly

The tension assembly consisted of two square plates and two long rectangular plates. The square plates were 12 5/8 inches (320.7 mm) across and 2 ½ inches (63.5 mm) thick. Each square plate had ribs welded to them the increase the moment of inertia and therefore accommodate the expected bending stresses. The rectangular plates were 86 inches (2184.4 mm) long and 3/4 inch (19 mm) thick. The two thicker plates were placed on each end with the two long plates welded between them. The bottom plate had eight, 3/4 inch (19 mm) holes drilled in it to allow penetration of the exposed prestressing strands from the concrete specimens which were secured with prestressing chucks. The long plates had bolt holes drilled into them for the bolted connection used for the steel specimens.

4.8   Pull-Out Testing

4.8.1 Set-Up

After the seal slabs were allowed to cure for the allowable minimum of 72 hours [1], the pull-out testing of the specimens was performed. To conduct the testing, the following steps were undertaken: placement of a grout layer, assembly and connection of the hydraulic testing apparatus, attachment of the data acquisition system, and application of loading until failure.

4.8.1.1   Leveling Grout Pad

Since concrete vibration is not used in seal slab construction [1] due to possible aggregate segregation in the submerged environment, various degrees of surface roughness developed according to the pour condition. The bentonite pour condition had the greatest degree of evenness and control had the least. To perform the vertical tensional load application as specified in the test program, the uneven surfaces needed to be compensated for. A secondary layer of high strength grout was placed upon each simulated cofferdam.

The grout was poured and finished two days after the placement of the CIP seal slab. Since the debonded portion of each pile specimen extended well above the CIP slab, there were no difficulties with possible bonding of the grout to the piles. Figs 4.30 and 4.31 show the placement of the grout and the finished grout layer.

Figure 4.30 Placement of high strength grout layer.

Figure 4.31 Finished layer of high strength grout.

4.8.1.2   Frame Assembly

First, the tension assembly and the compression assembly were arranged with the hydraulic jack supporting the tension assembly (Fig. 4.32). Then, while the entire frame was elevated above the concrete slab with a forklift (Fig. 4.33), the bottom of the tension assembly was connected to the specimen to be tested.
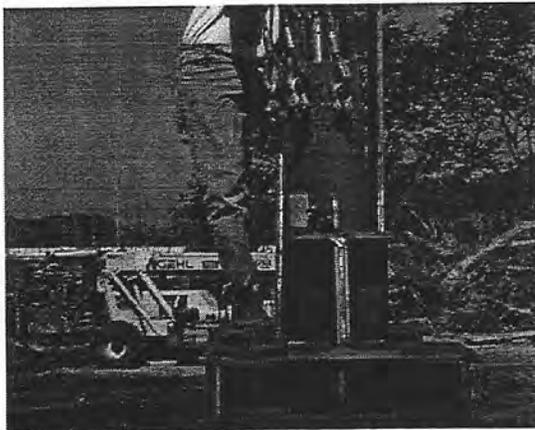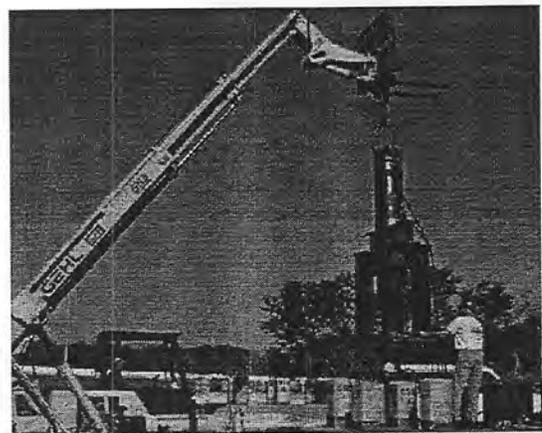

Figure 4.32 Assembly of hydraulic pullout frame.

Figure 4.33 Positioning frame using a crane and a forklift.

The type of connection depended on specimen type. In the case of the prestressed concrete specimens, the exposed prestressing strands were threaded through the holes in the bottom plate. They were then secured by prestressing chucks (Fig. 4.34). These chucks incorporate wedges which grip the strands. With the chucks in place, the concrete pile could be tested. With the steel specimens, extension plates were attached to the tension straps using 7/8 inch (22 mm) diameter bolts . The plates were then used to connect the frame to the pile specimen.
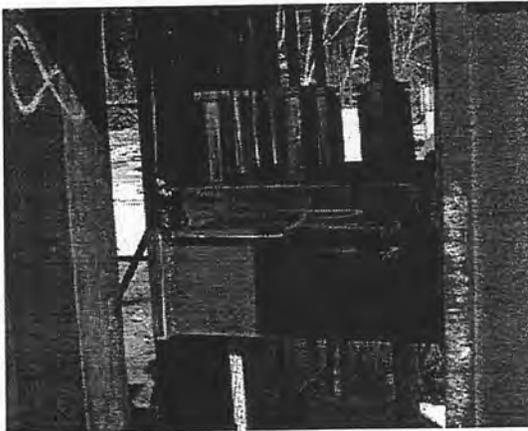
Figure 4.34 Concrete pile connection using prestressing chucks.

Figure 4.35 Steel pile connection using bolts.

4.8.2 Data Acquisition

As with the pilot study, the Megadac data acquisition system by the Optim Electronics Corporation was used for collecting and recording the test data generated by the pull-out testing. Along with the Megadac, a load cell and two electronic displacement gages (LVDTs)

79

were used to monitor each pile specimen as it was tested. The load cell had a capacity of 600 kips (2670 kN). The electronic displacement gages had a 2 inch (50.8 mm) range. Their placement depended on pile type.

For the concrete specimens, one LVDT was magnetically attached to the bottom of the tension assembly and positioned to register displacement with respect to an external reference beam (Fig. 4.36). The other LVDT recorded relative displacement between the tension assembly and the top of the pile specimen (Fig. 4.37). This accounted for any possible slippage of the prestressing chucks.
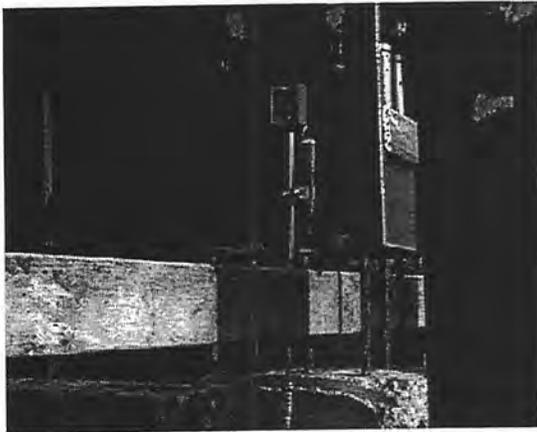
Figure 4.36 LVDT referenced from frame to external beam.
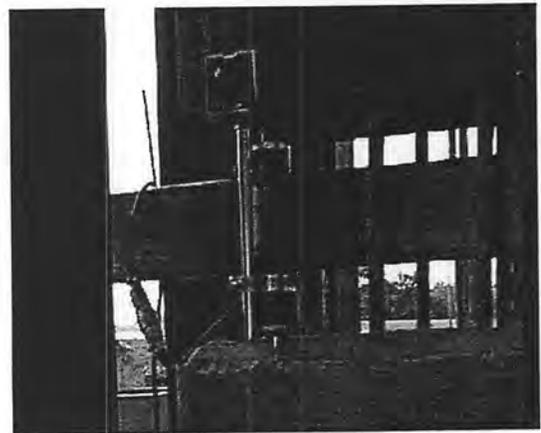
Figure 4.37 LVDT referenced to top of pile specimen.

For the steel specimens, one displacement gage was magnetically attached to the pile and referenced to the top of the slab (Fig. 4.38). The other gage, for redundancy, was magnetically attached to the pile and a referenced to an external beam (Fig. 4.39).

80

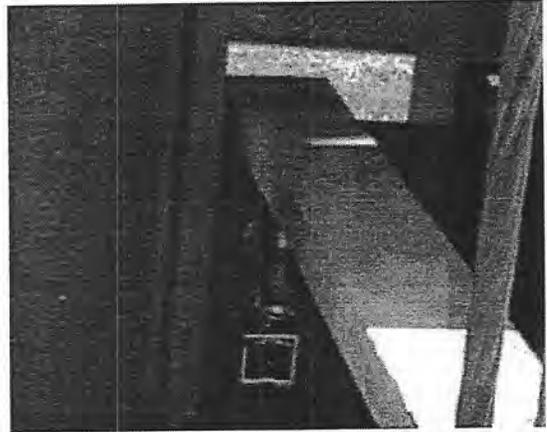**Figure 4.38** LVDT referenced for steel specimen to top of CIP slab.

Figure 4.39 LVDT referenced from steel specimen to external frame.

4.8.3   Test Procedure

Once the set-up procedure was completed, the pull-out testing could be conducted. The tensile load was increased slowly using a manually operated toggle switch which intermittently engaged the power to the hydraulic pump (Figs 4.40 and 4.41). The load was increased slowly to reduce any possible dynamic stiffening of the system. Each specimen was displaced upward at least one inch (25.4 mm) to ensure that the bond interface had been displaced.
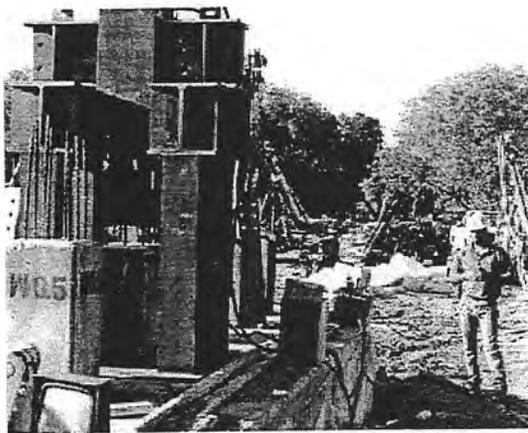
Figure 4.40 Operating Hydraulic Pump.

Figure 4.41 Pullout Testing in Progress.

81

Figs 4.42 and 4.43 show typical load versus slip graphs for both a concrete and a steel pile specimen. A load versus slip plot was produced for each pullout test. The complete record for the full-scale study is presented in Appendix II.
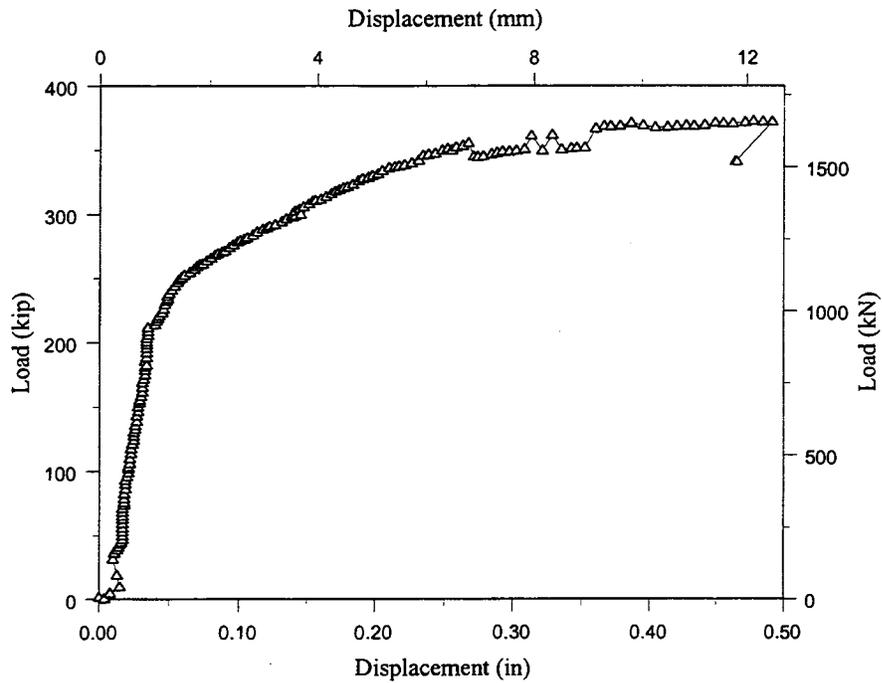
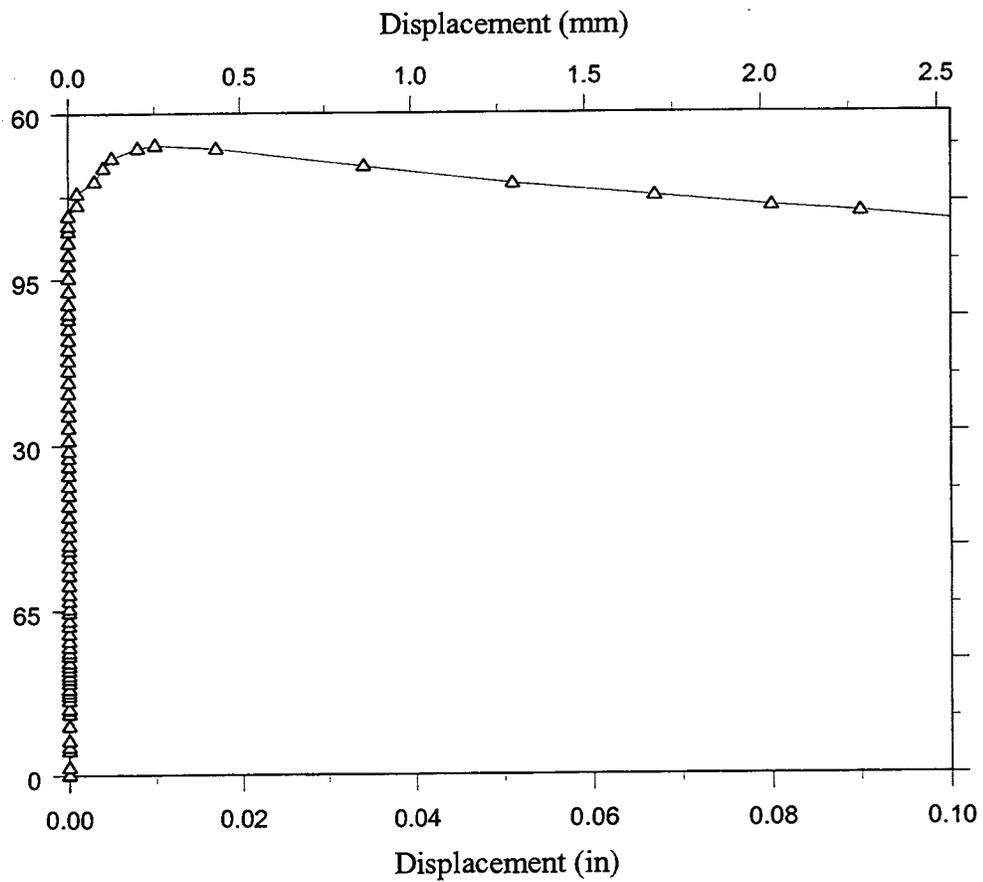**Figure 4.42** Typical Load vs Displacement Plot of a Concrete Specimen.

Figure 4.43 Typical Load vs Displacement Plot of a Steel Specimen.

References

1. Standard Specifications for Road and Bridge Construction (1999). Florida Department of Transportation, State Specifications Office, Tallahassee, FL.

CHAPTER 5

FULL-SCALE TEST RESULTS

5.1   Introduction

The results of the full-scale investigations are summarized in this chapter. The implications of these results are assessed in the next chapter that includes recommendations for possible incorporation in design specifications. Section 5.2 provides results for the prestressed pile specimens for the four different cofferdam conditions. Section 5.3 presents the corresponding results for the steel specimens. The principal conclusions are summarized in Section 5.4.

5.2   Concrete Specimens

The same format adopted for the presentation of the results of the pilot study is used. As before, results are grouped for the different simulated cofferdam conditions that were outlined in the previous chapter. All results are presented in two ways: in tabular form and also as bar diagrams. Each table contains information from the test relating to the specimen number, the average concrete strength, the measured area of the pile in contact with the seal

slab and the maximum recorded load. The corresponding bond stress and average bond

stress are also included. For conditions other than the control, average bond stress values are

normalized with respect to those for the control for the same embedment depth. The bar

diagrams contain information only on the maximum load and the average bond stresses. A

detailed description of each of the conditions is presented in succeeding sub-sections.

5.2.1   Control Condition

Table 5.1 presents the test results for the concrete control specimens. The maximum

load varied between 258 kips to 454 kips. The computed average bond stresses ranged

between 341 to 658 psi and displayed the same non-linearity observed in the pilot study. A

discussion on the strain distribution from the instrumented specimens is presented later in

Section 5.2.5. Figs. 5.1-5.2 present the same information in the form of a bar diagram.

Table 5.1 Summary for Control Concrete Specimens.

Specimen	f'c (psi)	Bond Length	Bond Area (in²)	Max Load (kip)	Bond Stress (psi)	Average (psi)
C0.5	4590	0.5d	392.9	258.7	658	658
C1.0A	4590	1d	794.5	372.2	468	460
C1.0B	4590	1d	788.4	355.2	451	
C1.5A	4590	1.5d	1179.9	356.1	302	341
C1.5B	4590	1.5d	1193.1	454.0	381	
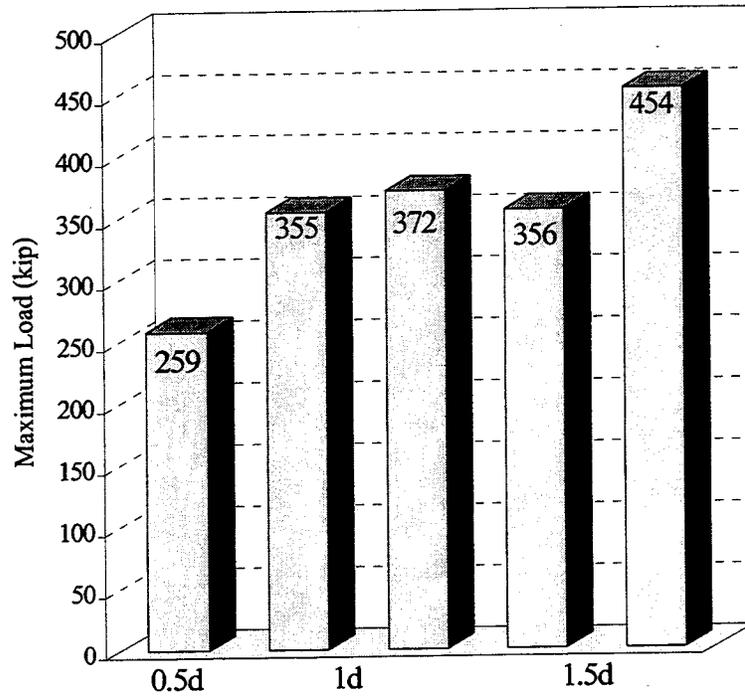
Figure 5.1 Force Summary For Control Concrete Specimens.
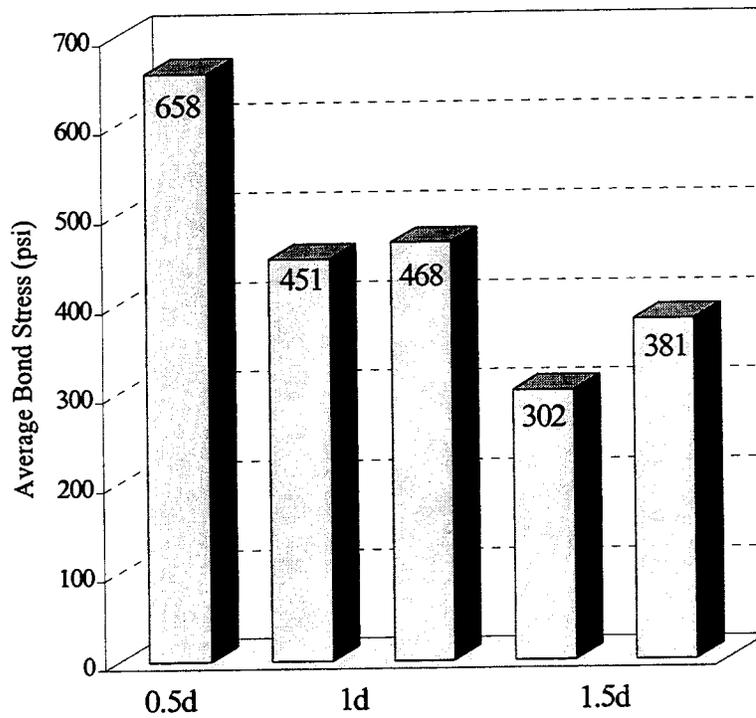
Figure 5.2 Average Bond Stress For Control Concrete Specimens.

86

5.2.2 Fresh Water Condition

Table 5.2 presents the test results for the fresh water control specimens. Compared to the controls, the maximum pullout loads (and computed bond stresses) tends to be lower ranging between 78-87% of its value. This may be because the concrete strength was somewhat lower (3940 vs 4590). The maximum load ranged between 200-357 kips. The computed average bond stress ranged between 297-512 psi. As with the control concrete specimens, there was a decrease in average bond stress from 0.5d to 1.5d. Results for the instrumented pile is presented in Section 5.2.5. Results in bar diagram form are shown in Figs. 5.3-5.4.

Table 5.2 Summary for Fresh Water Concrete Specimens.

Specimen	f'c (psi)	Bond Length	Bond Area (in²)	Max Load (kip)	Bond Stress (psi)	Average (psi)	Percent of Control
W0.5	3940	0.5d	392.0	200.6	512	512	78
W1.0A	3940	1.0d	780.1	305.2	391	387	84
W1.0B	3940	1.0d	784.9	300.4	383		
W1.5A	3940	1.5d	1183.9	357.7	302	297	87
W1.5B	3940	1.5d	1176.0	343.3	292		
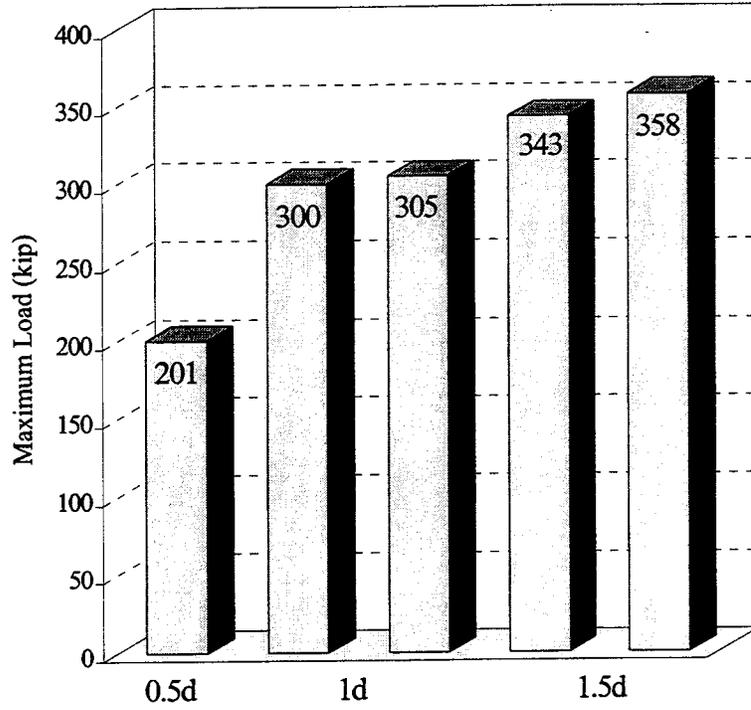
Figure 5.3 Force Summary For Fresh Water Concrete Specimens.
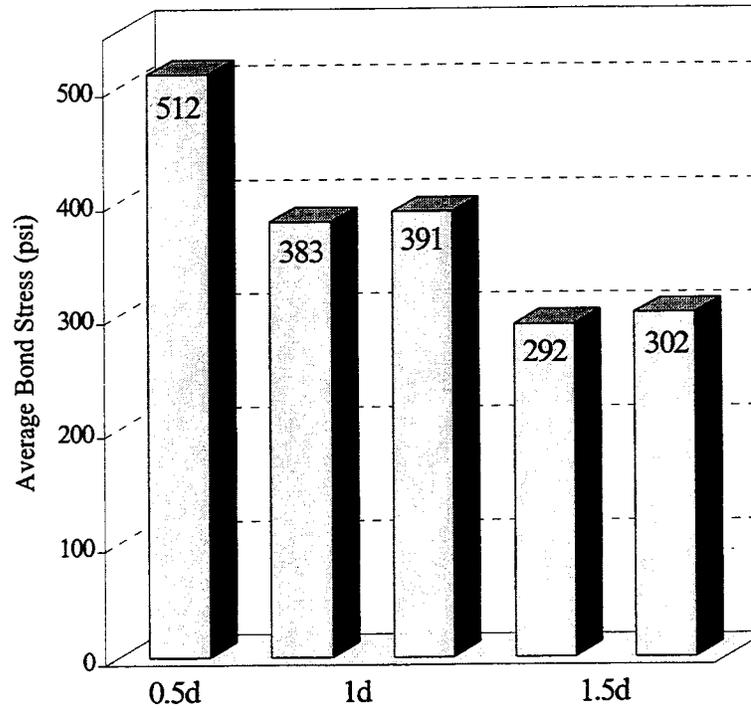
Figure 5.4 Average Bond Stress For Fresh Water Concrete Specimens.

88

5.2.3 Bentonite Slurry Condition

Table 5.3 presents the test results for the concrete bentonite slurry specimens. Additionally, Figs 3.5 and 3.6 graphically depict the experimental results. The maximum load varied between 286-365 kips and corresponding bond stresses between 216-368 psi. No results were available for the 2d controls but those for 1d embedment were 80% of that of the control. This is significantly higher than the approximately 30% values obtained from the pilot testing.

Table 5.3 Summary for Bentonite Specimens.

Specimen	f'c (psi)	Bond Length	Bond Area (in²)	Max Load (kip)	Bond Stress (psi)	Average (psi)	Percent of Control
B1B	3360	1d	804.6	300.7	374	368	80
B1D	3360	1d	791.4	286.5	362		
B2A	3360	2d	1595.1	365.2	229	216	-
B2B	3360	2d	1585.5	323.2	204		
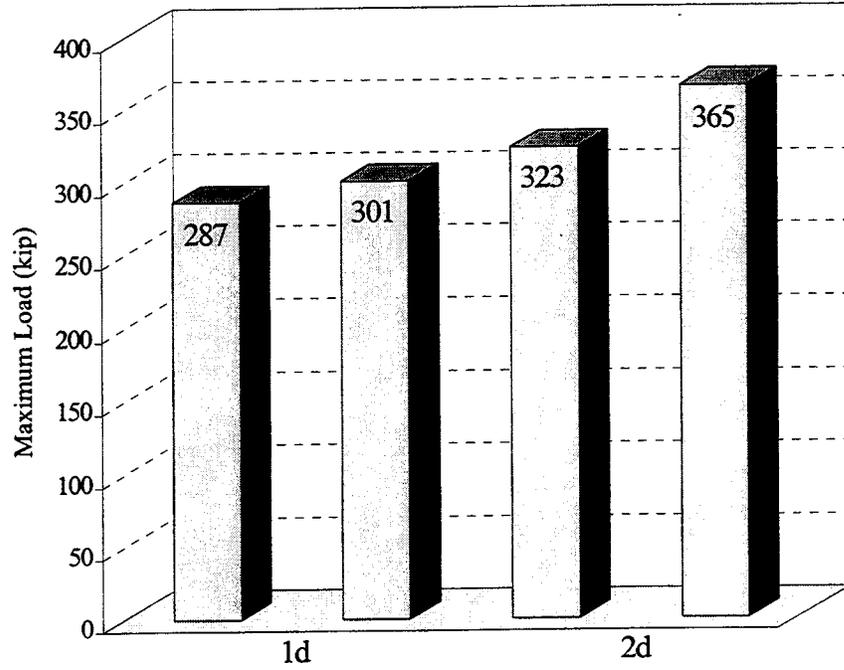
Figure 5.5 Force Summary For Concrete Bentonite Specimens.
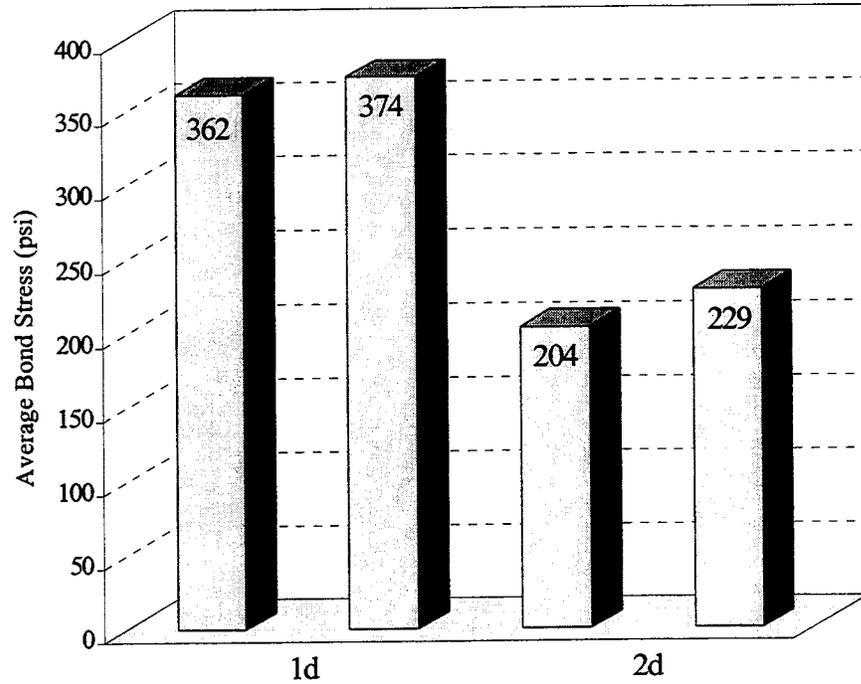
Figure 5.6 Average Bond Stress For Bentonite Concrete Specimens.

5.2.4 Soil-Caked Condition

Table 5.4 presents the test results for the concrete soil-caked specimens. Additionally, Figs 5.7 and 5.8 graphically depict the experimental results. Only two specimens were tested and the maximum load varied between 128-209 kips. The corresponding computed bond stresses were 161-264 psi.

As in the laboratory-scale study, the soil-caked condition has a significant negative impact on bond (35% and 57% of the controls at 1d). The results of the full-scale investigation confirm that bonding under soil-caked conditions is undesirable in actual construction conditions due to the unreliability of the capacity. The results for the instrumented pile is presented in the next section.

Table 5.4 Summary for Soil-Caked Specimens.

Specimen	Pour Condition	f'c (psi)	Bond Length	Bond Area (in²)	Max Load (kip)	Bond Stress (psi)	Percent of Control
B1A	bentonite	3360	1d	792.3	209.2	264	57
B1C	bentonite	3360	1d	795.4	128.2	161	35
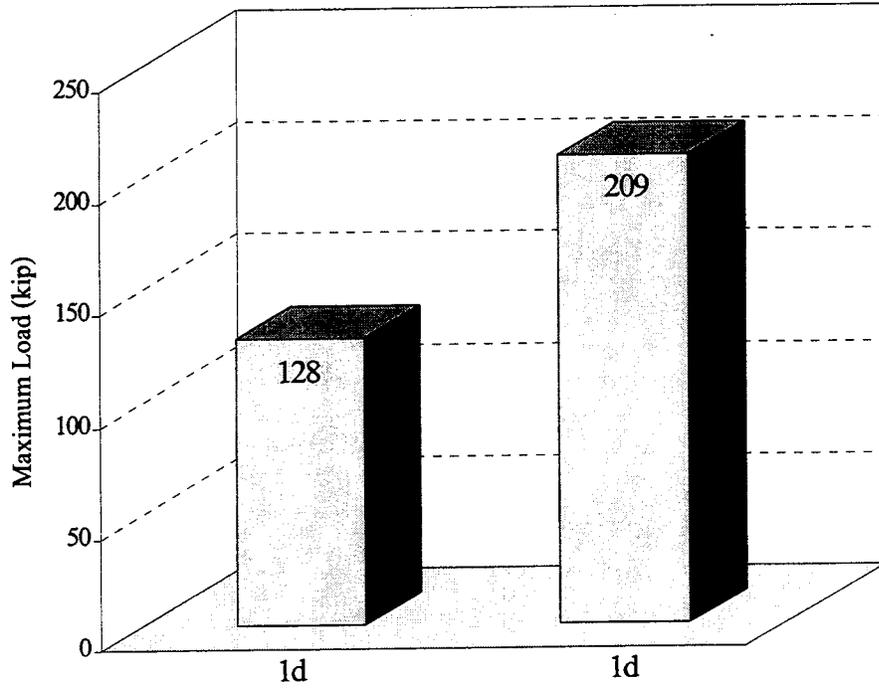
Figure 5.7   Force Summary For Concrete Soil-Caked Specimens.
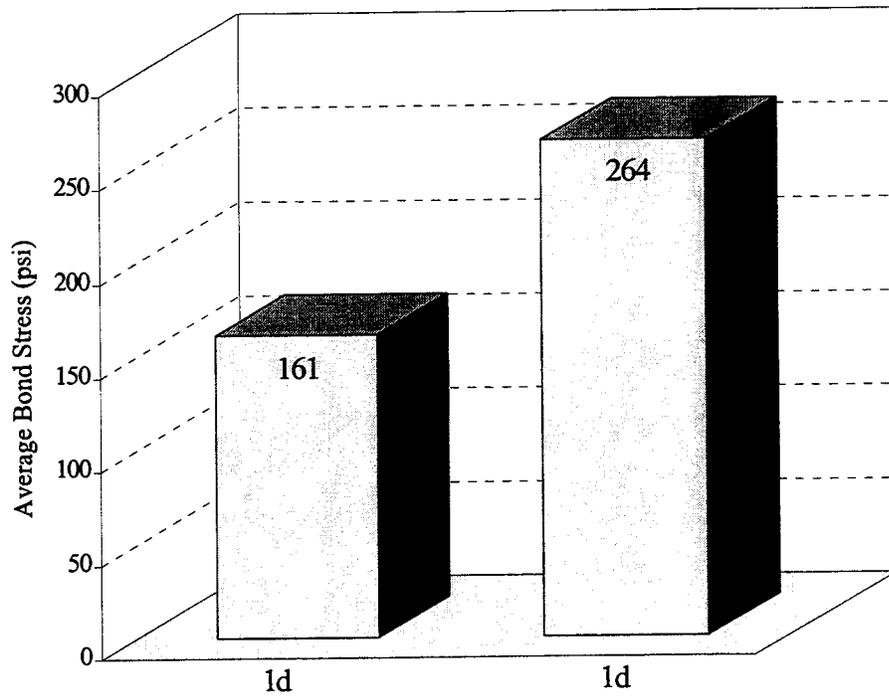
Figure 5.8   Average Bond Stress For Soil-Caked Concrete Specimens.

5.2.5 Strain Variation

To determine the nature of the load transfer across the bond interface, pile specimens were instrumented with embedded strain gages. Due to the scale and the required resources involved in the full-scale investigation, only four pile specimens were fitted with gages. One pile in each of the control and fresh water condition corresponding to an embedment depth of 1d were instrumented. Two piles with embedment depths of 1d and 2d in the bentonite bed were additionally instrumented.

Figs 5.9 through 5.13 show the strains along the bond interface during testing for each instrumented pile specimens. Strains were recorded for each pile at three levels: at the top of the bond interface, at the middle, and at the bottom of the bond interface.

Examining the general difference between strain gage levels during the initial loading, the force is transferred gradually from the top to the bottom of the bond interface. Also, later in the loading, there seems to be a loss of resistance at the top of the bond surface which is indicated by a significant increase in strain at the lower gage levels. This may indicated that a crack had formed along the pile and CIP seal slab bond interface.

In Fig 5.9, only the top and middle strain gages register strains. This suggests that only half the embedment depth is effective or that the gage was not working. In Fig. 5.10, however, all three gages show significant strains. This indicates that the effective depth is the full embedment depth. This is also borne out by the strain distribution for the bentonite bed having the same embedment (Fig. 5.11). In contrast, the strain at the bottom of the embedment for the 2d bentonite case (Fig. 5.12) registered no strain.
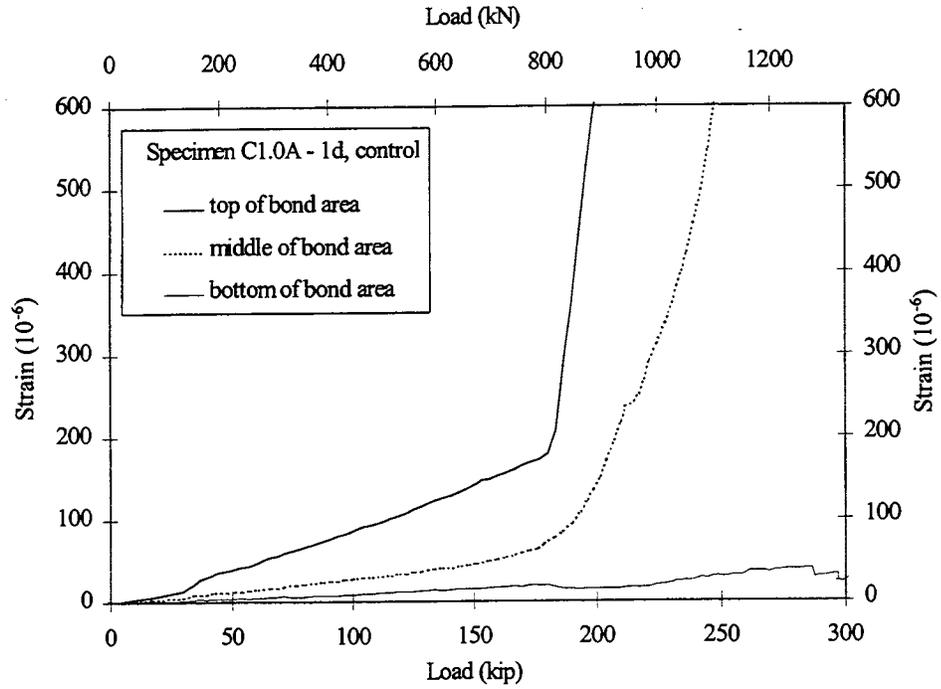
Figure 5.9 Change in strain with respect to load for Specimen C1.0A (control, 1d embedment).
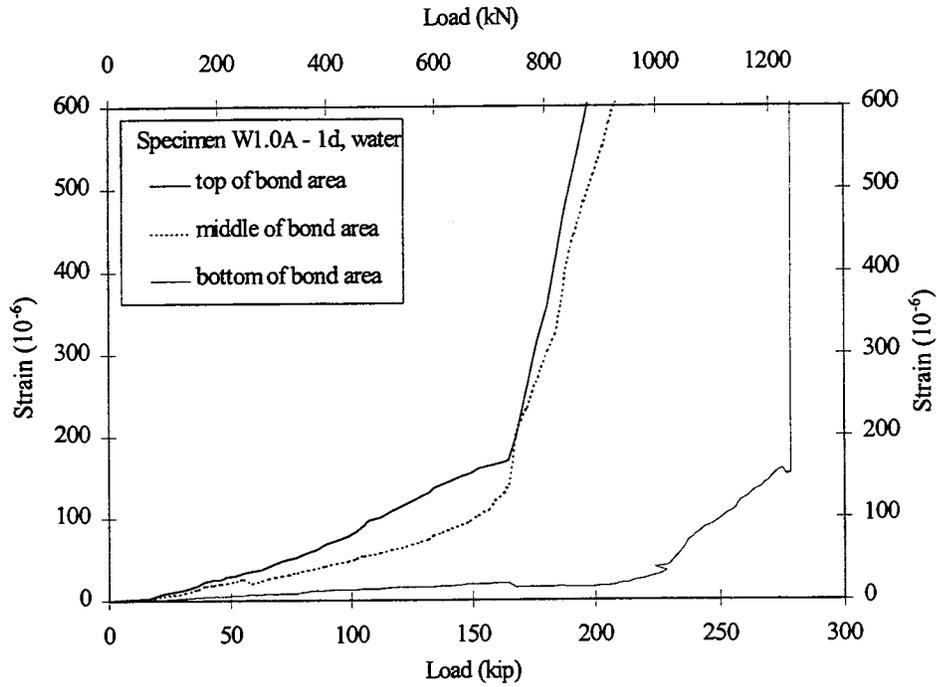
Figure 5.10 Change in strain with respect to load for Specimen W1.0A (fresh water, 1d embedment).

94
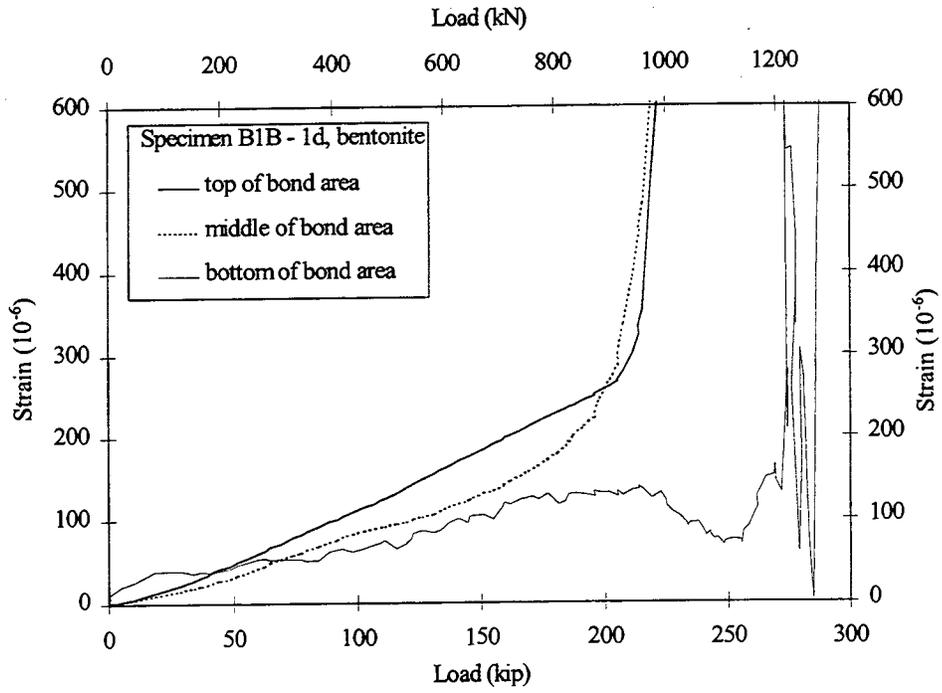
Figure 5.11 Change in strain with respect to load for Specimen B1A (bentonite, 1d embedment).
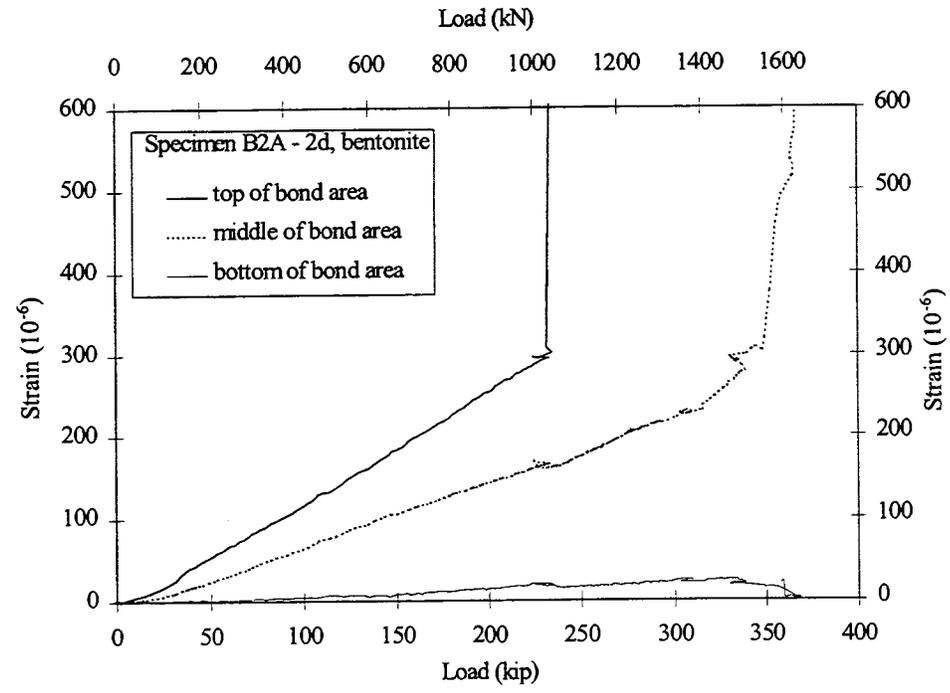
Figure 5.12 Change in strain with respect to load for Specimen B2A (bentonite, 2d embedment).

5.3   Steel Specimens

5.3.1 Control Condition

Table 5.5 presents the test results for the steel control specimens. Additionally, Figs 5.13 and 5.14 graphically depict the experimental results. Fig 5.13 shows the maximum pull-out force for each specimen. Fig. 5.14 is a graphical presentation of the average stress along the bond interface. This was calculated by dividing the maximum pull-out force by the bonded surface area.

The maximum load varied between 139-267 kips and the corresponding bond stresses ranged between 143-233 psi. These are substantially lower than the values obtained for the concrete specimens. As in the pilot study, average bond stresses decreased with increasing embedment indicating that the distribution was non-linear. Unfortunately, it was not possible to instrument any of the specimens as embedded gages could not be used for the steel specimens.

Table 5.5 Summary for Control Steel Specimens.

Specimen	f'c (psi)	Bond Length	Bond Area (in²)	Max Load (kip)	Bond Stress (psi)
SC0.5	4590	0.5d	597	139.1	233
SC1.0A	4590	1d	1193	229.2	192
SC1.0B	4590	1d	1193	247.6	208
SC1.5A	4590	1.5d	1790	256.5	143
SC1.5B	4590	1.5d	1790	267.3	149
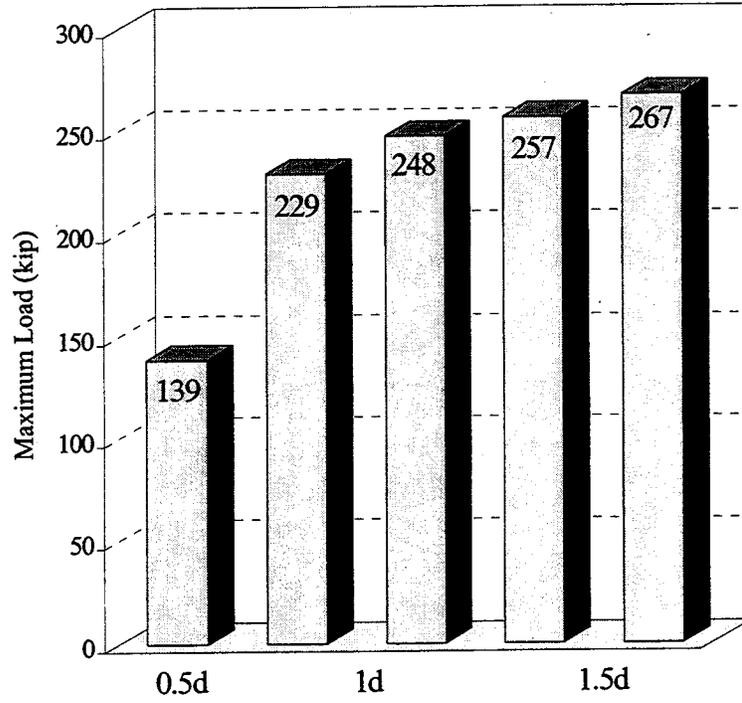
Figure 5.13 Force Summary For Control Steel Specimens.
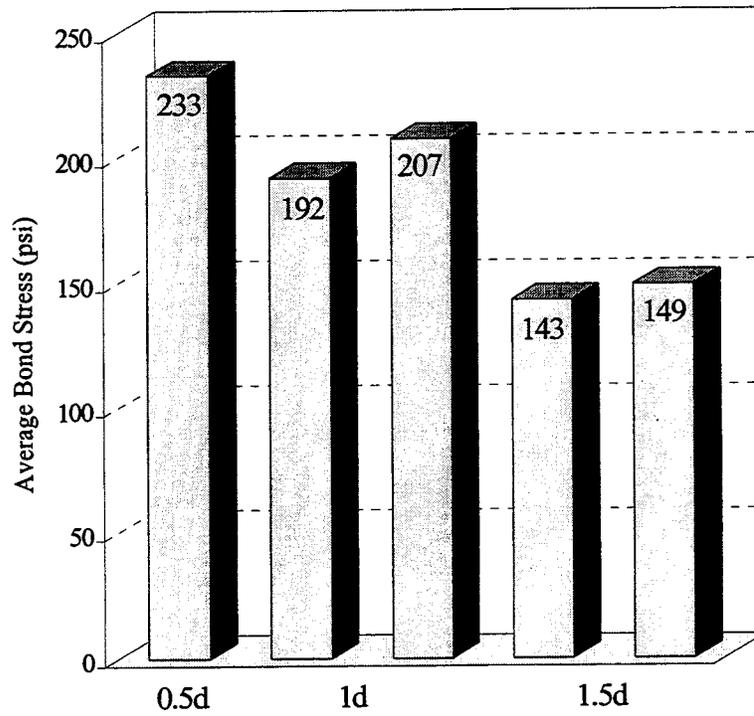
Figure 5.14 Average Bond Stress For Control Steel Specimens.

5.3.2 Fresh Water Condition

Table 5.6 presents the test results for the steel fresh water specimens. Additionally, Figs 5.15 and 5.16 graphically depict the experimental results. Fig. 5.15 shows the maximum pull-out force for each specimen. Fig. 5.16 is a graphical presentation of the average stress along the bond interface. This was calculated by dividing the maximum pull-out force by the bonded surface area.

Inspection of Table 5.6 shows that the maximum pullout load varied between 98-296 kips with the corresponding computed average bond stress varying between 153-187 psi. These stresses vary between 62-93% of the controls. The bond stresses increased from 0.5d to d but decreased for the 1.5d case. This suggests that the effective depth is less than 1.5d. This was observed in the instrumented concrete piles.

Table 5.6 Summary for Fresh Water Steel Specimens.

Specimen	f'c (psi)	Bond Length	Bond Area (in²)	Max Load (kip)	Bond Stress (psi)	Average (psi)	Percent of Control
SW0.5	3940	0.5d	597	98.5	165	165	71
SW1.0A	3940	1.0d	1193	226.2	190	187	93
SW1.0B	3940	1.0d	1193	219.5	184		
SW1.5A	3940	1.5d	1790	296.3	166	153	62
SW1.5B	3940	1.5d	1790	251.2	140		
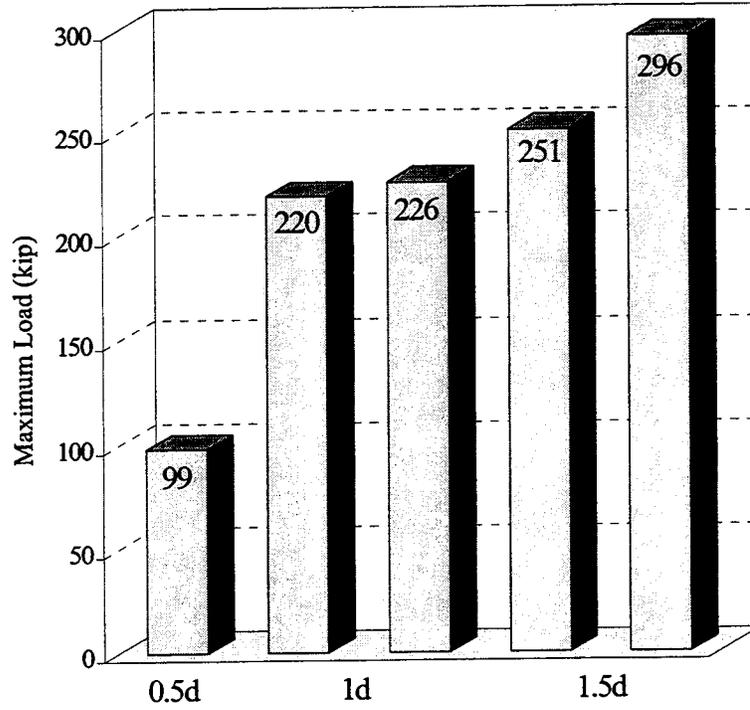
Figure 5.15 Force Summary For Fresh Water Steel Specimens.
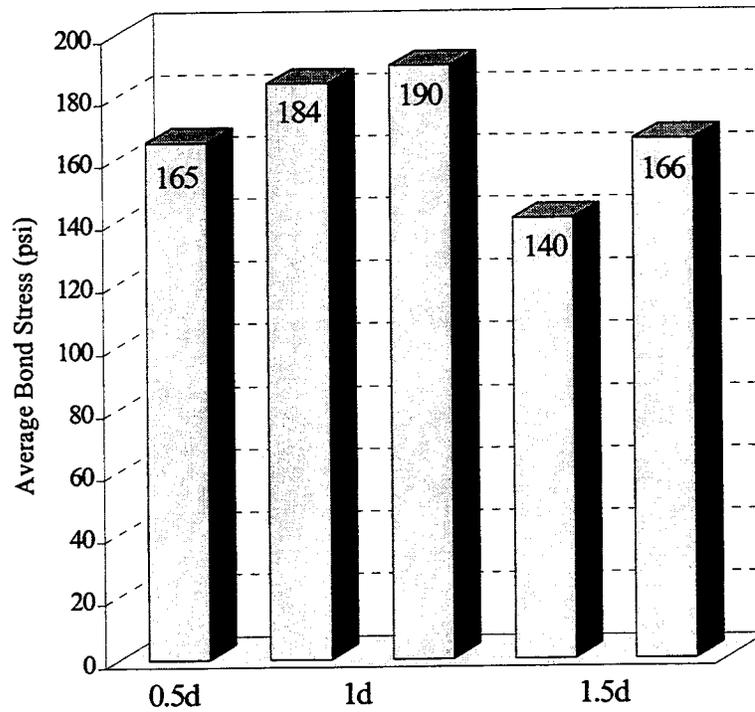
Figure 5.16 Average Bond Stress For Fresh Water Steel Specimens.

5.3.3 Bentonite Slurry Condition

Table 5.7 presents the test results for the steel bentonite slurry specimens. Additionally, Figs 5.17 and 5.18 graphically depict the experimental results. Fig. 5.17 shows the maximum pull-out force for each specimen. Fig. 5.18 is a graphical presentation of the average stress along the bond interface. This was calculated by dividing the maximum pull-out force by the bonded surface area. The maximum pullout load varied between 104-196 kips. The corresponding average bond stresses ranged between 72-126 psi.

While there is still some apparent experimental scatter, the trend of decreasing average bond stress with increasing embedment is continued. The magnitude of the bond capacity for the bentonite specimens is significantly lower than the controls (63% of the controls at 1d).

Table 5.7 Summary for Bentonite Steel Specimens.

Specimen	f'c (psi)	Bond Length	Bond Area (in²)	Max Load (kip)	Bond Stress (psi)	Average (psi)	Percent of Control
SB1B	3360	1d	1193	196.7	165	126	63
SB1D	3360	1d	1193	104.9	88		
SB2A	3360	2d	2387	186.1	78	75	-
SB2B	3360	2d	2387	172.5	72		
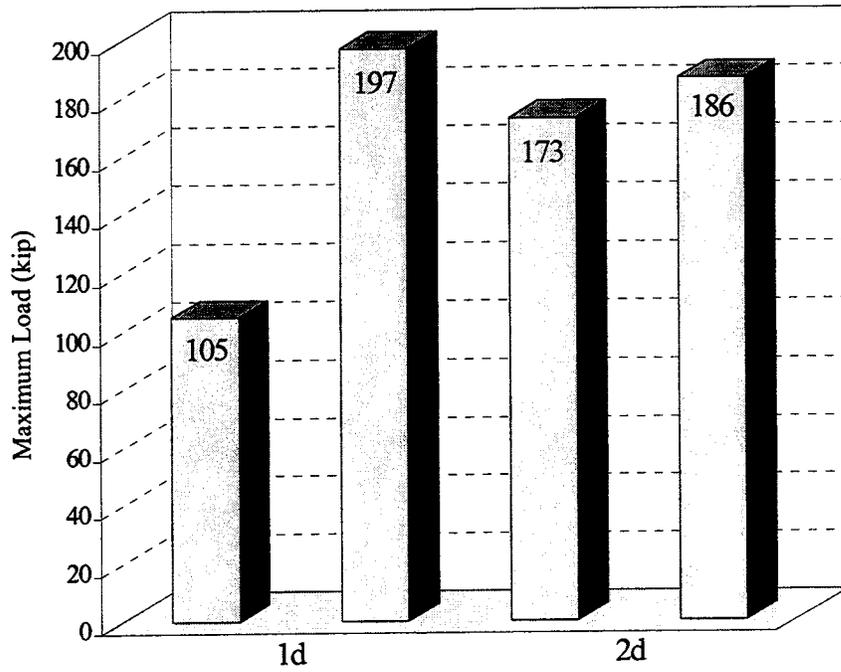
Figure 5.17 Force Summary For Steel Bentonite Specimens.
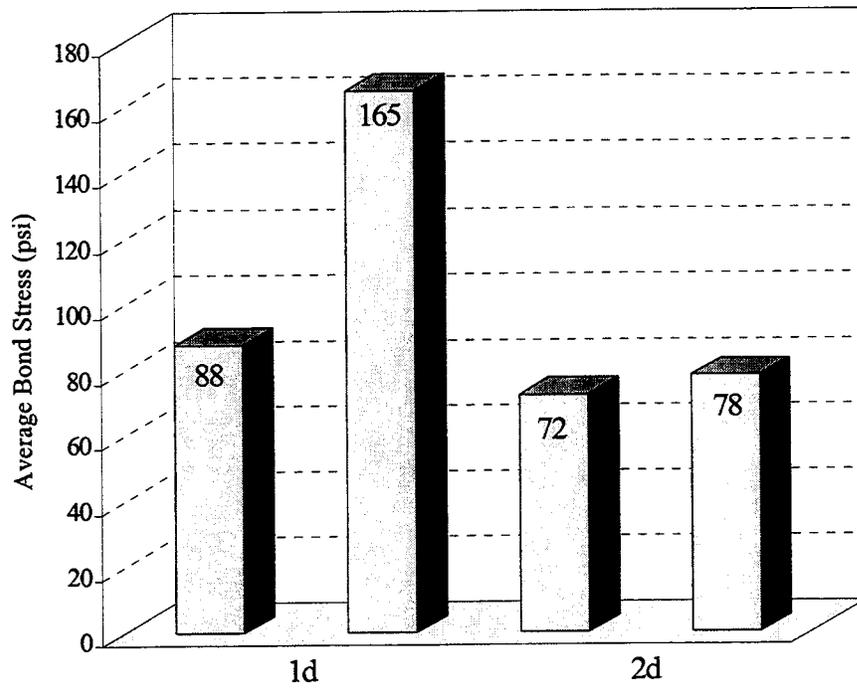
Figure 5.18 Average Bond Stress For Bentonite Steel Specimens.

101

5.3.4 Soil-Caked Condition

Table 5.8 presents the test results for the steel soil-caked specimens. Additionally, Figs 5.19 and 5.20 graphically depict the experimental results. Fig. 5.19 shows the maximum pullout force for each specimen. Fig. 5.20 is a graphical presentation of the average stress along the bond interface. This was calculated by dividing the maximum pullout force by the bonded surface area. The maximum pullout load varied between 141-169 kips and the corresponding bond stress between 119-142 psi.

As in the laboratory-scale study, the soil-caked condition has a significant negative impact on bond (26% and 71% of the controls at 1d). The results of the full-scale investigation confirm that bonding under soil-caked conditions is undesirable in actual construction conditions due to the unreliability of the capacity.

Table 5.8 Summary for Soil-Caked Steel Specimens.

Specimen	Pour Condition	f'c (psi)	Bond Length	Bond Area (in²)	Max Load (kip)	Average Bond Stress (psi)	Percent of Control
SB1A	bentonite	3360	1d	1194	141.6	119	26
SB1C	bentonite	3360	1d	1194	169.4	142	71
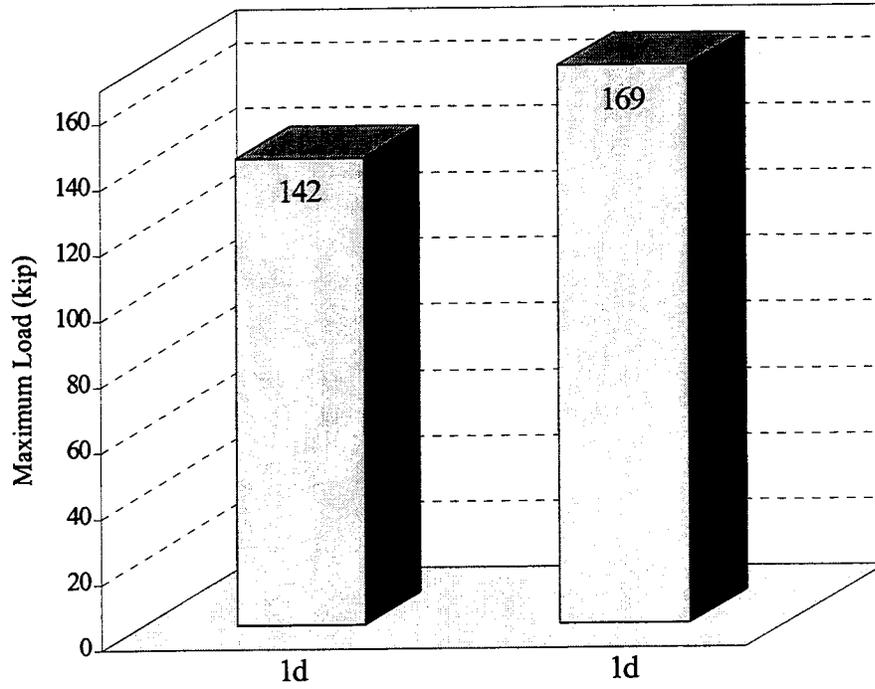
Figure 5.19 Force Summary For Steel Soil-Caked Specimens.
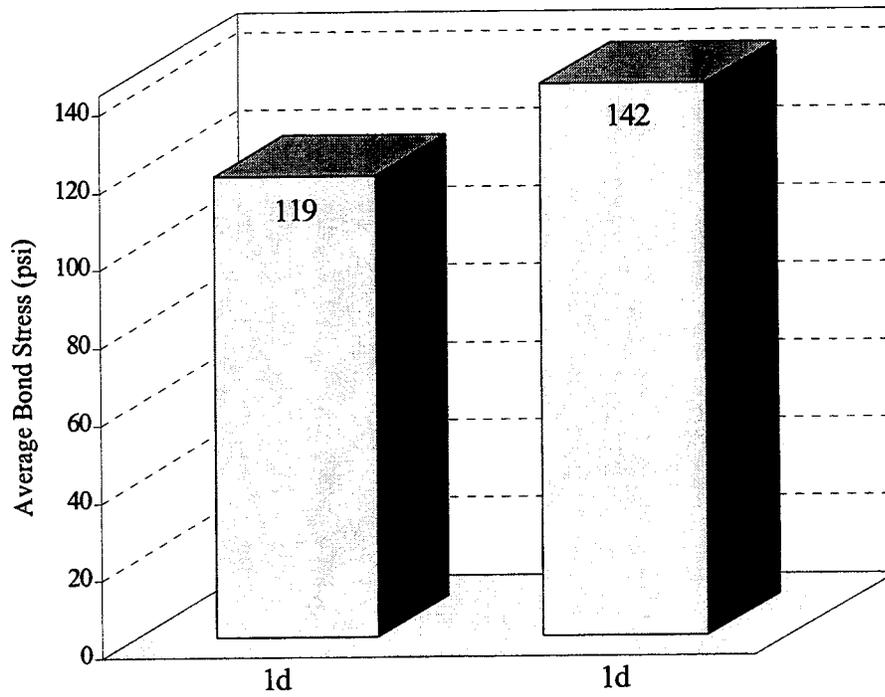
Figure 5.20 Average Bond Stress For Soil-Caked Steel Specimens.

5.4 Conclusions

The results from the full-scale tests provided information that confirmed several of the findings from the pilot study. The following conclusions may be drawn:

(1) Measurement of shear strain indicated that only a depth d was effective. (See Figs 5.9-5.12). The strain gage at depth 2d did not record any strains.

(2) Prestressed concrete piles cracked before the full pullout load was reached (see Fig. 5.21-5.22).

(3) The seal slab also cracked before the full pullout load was developed (see Fig. 5.22-5.23). Thus, structural failure of the seal slab and/or the piles themselves should be considered in any rational design process.

(4) Average bond stress for concrete interfaces were higher than those for steel for the same embedment depth.
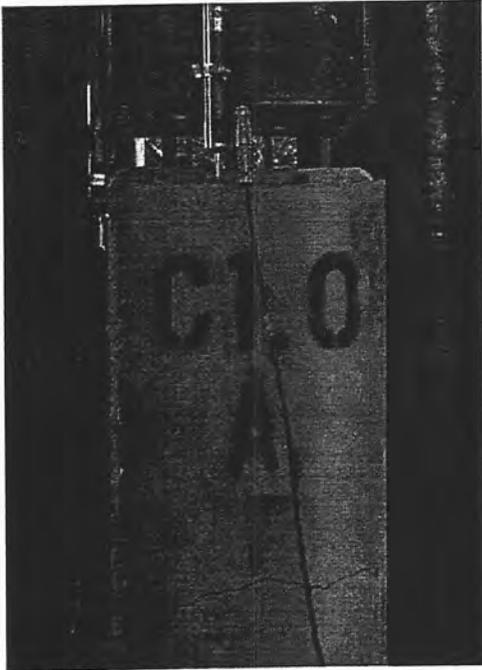
Figure 5.21 Cracking of concrete specimen during pullout testing.
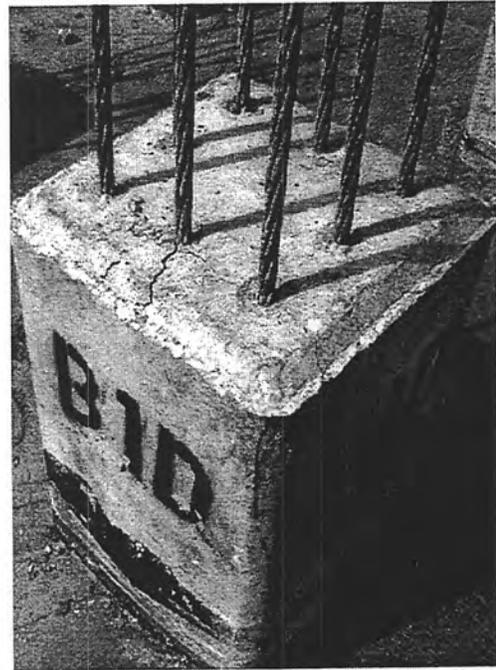
Figure 5.22 Radial cracks in a concrete specimen after testing.

Figure 5.23 Cracks at top of CIP slab extending radially from pile specimen.

Figure 5.24 Vertical crack at edge of CIP seal slab.

105

CHAPTER 6

ANALYSIS OF RESULTS

6.1   Introduction

This chapter provides a detailed analysis of the experimental results that form the basis of the proposed recommendations for interface seal/slab bond for the prestressed and steel piles presented in the next chapter.

6.2   Concrete Piles

The experimental results from both the pilot and full-scale studies are summarized in Table 6.1 and presented graphically in Fig. 6.1.

6.2.1   Effective Embedment Length

Four of the sixteen prestressed piles tested were fabricated with embedded gages to determine the variation of strain with embedment depth. The results plotted in Figs. 5.9-5.12 show that the strain variation is not uniform. At relatively small loads, only gages at the top

Table 6.1 Result Summary for Prestressed Piles.

Condition	Bond Length	Scale	Bond Stress (psi)		
			Lowest	Highest	Average
Control	0.5d	Pilot	No Data		
		Full	658	658	658
	1d	Pilot	544	568	556
		Full	451	468	460
	1.5d	Pilot	609	628	618
		Full	302	381	341
	2d	Pilot	479	480	479
		Full	No Data		
Fresh Water	0.5d	Pilot			
		Full	512	512	512
	1d	Pilot	536	622	579
		Full	383	391	387
	1.5d	Pilot	572	617	595
		Full	292	302	297
	2d	Pilot	423	467	445
		Full	No Data		
Salt Water	0.5d	Pilot	No Data		
		Full			
	1d	Pilot	591	592	592
		Full	No Data		
	1.5d	Pilot	594	634	614
		Full	No Data		
	2d	Pilot	480	515	498
		Full	No Data		
Bentonite Slurry	1d	Pilot	214	224	219
		Full	362	374	368
	1.5d	Pilot	238	561	400
		Full	No Data		
	2d	Pilot	154	412	283
		Full	204	229	216

and middle of the bonded region recorded strains. At ultimate, the gages located at the bottom at 1d embedment recorded strains. However, this was not the case where the strain gage was located at 2d depth. In this case, there was practically no strain recorded in the pile. Thus, the use of an effective depth equal to d (*or actual depth if it is shallower*), appears to be reasonable for design.

6.2.2 Average Stress

Fig. 6.1 plots the variation in average bond stress with embedment depth for the various surface conditions from both the pilot and full-scale studies. Inspection of Fig. 6.1 shows that excepting for bentonite, the average bond stress always exceeds 300 psi for an assumed effective embedment depth of **d** or less. Thus, the use of a constant value of 300 psi for the associated effective embedment depth is reasonable for the salt water and fresh water conditions. It is proposed that this value be used in designing the seal slab.

For bentonite, the average bond stress from the full-scale tests exceeded 300 psi but those from the pilot tests fell below 300 psi. In the latter case, the measured bond stresses were approximately one-third of those for the control (see Table 3.4). In view of this, it is proposed that a value of 100 psi be used for this condition.

6.2.3 Assessment

Tables 6.2-6.3 evaluate the proposed values by applying them to the experimental conditions from both the pilot and full-scale tests. Only the cases where fresh water, salt
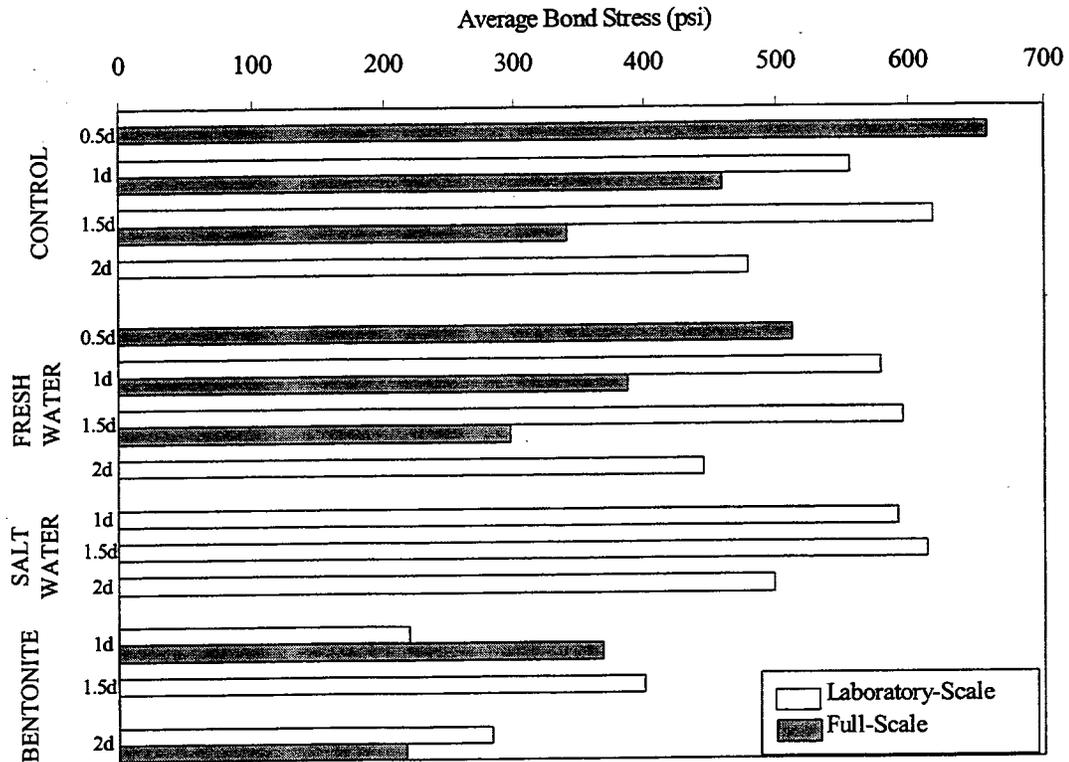
Figure 6.1 Result Summary For Prestressed Piles.

water or bentonite slurry are used are considered. The tables provide information on the mean safety factors for different embedment depths and for all the results.

The calculated capacities in Tables 6.2-6.3 were obtained by multiplying the effective area by the assumed constant bond stress. For the 6 in. piles, the effective area is 144 in^2 (6 x 4 x 6) and the assumed stress is either 300 psi or 100 psi giving capacities of 43.2 kips or 14.4 kips (for bentonite). For the full-scale tests where the pile size was 14 in., the effective area is 784 in^2 (14 x 4 x 14) giving capacities of 235.2 kips or 78.4 kips in bentonite.

Inspection of Tables 6.2-6.3 shows that the proposed values consistently underestimate the measured capacities. The predictions are more conservative, the greater

Table 6.2 Experimental vs Proposed - Pilot Study.

Specimen	Depth	Condition	f'c	Experimental (kips)	Calculated (kips)	Exp/Cal
C1	d	Bentonite	4270	31.7	14.4	2.2
C2	d			33.4		2.3
C3	1.5d			125.3		8.7**
C4	1.5d			53.3		3.7
C5	2d			46.2		3.2
C6	2d			122.0		8.5**
C8	d	Salt Water	4270	89.4	43.2	2.1
C9	d			85.1		2.0
C10	1.5d			141.9		3.3
C11	1.5d			132.9		3.1
C12	2d			146.3		3.4
C13	2d			154.8		3.6
C15	d	Fresh Water	4270	79.5	43.2	1.8
C16	d			93.8		2.2
C17	1.5d			139.3		3.2
C18	1.5d			128.7		3.0
C19	2d			125.9		2.9
C20	2d			139.8		3.2
Mean	d	2.1				
	1.5d	3.3				
	2d	3.3				
	All	2.85				

** Excluded from averages

110

Table 6.3 Experimental vs Proposed - Full-Scale Study.

Specimen	Depth	Condition	f'c	Experimental (kips)	Calculated (kips)	Exp/Cal
B1B	d	Bentonite	3360	300.7	78.4	3.8
B1D	d			286.5		3.6
B2A	2d			365.2		4.6
B2B	2d			323.2		4.1
B1A	d	Soil Caked		209.2		2.6
B1C	d	Bentonite		128.2		1.6
W0.5	0.5d	Fresh Water	3940	200.6	117.6	1.7
W1.0A	d			305.2	235.2	1.3
W1.0B	d			300.4		1.27
W1.5A	1.5d			357.7		1.5
W1.5B	1.5d			343.3		1.46
Mean	0.5d	1.7				
	d	2.36				
	1.5d	1.48				
	2d	4.35				
	All	2.50				

the embedment depth. The overall factor of safety was 2.85 for the pilot study and 2.5 for the full-scale tests.

6.3 Steel Piles

The experimental results from both the pilot and full-scale studies are summarized in Table 6.4 and presented graphically in Fig. 6.2. The average bond stresses for the steel piles were consistently lower than those for the prestressed piles.

Although steel piles were not instrumented to obtain strain variation, the underlying trends were similar to those for the prestressed piles, i.e. calculated average stresses reduced as the embedment depth increased. In view of this, effective depth for the steel piles will also be assumed to be d (or the actual embedment depth if it is smaller). The average bond stress is taken as 150 psi for fresh/salt water and 50 psi in bentonite.
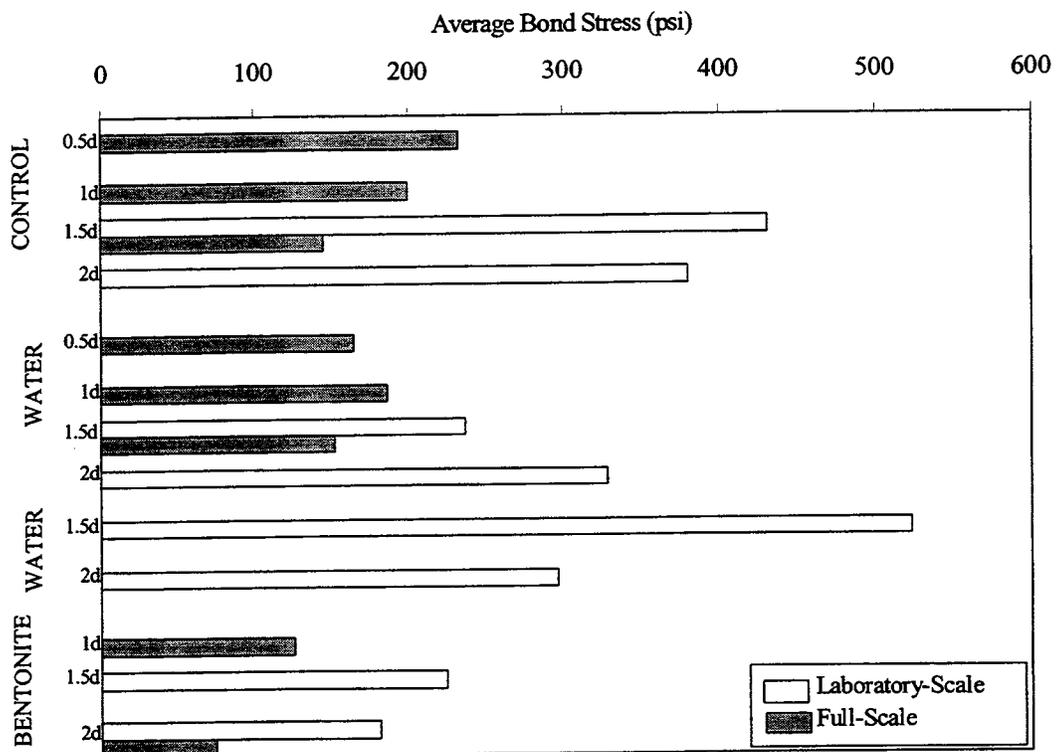
Figure 6.2 Result Summary For Steel Piles.

Table 6.4 Result Summary for Steel Piles.

Condition	Bond Length	Scale	Bond Stress (psi)		
			Lowest	Highest	Average
Control	0.5d	Pilot	No Data		
		Full	233	233	233
	1d	Pilot	No Data		
		Full	192	208	200
	1.5d	Pilot	431	431	431
		Full	143	149	146
	2d	Pilot	380	380	380
		Full	No Data		
Fresh Water	0.5d	Pilot			
		Full	165	165	165
	1d	Pilot	No Data		
		Full	184	190	187
	1.5d	Pilot	237	237	237
		Full	140	166	153
	2d	Pilot	328	328	328
		Full			
Salt Water	0.5d	Pilot	No Data		
		Full			
	1d	Pilot			
		Full			
	1.5d	Pilot	524	524	524
		Full	No Data		
	2d	Pilot	297	297	297
		Full	No Data		
Bentonite Slurry	1d	Pilot			
		Full	88	165	126
	1.5d	Pilot	225	225	225
		Full	No Data		
	2d	Pilot	182	182	182
		Full	72	78	75

113

6.3.1 Assessment

Tables 6.5-6.6 evaluate the application of the proposed values by applying them to the experimental conditions obtained for both the pilot and full-scale tests. Only the water or bentonite slurry conditions are used. The tables also provide mean values. Standard deviations are omitted since the samples are small.

Table 6.5 Experimental vs Proposed - Pilot Study.

Specimen	Depth	Condition	f'c	Experi-mental (kips)	Calcu-lated (kips)	Exp/Cal
H11	1.5d	Bentonite	4460	71.9	10.6	6.8
H12	2d			·77.3		7.3
H21	1.5d	Salt Water	4460	167.4	31.8	5.3
H22	2d			126.6		4.0
H31	1.5d	Fresh Water	4460	75.6	31.8	2.4
H32	2d			139.6		4.4
Mean	1.5d	4.8				
	2d	5.2				
	All	5.0				

The calculated capacities in Table 6.5-6.6 were obtained as the product of the nominal interface areas times the assumed constant bond stress of 150 psi (or 50 psi for bentonite). The effective area is 212 in² for the pilot study (half value for 2d in Table 3.6) and 1190 in² for the full-scale study (from Table 5.5). This gives capacities of 31.8 kips and 178.5 kips for the pilot and full-scale studies respectively. In bentonite, these values are reduced by a factor of 3.

Table 6.6 Experimental vs Proposed - Full-Scale Study.

Specimen	Depth	Condition	f'c	Experimental (kips)	Calculated (kips)	Exp/Cal
SB1B	d	Bentonite	3360	196.7	59.5	3.3
SB1D	d			104.9		1.7
SB2A	2d			186.1		3.1
SB2B	2d			172.5		2.9
SB1A	d	Soil Caked Bentonite		141.6		2.4
SB1C	d			169.4		2.8
SW0.5	0.5d	Fresh Water	3940	98.5	89.3	1.1
SW1.0A	d			226.2	178.5	1.27
SW1.0B	d			219.5		1.23
SW1.5A	1.5d			296.3		1.66
SW1.5B	1.5d			251.2		1.41
Mean	0.5d	1.1				
	d	2.12				
	1.5d	1.54				
	2d	3.0				
	All	2.08				

Inspection of Tables 6.5-6.6 show that the assumed effective area and average bond stress consistently underestimate the measured capacities. As for concrete, the predictions are more conservative, the greater the embedment depth. The overall factor of safety is 5 for the pilot study and 2.08 for the full-scale study.

CHAPTER 7

CONCLUSIONS AND RECOMMENDATIONS

Based on the experimental results obtained and the analysis of data presented in the previous chapter, the following recommendations are made:

1. Uplift forces supported by piles (*depth* d, *perimeter* p, *embedded depth* D *in seal slab*) may be determined from the allowable bond stress, F_b, listed in Table 7.1. This stress may be assumed to be uniform over an effective area A_e given by:

$$A_e = pD \qquad \text{if } D < d$$
$$A_e = pd \qquad \text{if } D > d$$

Table 7.1 Allowable Bond Stress.

Pile	Condition	F_b (psi)
Concrete	Salt/Fresh Water	300
	Bentonite	100
Steel	Salt/Fresh Water	150
	Bentonite	50

2. The allowable loads obtained using values in Table 7.1 shall not exceed the cracking load of the prestressed pile in tension.

3. The thickness of the seal slab shall be checked to ensure that it does not crack in bending or shear due to uplift forces.

116

APPENDICES

Appendix I Laboratory-Scale Test Data
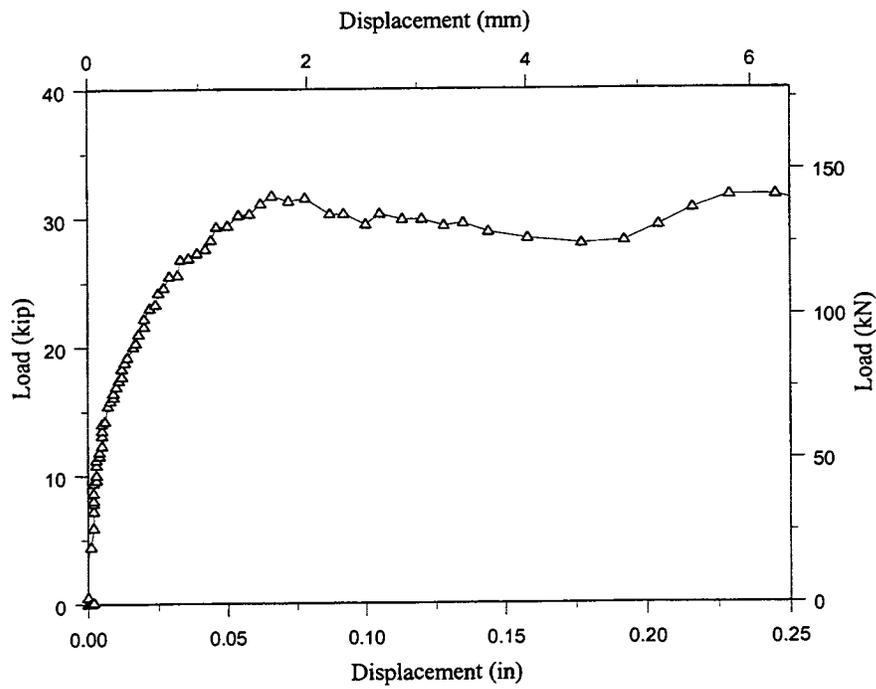
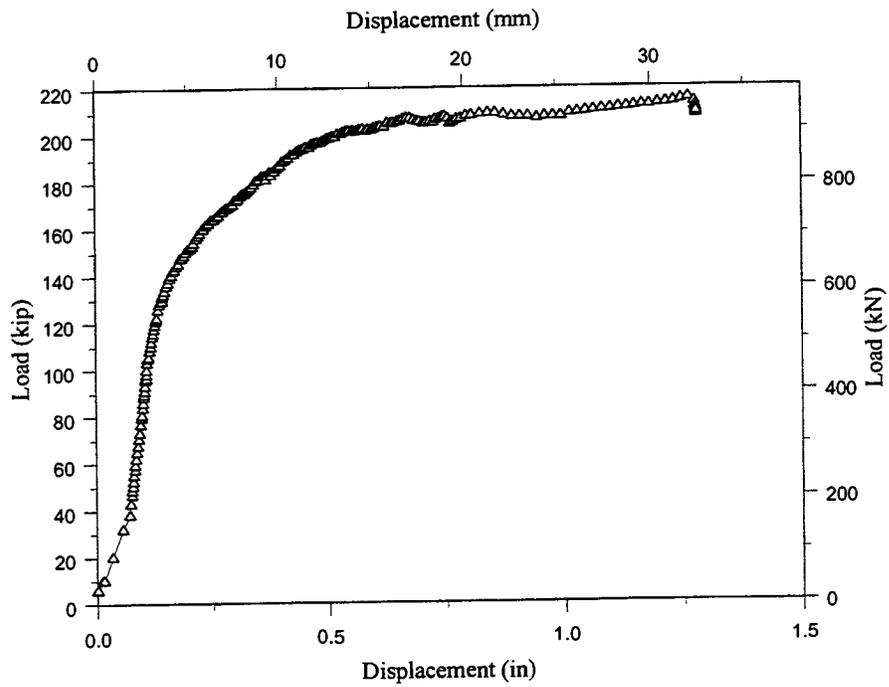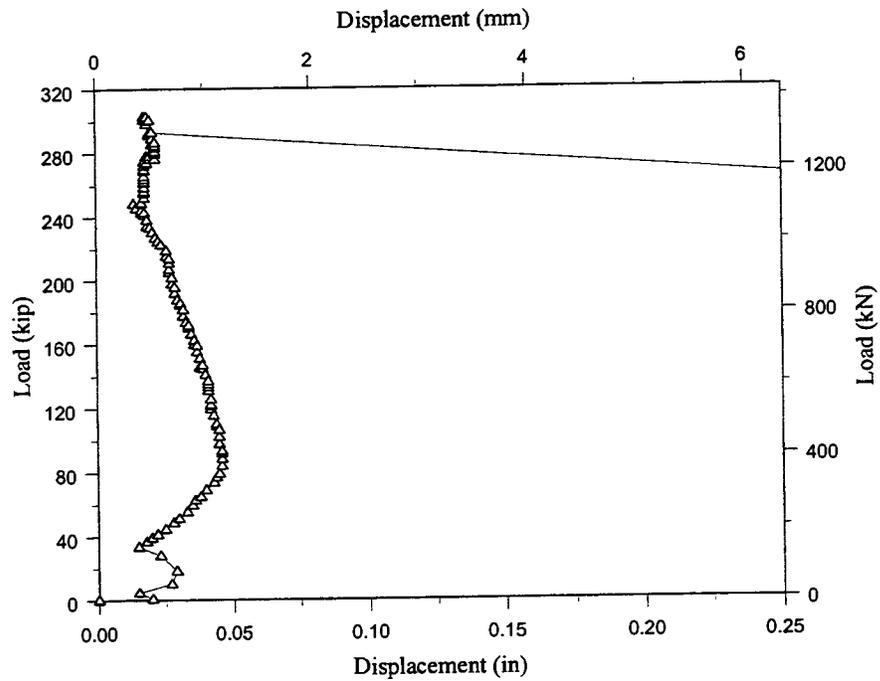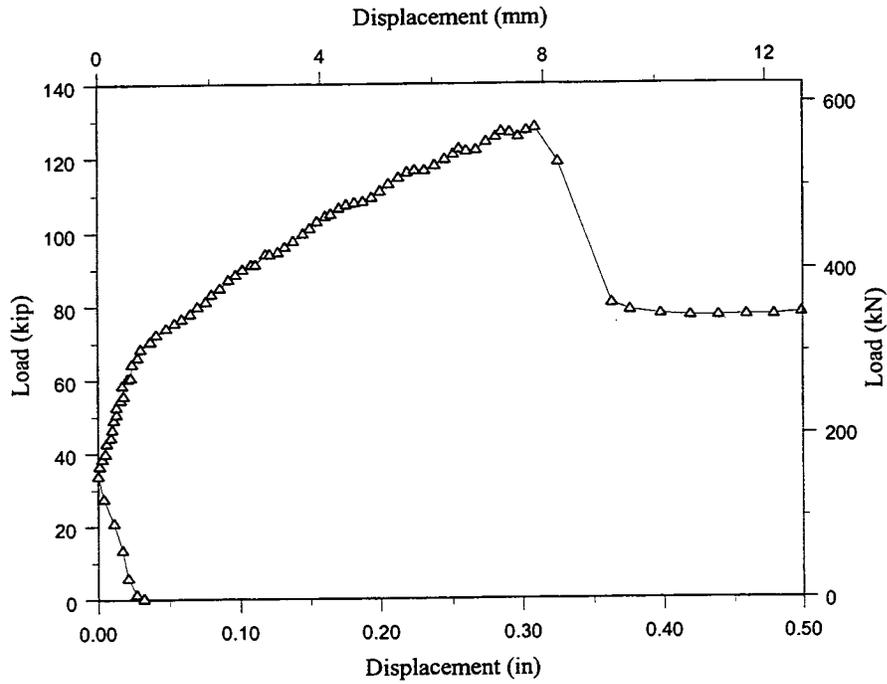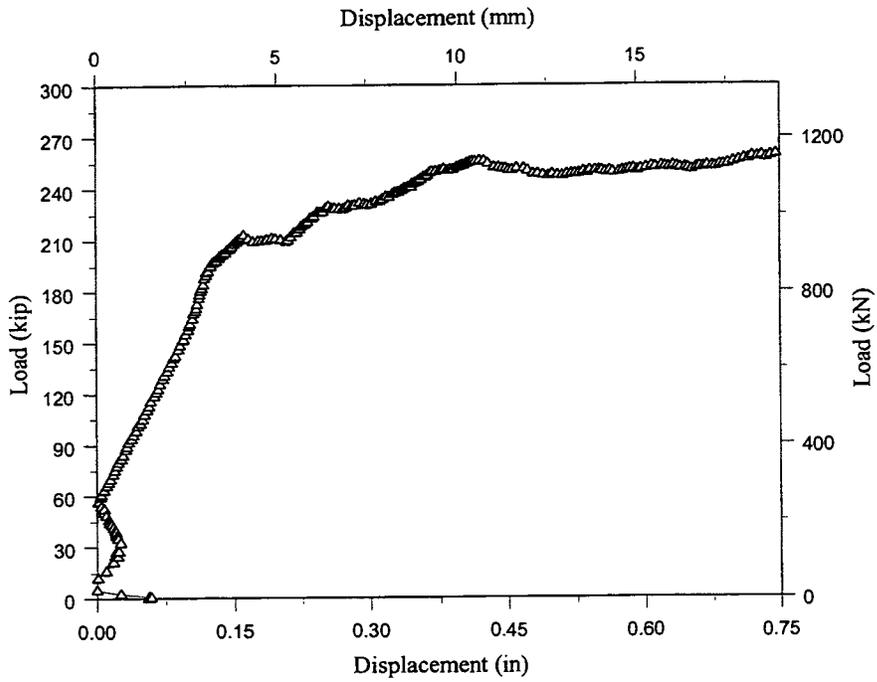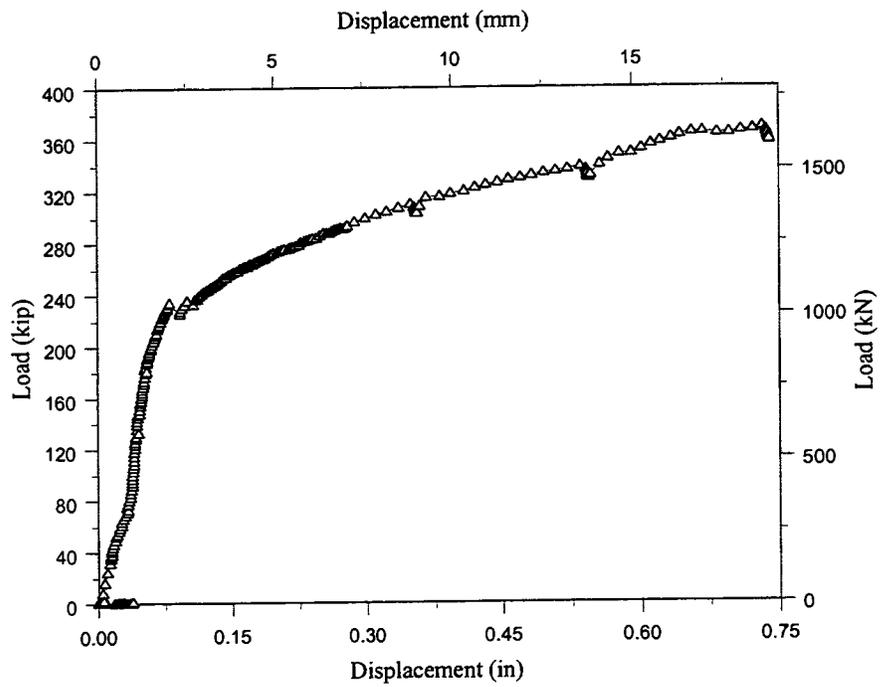Figure I-1 Load vs. displacement - specimen C1 (concrete, 1d, bentonite).
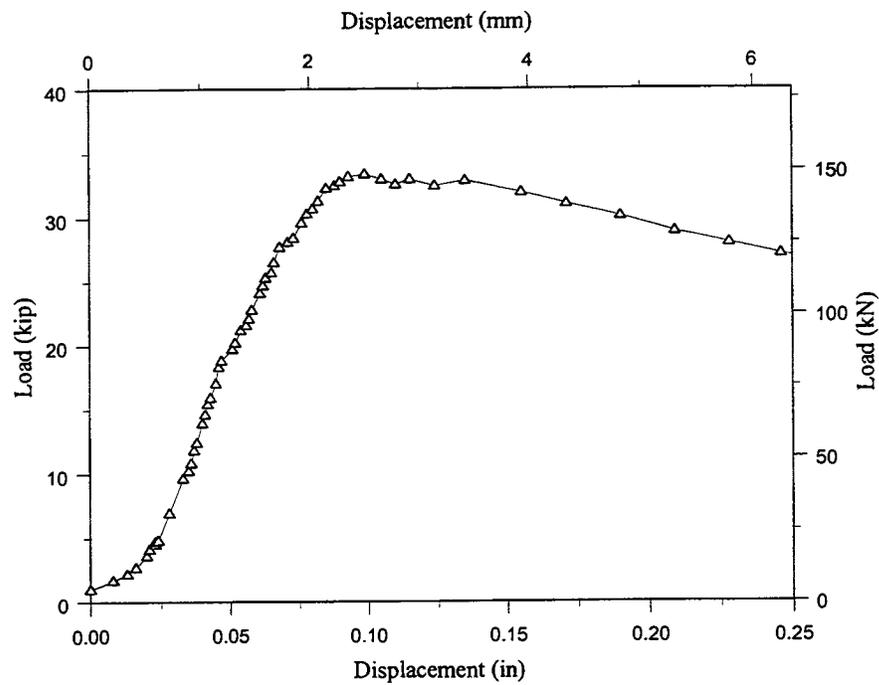
Figure I-2 Load vs. displacement - specimen C2 (concrete, 1d, bentonite).

118
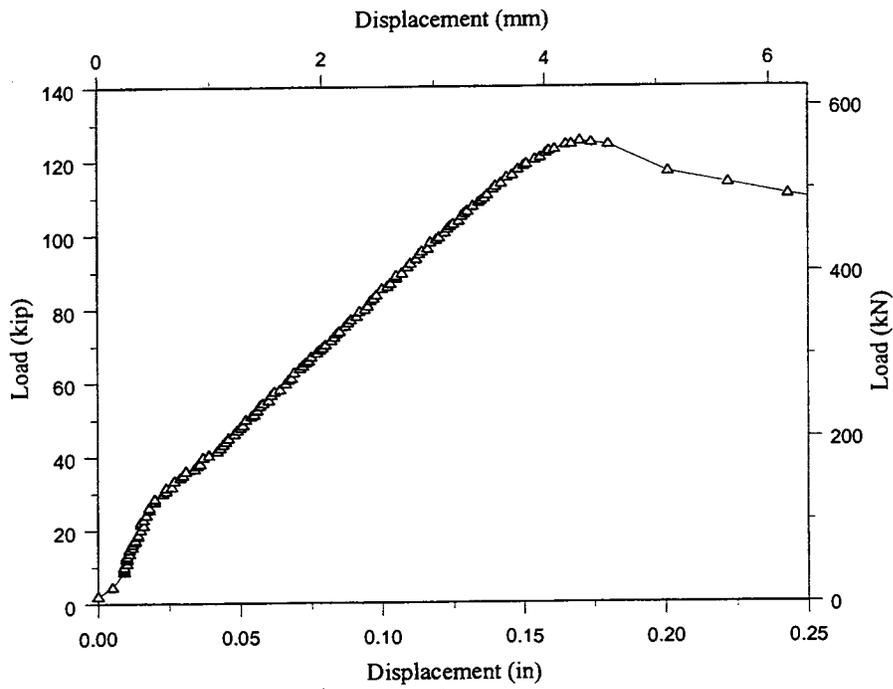
Figure I-3 Load vs. displacement - specimen C3 (concrete, 1.5d, bentonite).
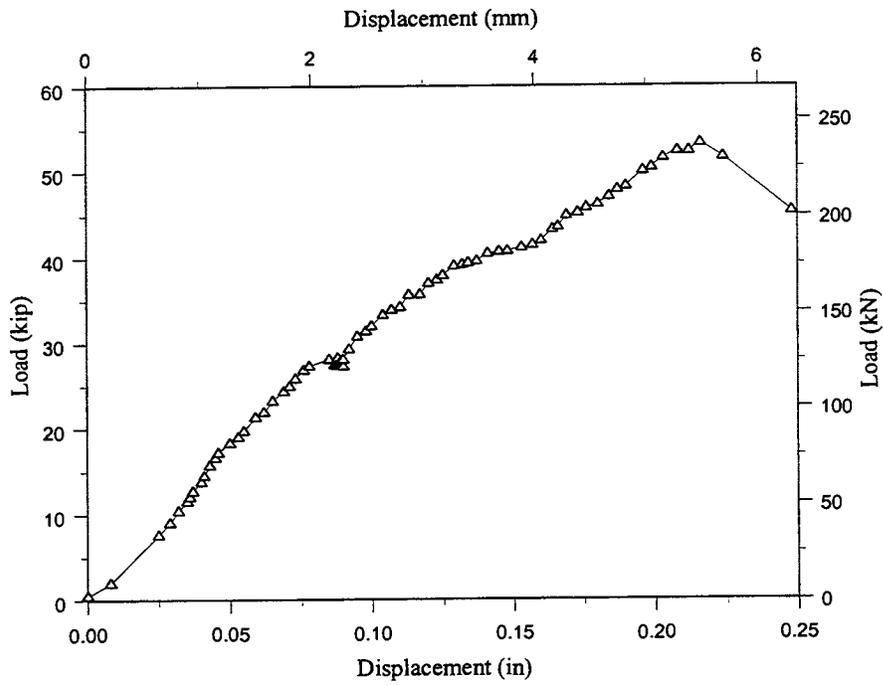
Figure I-4 Load vs. displacement - specimen C4 (concrete, 1.5d, bentonite).
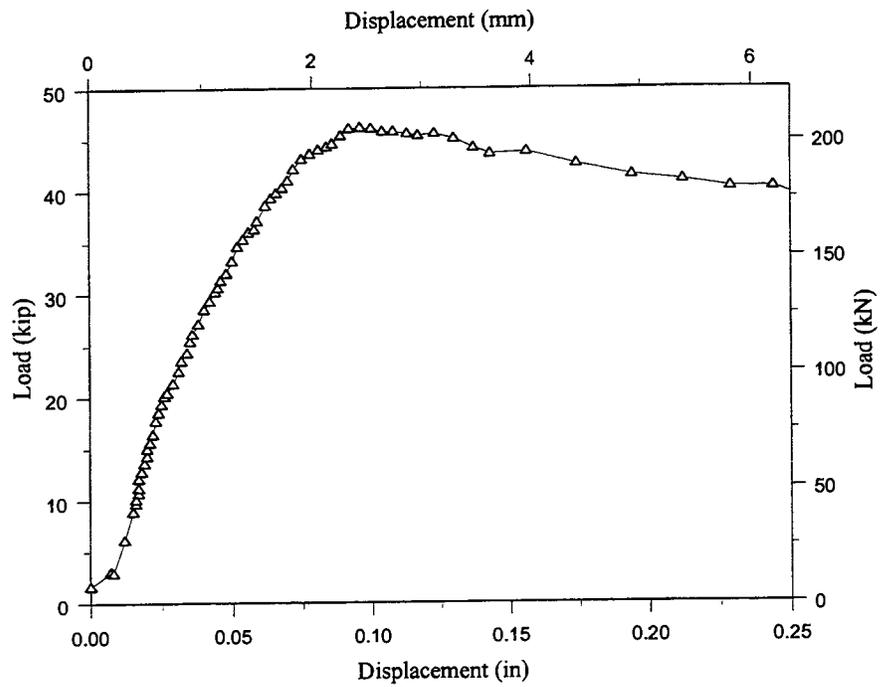
Figure I-5 Load vs. displacement - specimen C5 (concrete, 2d, bentonite).
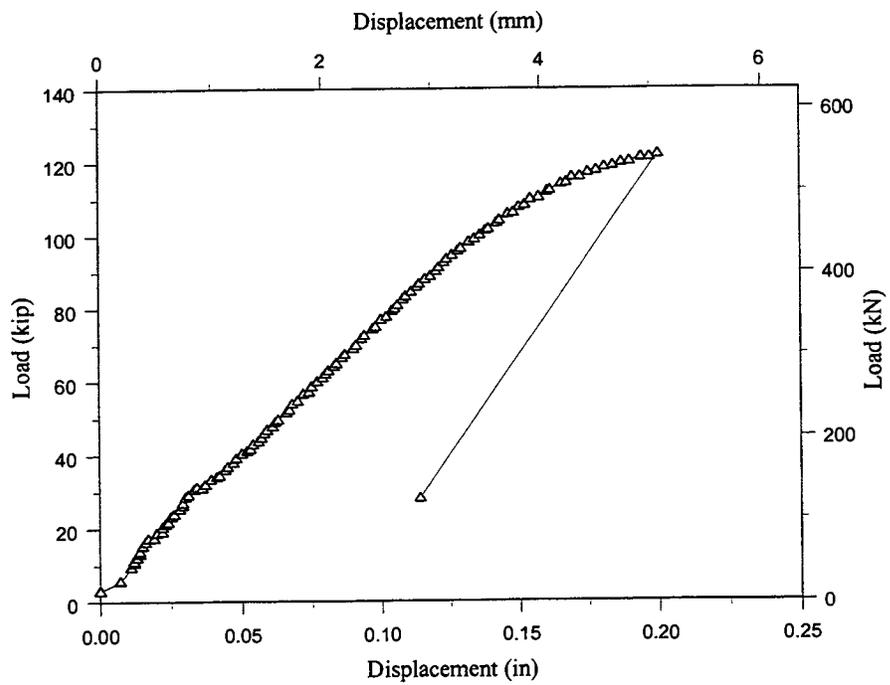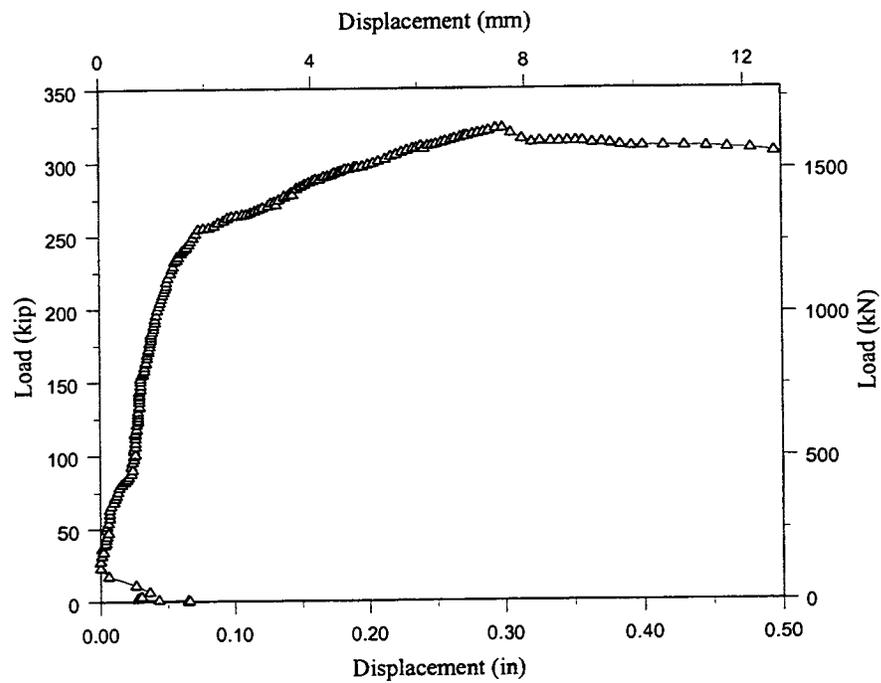

Figure I-6 Load vs. displacement - specimen C6 (concrete, 2d, bentonite).

120

Appendix I (continued)
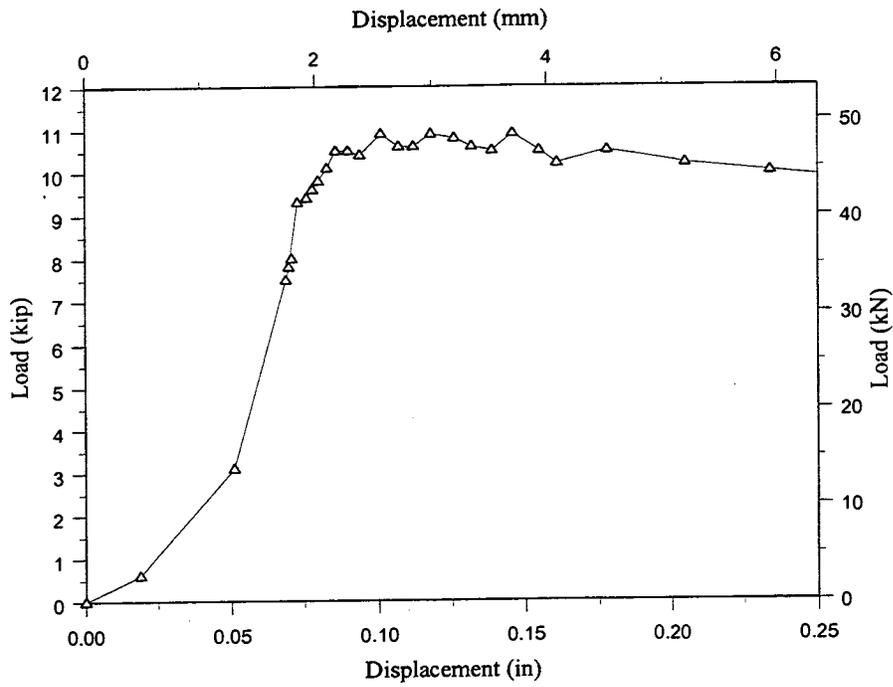
Figure I-7 Load vs. displacement - specimen C7 (concrete, 2d, bentonite, soil-caked).
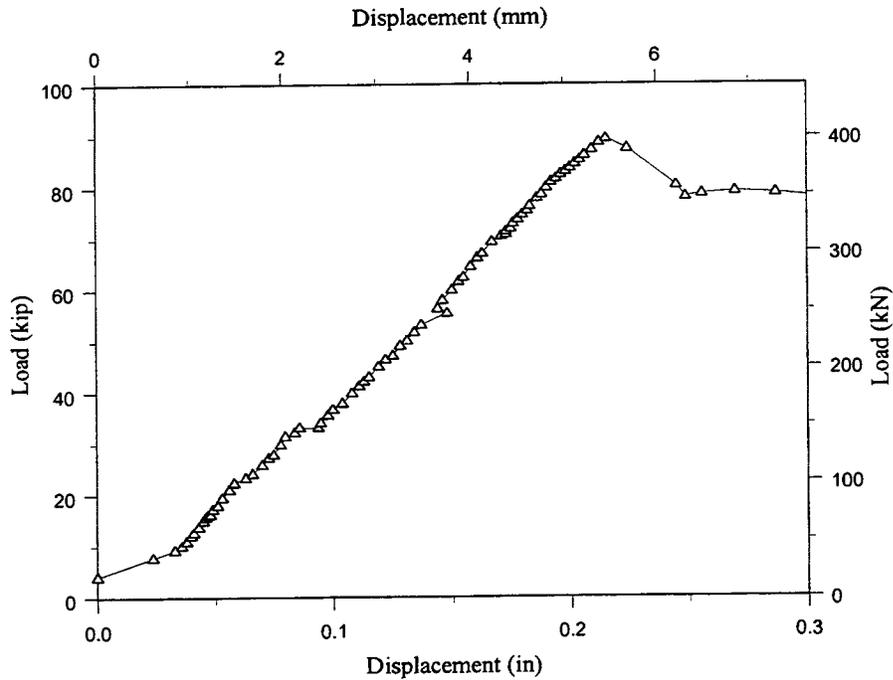
Figure I-8 Load vs. displacement - specimen C8 (concrete, 1d, salt water).

121
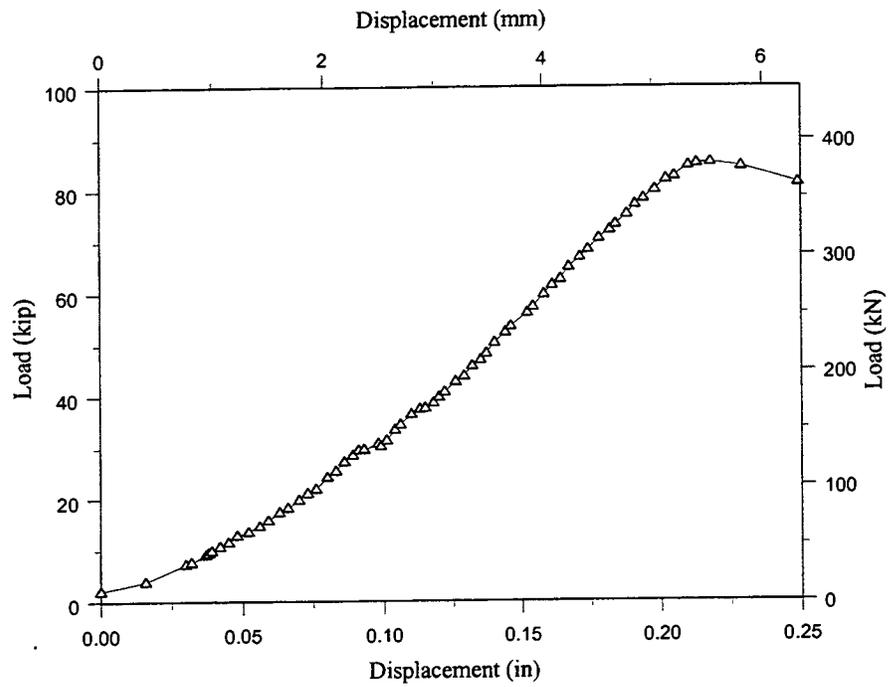
Figure I-9 Load vs. displacement - specimen C9 (concrete, 1d, salt water).
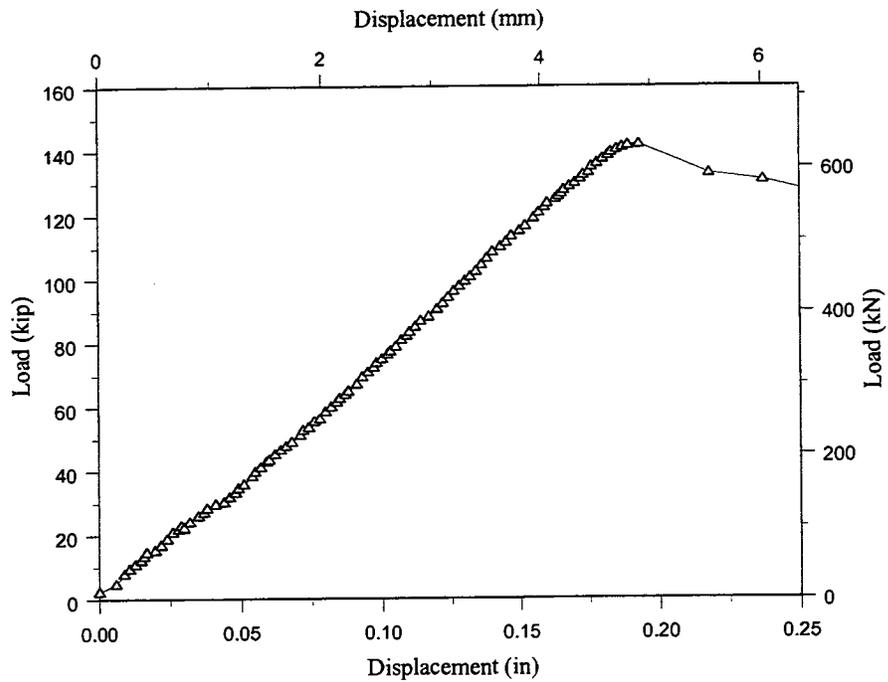
Figure I-10 Load vs. displacement - specimen C10 (concrete, 1.5d, salt water).
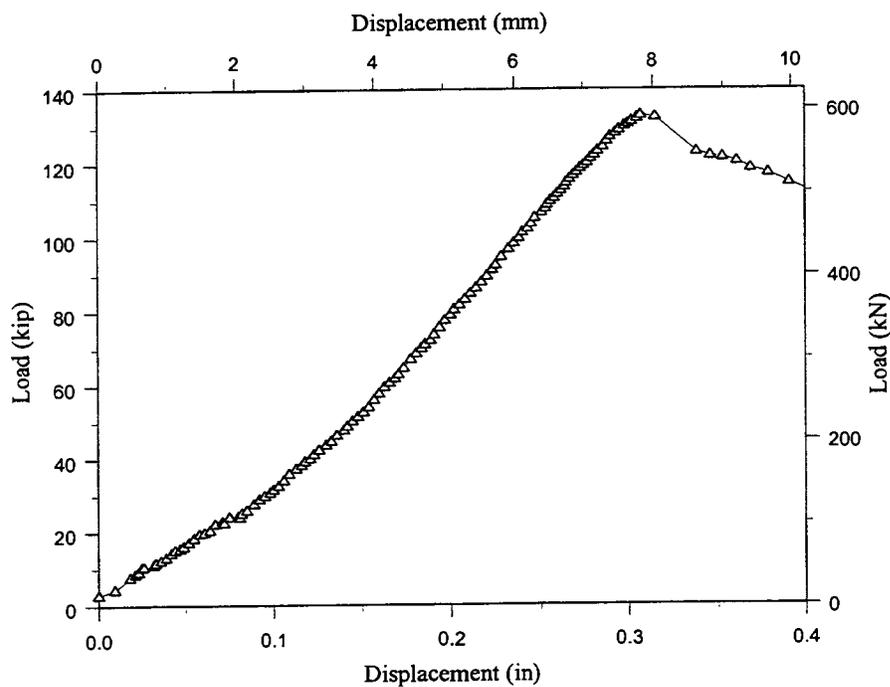
Figure I-11 Load vs. displacement - specimen C11 (concrete, 1.5d, salt water).
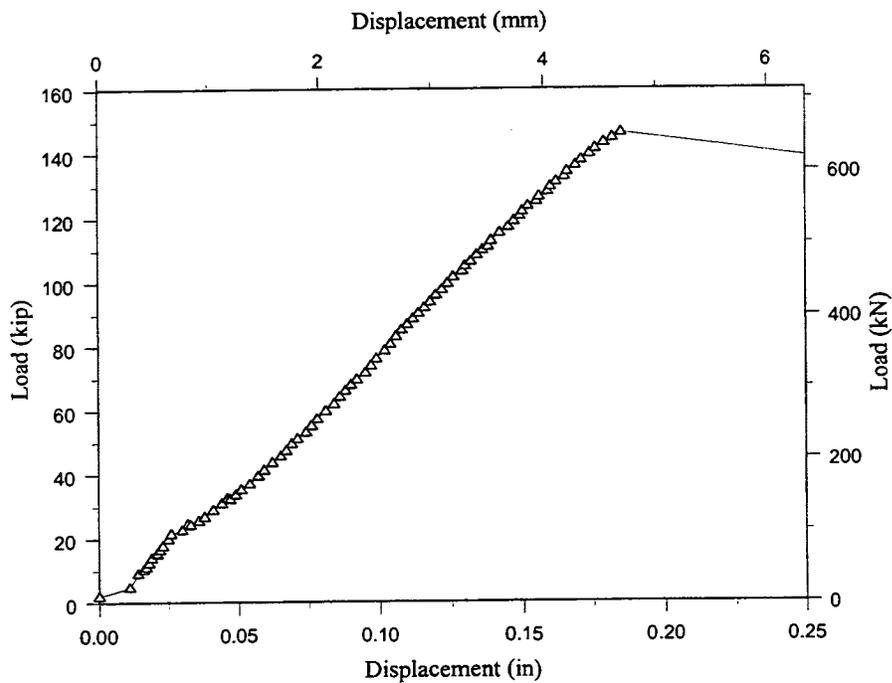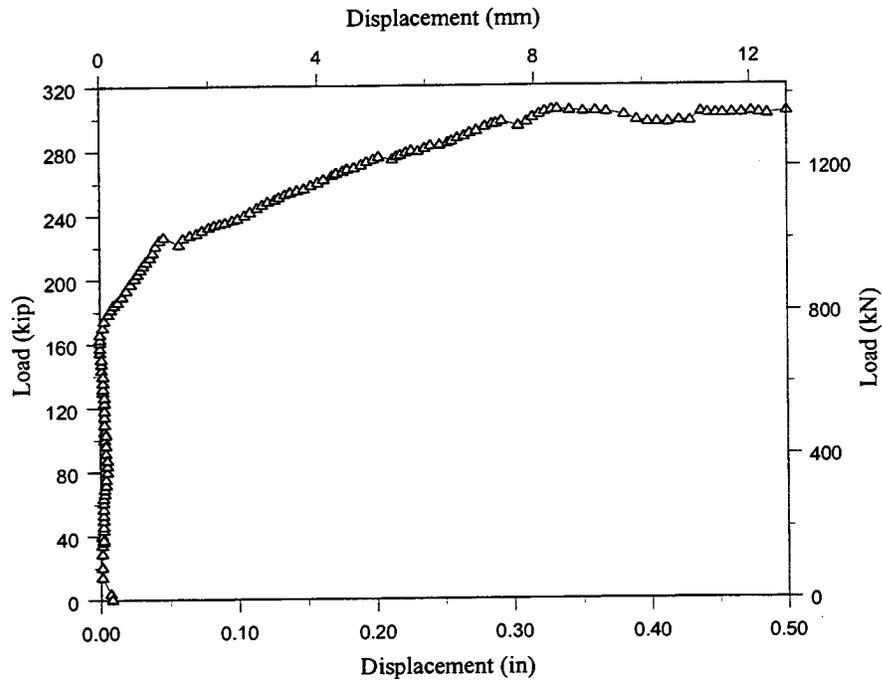

Figure I-12 Load vs. displacement - specimen C12 (concrete, 2d, salt water).

123

Appendix I (continued)
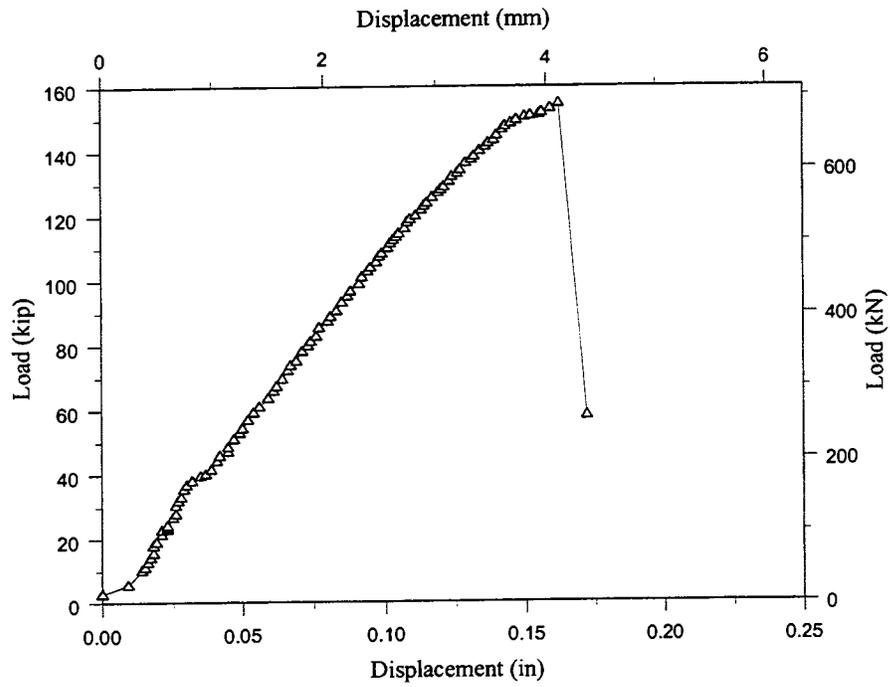
Figure I-13 Load vs. displacement - specimen C13 (concrete, 2d, salt water).
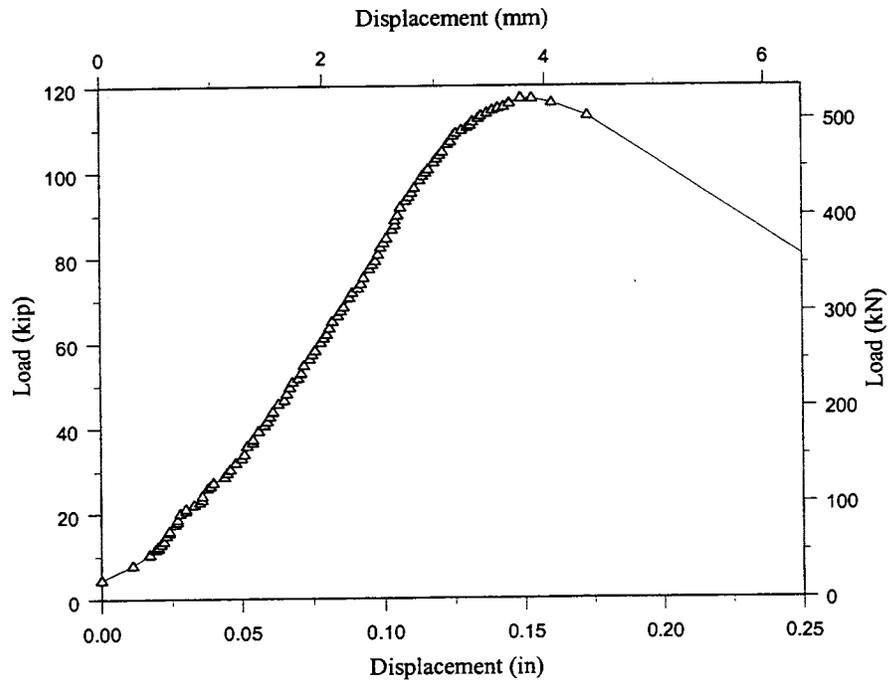
Figure I-14 Load vs. displacement - specimen C14 (concrete, 2d, salt water, soil-caked).
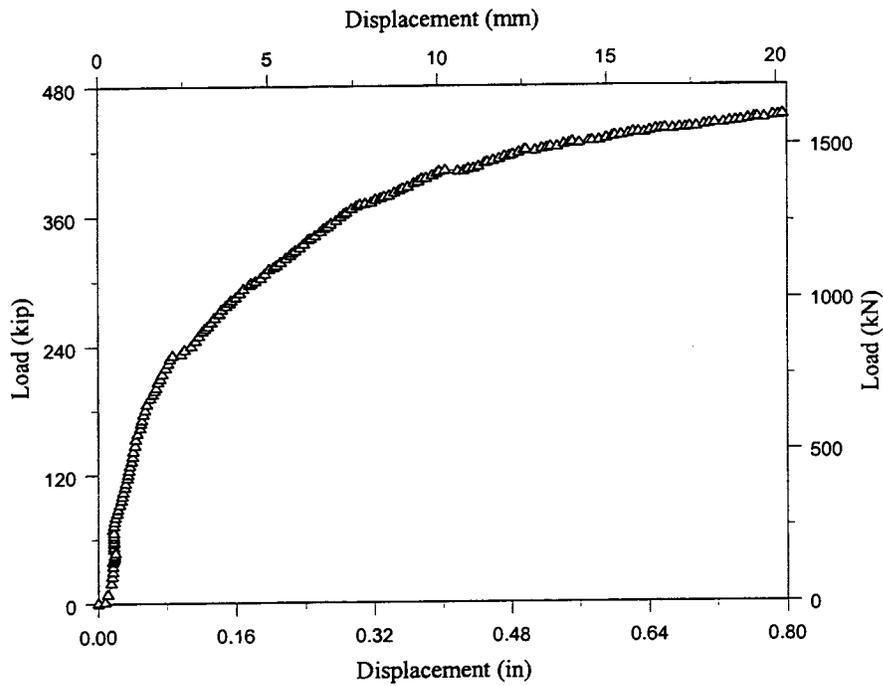
124

Appendix I (continued)
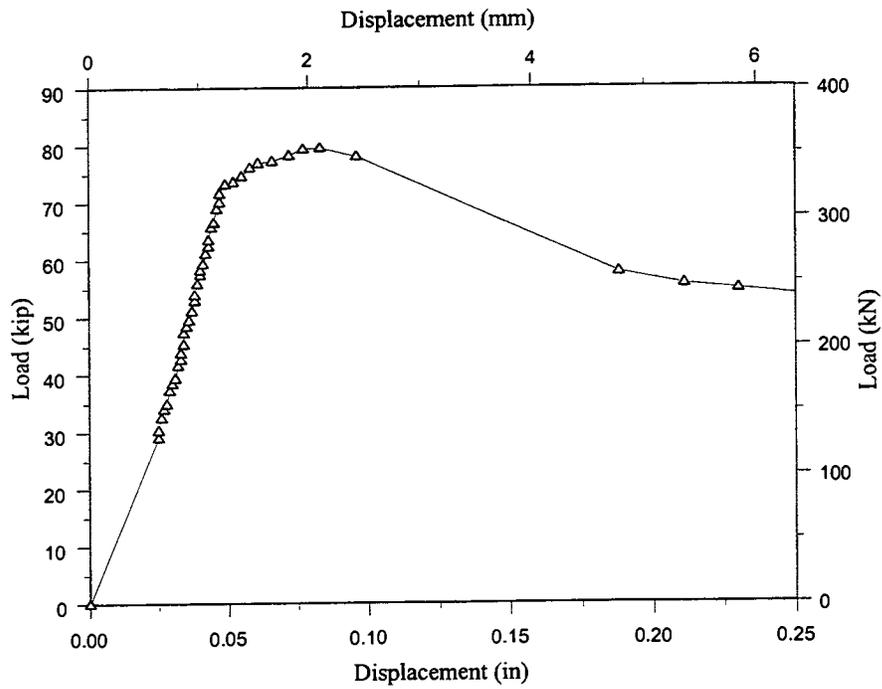
Figure I-15 Load vs. displacement - specimen C15 (concrete, 1d, fresh water).
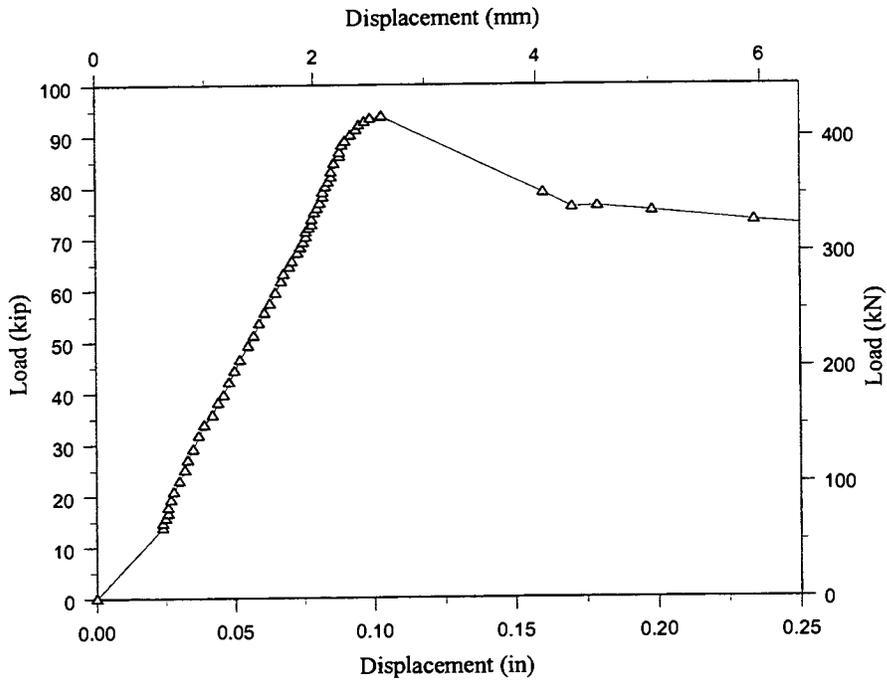
Figure I-16 Load vs. displacement - specimen C16 (concrete, 1d, fresh water).

125
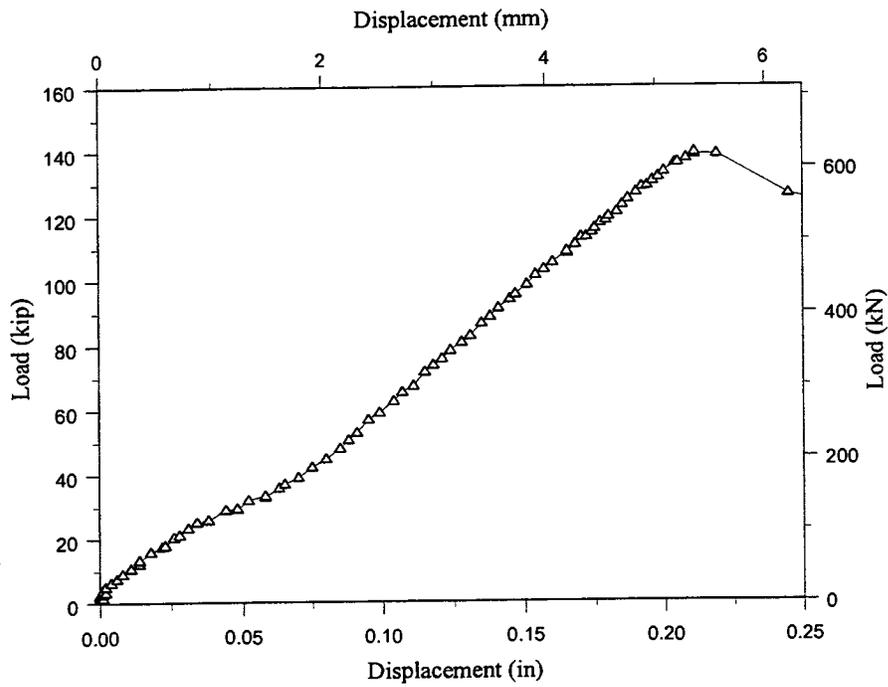
Displacement (mm)

Figure I-17 Load vs. displacement - specimen C17 (concrete, 1.5d, fresh water).
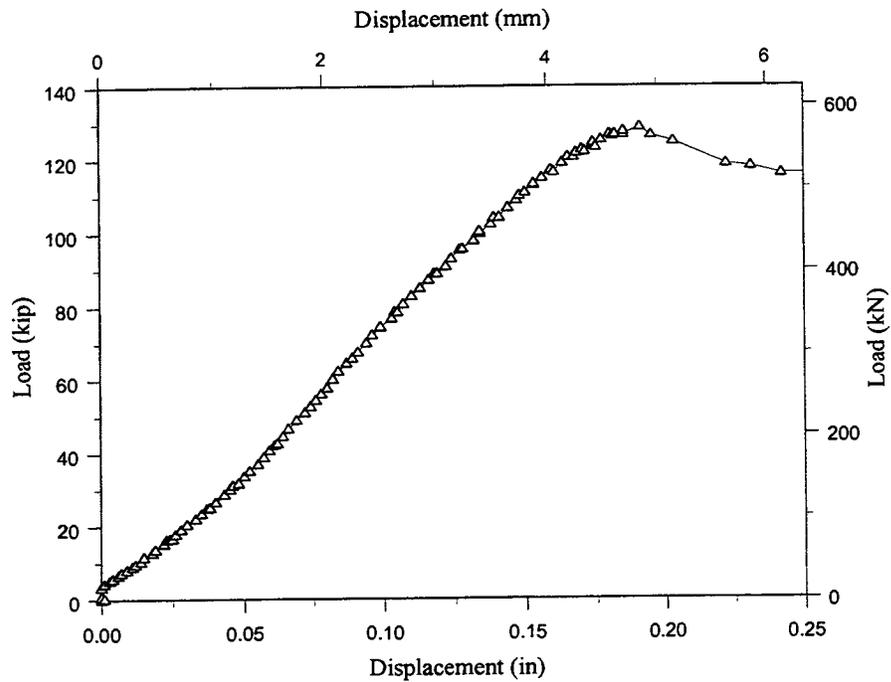
Displacement (mm)

Figure I-18 Load vs. displacement - specimen C18 (concrete, 1.5d, fresh water).

126
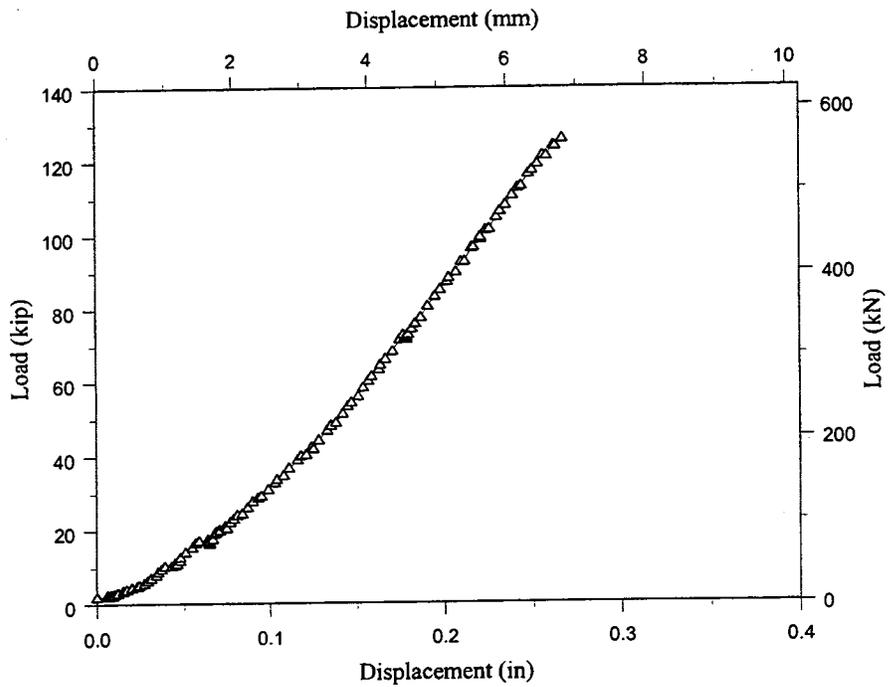
Figure I-19 Load vs. displacement - specimen C19 (concrete, 2d, fresh water).
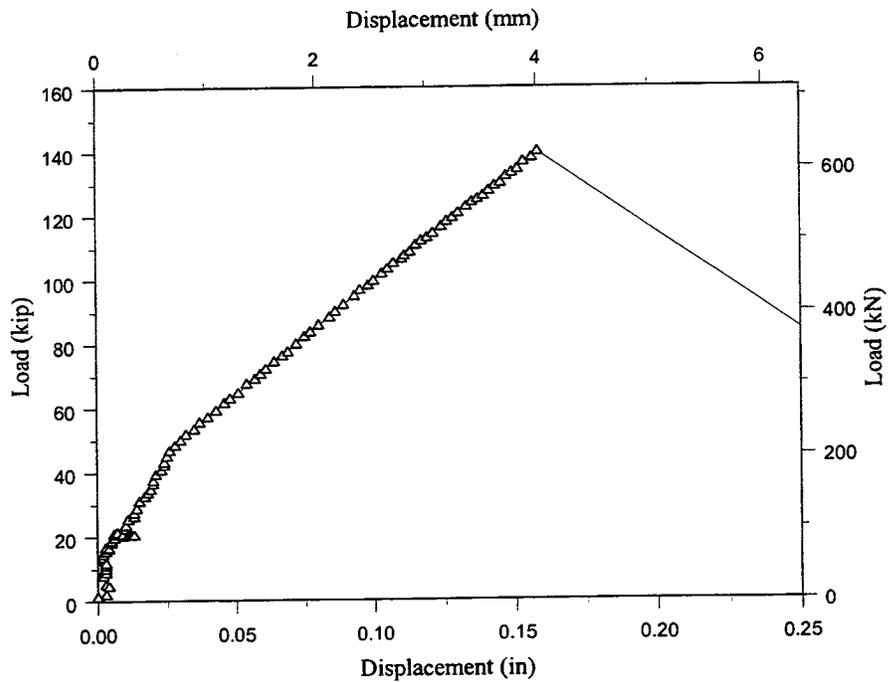
Figure I-20 Load vs. displacement - specimen C20 (concrete, 2d, fresh water).
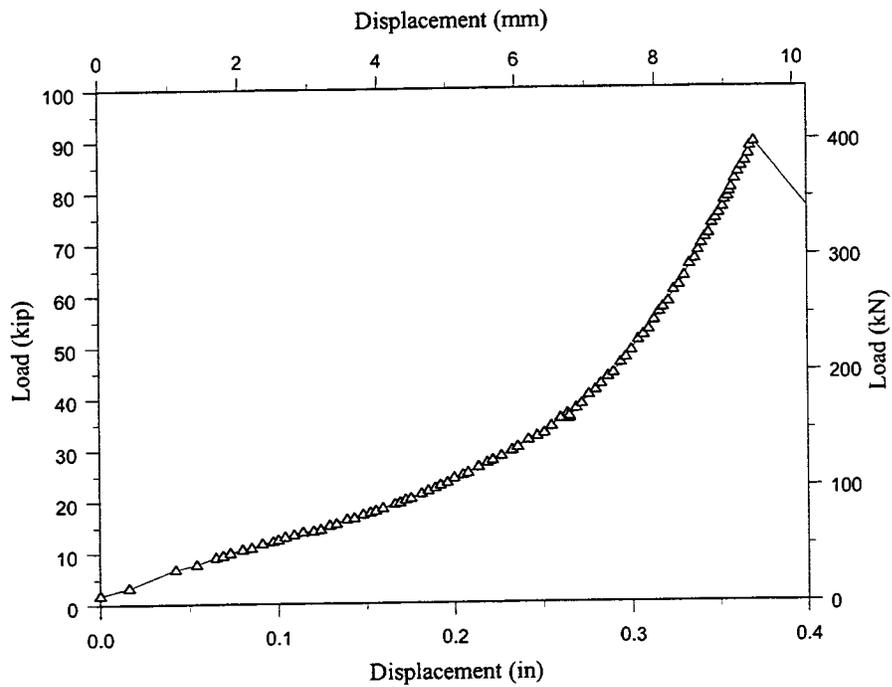
Figure I-21 Load vs. displacement - specimen C21 (concrete, 2d, fresh water, soil-caked).
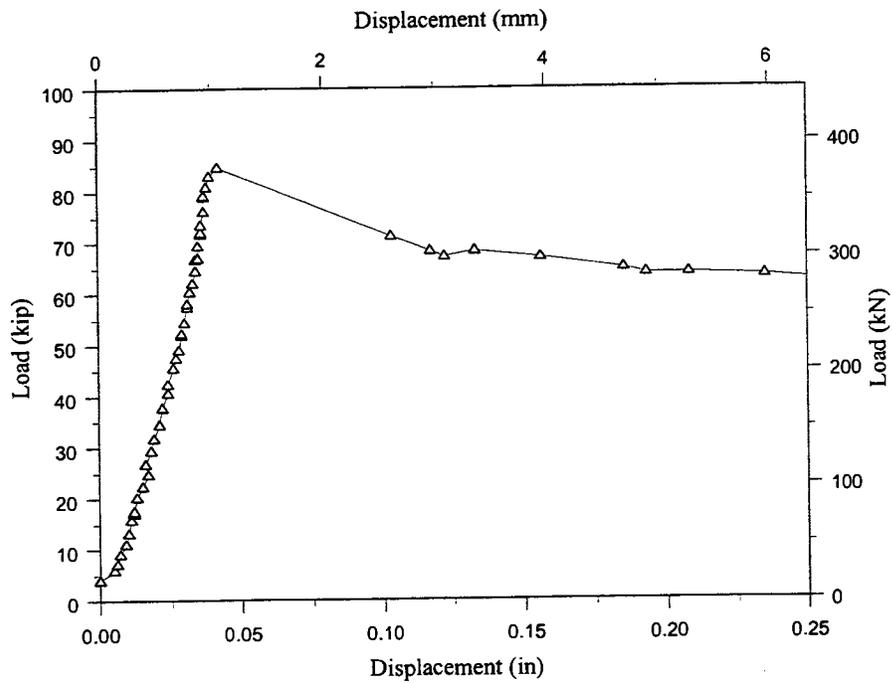
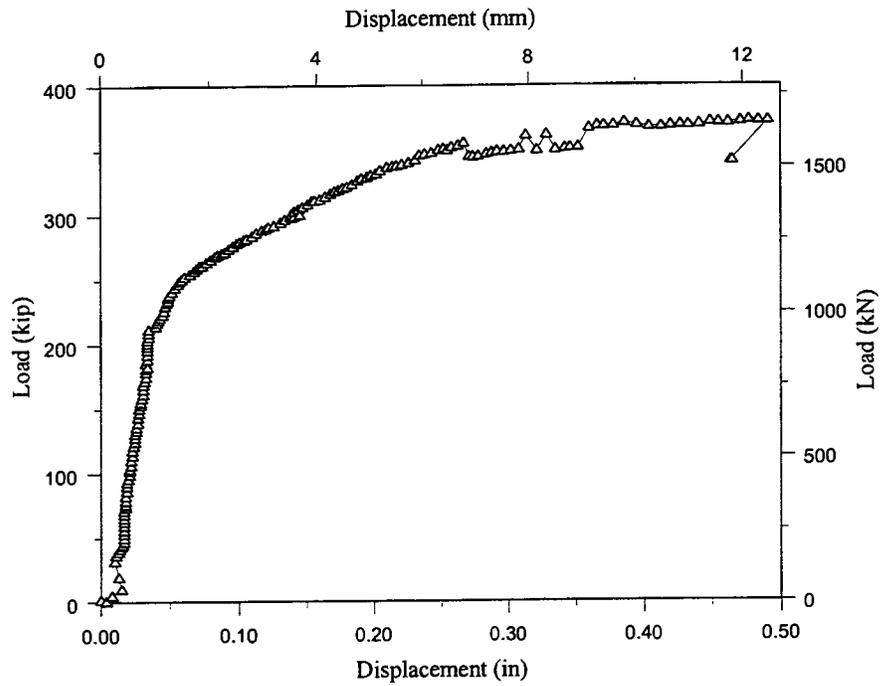Figure I-22 Load vs. displacement - specimen C22 (concrete, 1d, control).
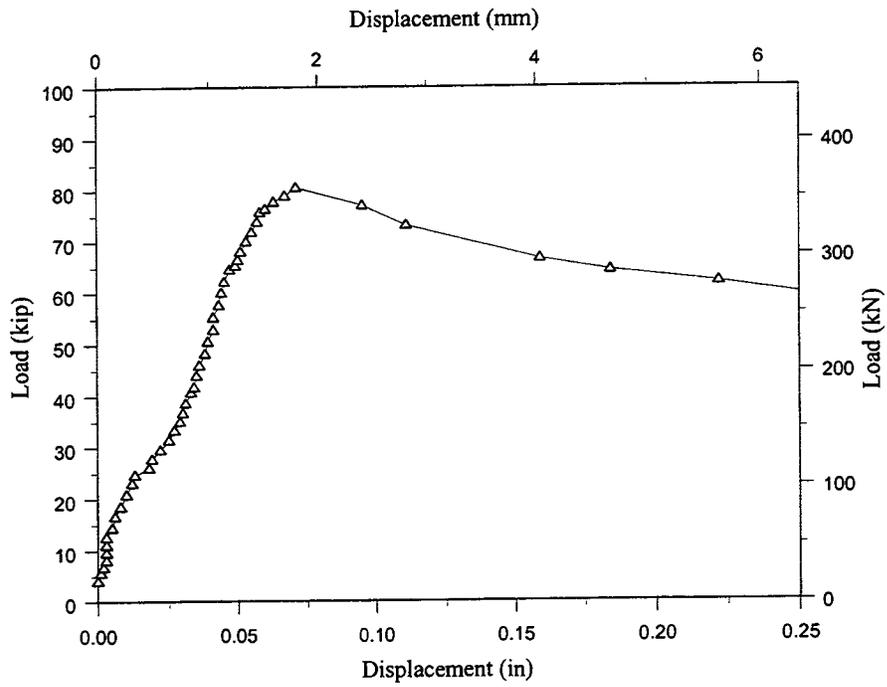
Figure I-23 Load vs. displacement - specimen C23 (concrete, 1d, control).
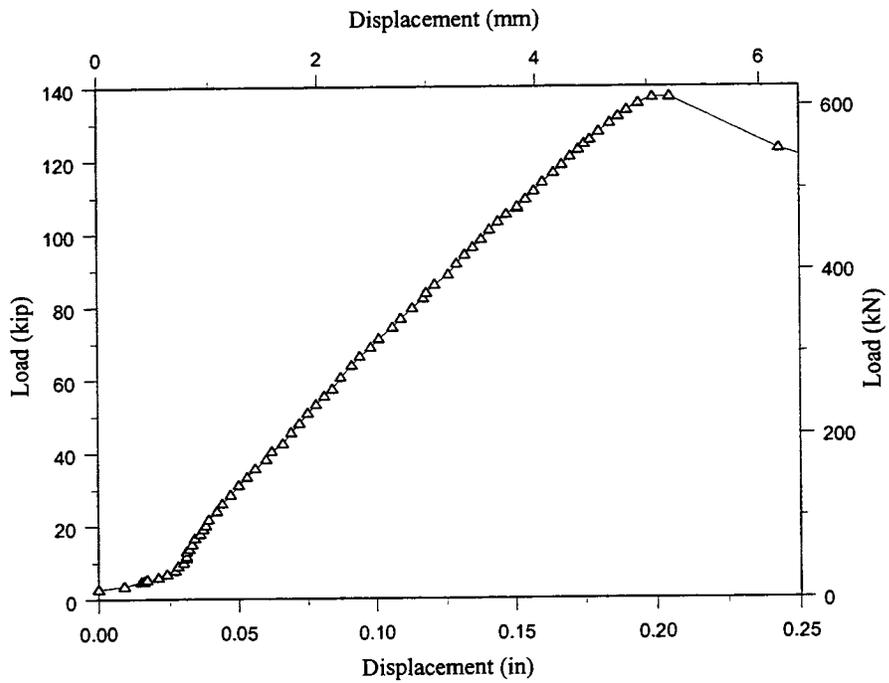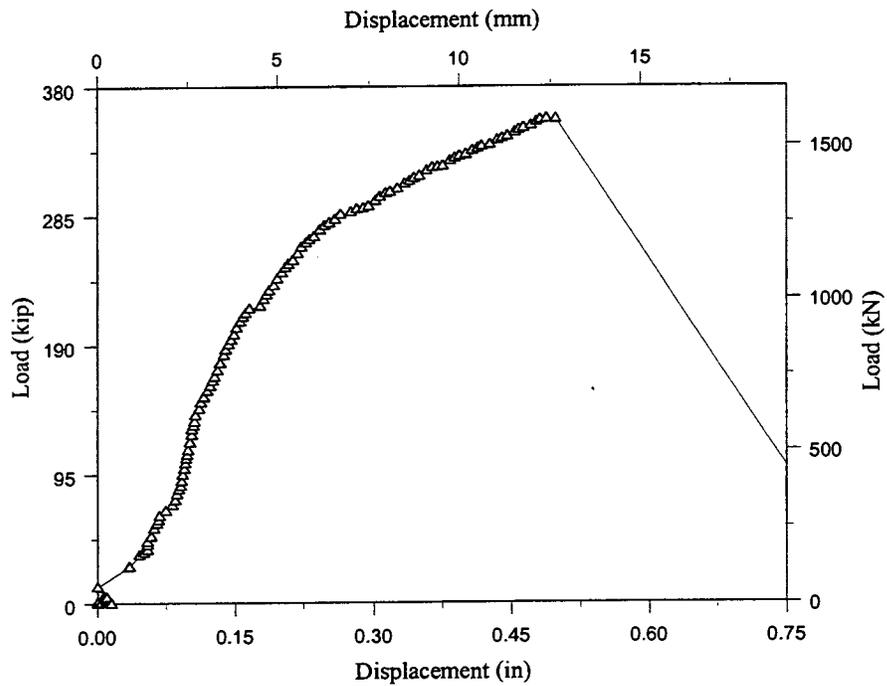

Figure I-24 Load vs. displacement - specimen C24 (concrete, 1.5d, control).
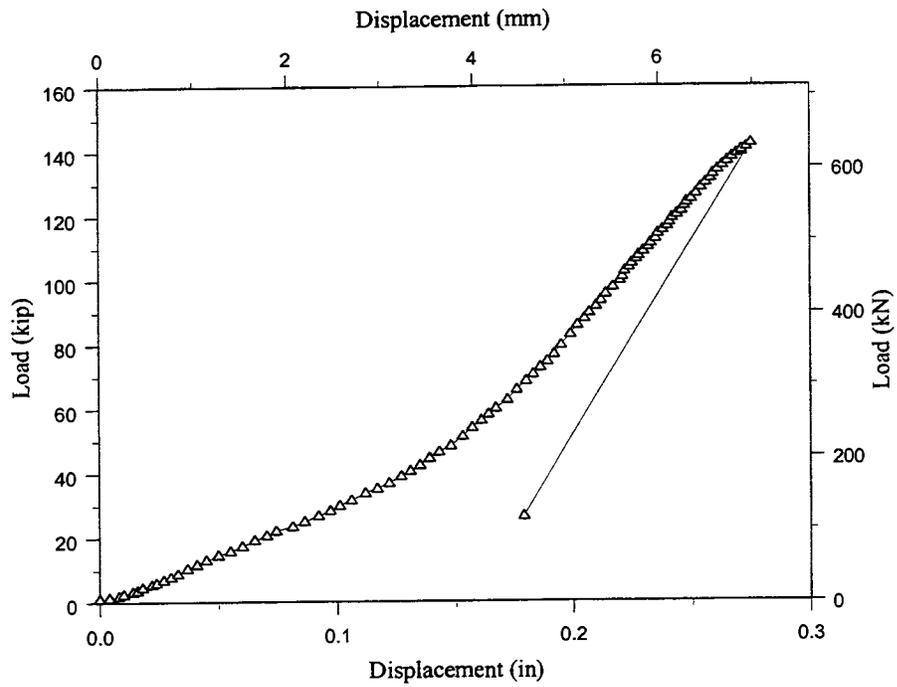
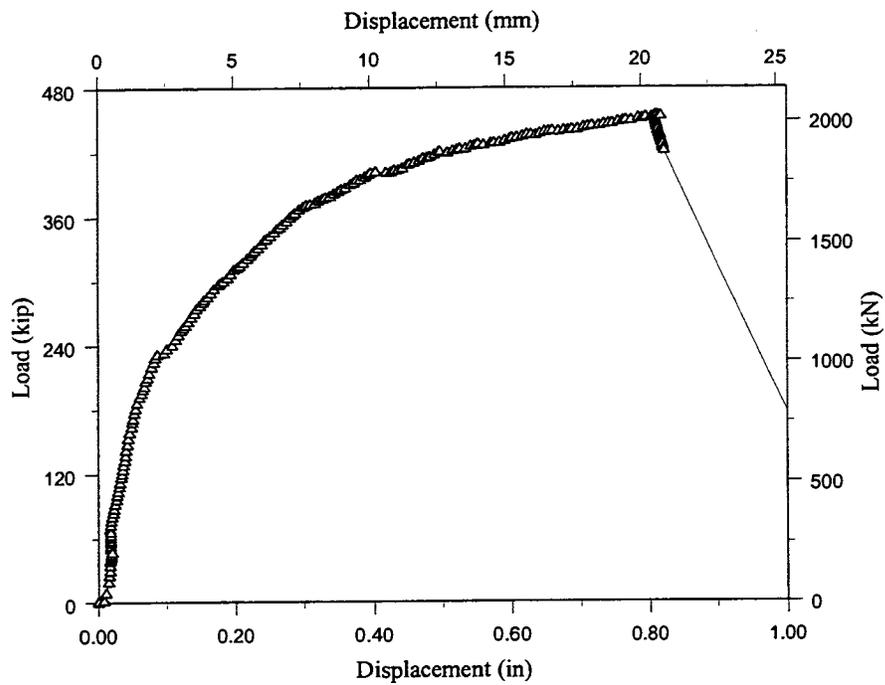Figure I-25 Load vs. displacement - specimen C25 (concrete, 1.5d, control).
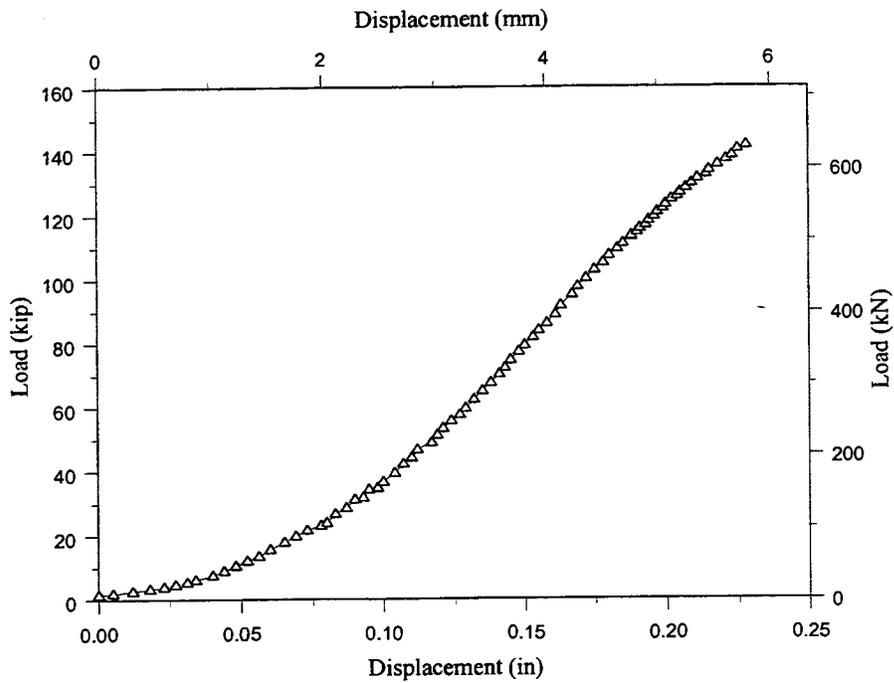
Figure I-26 Load vs. displacement - specimen C26 (concrete, 2d, control).
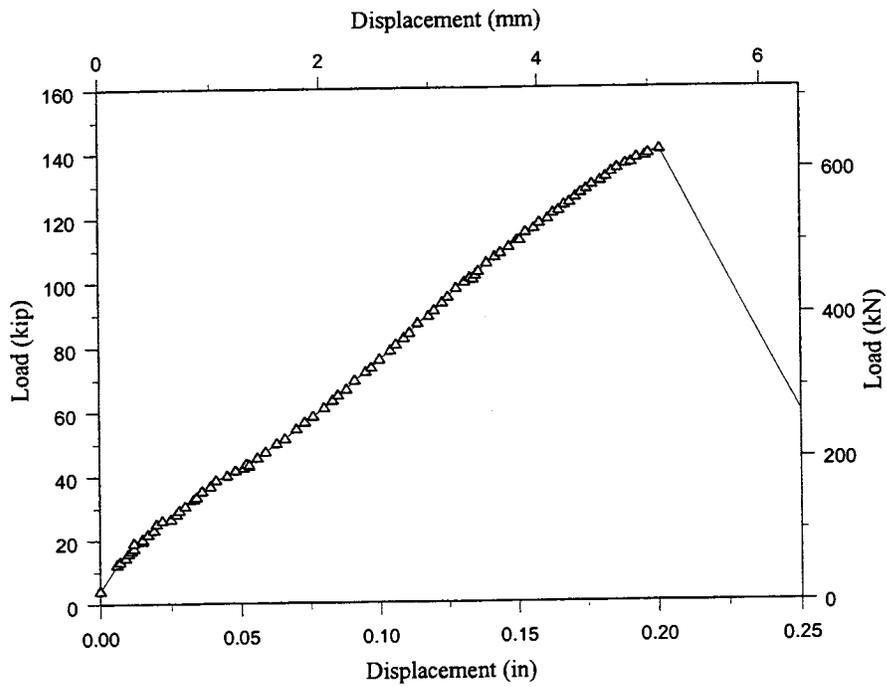
Figure I-27 Load vs. displacement - specimen C27 (concrete, 2d, control).
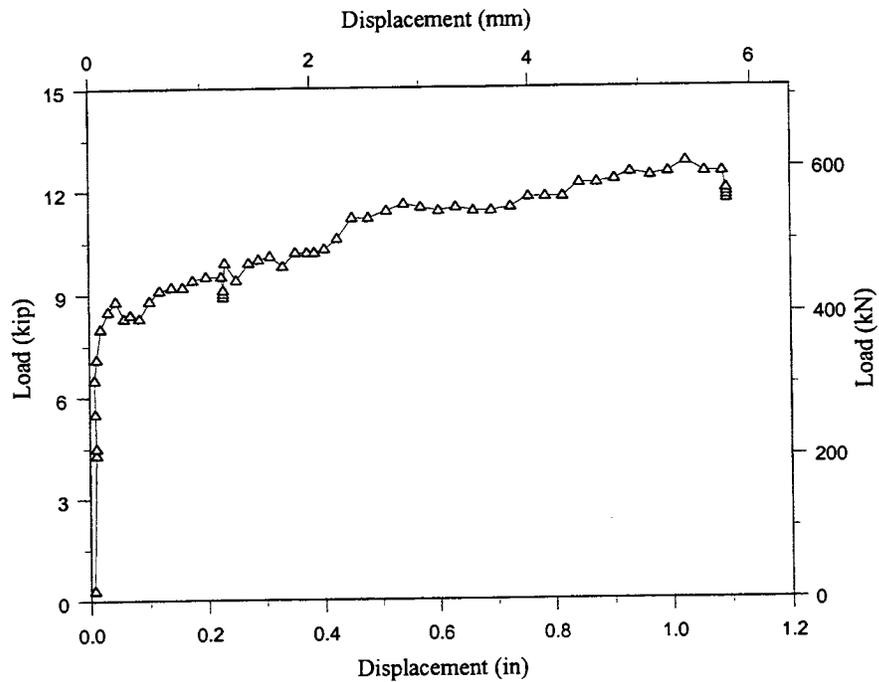
Figure I-28 Load vs. displacement - specimen C28 (concrete, 2d, control, soil-caked).

131
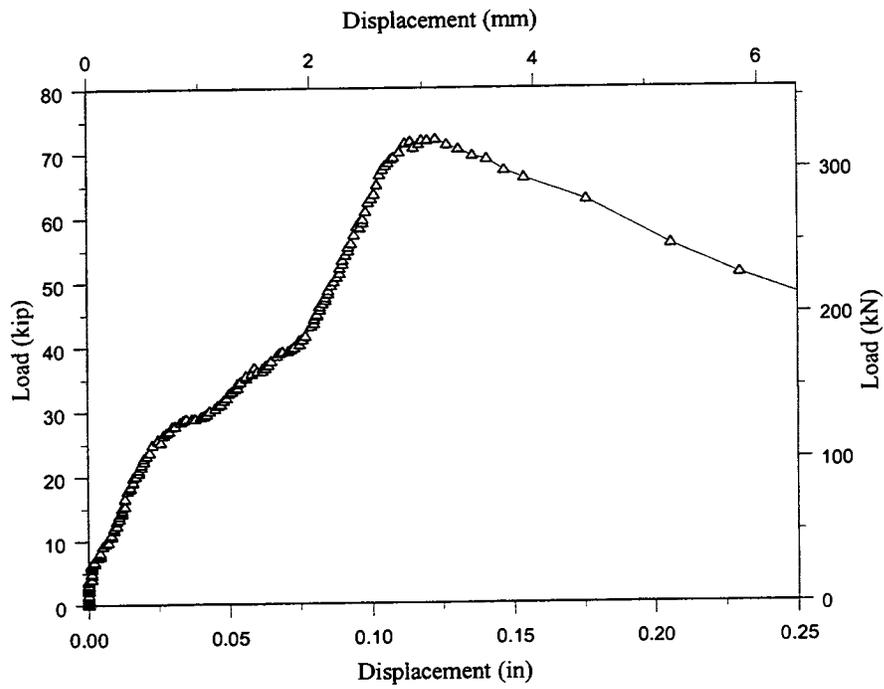
Figure I-29 Load vs. displacement - specimen H11 (steel, 1.5d, bentonite).
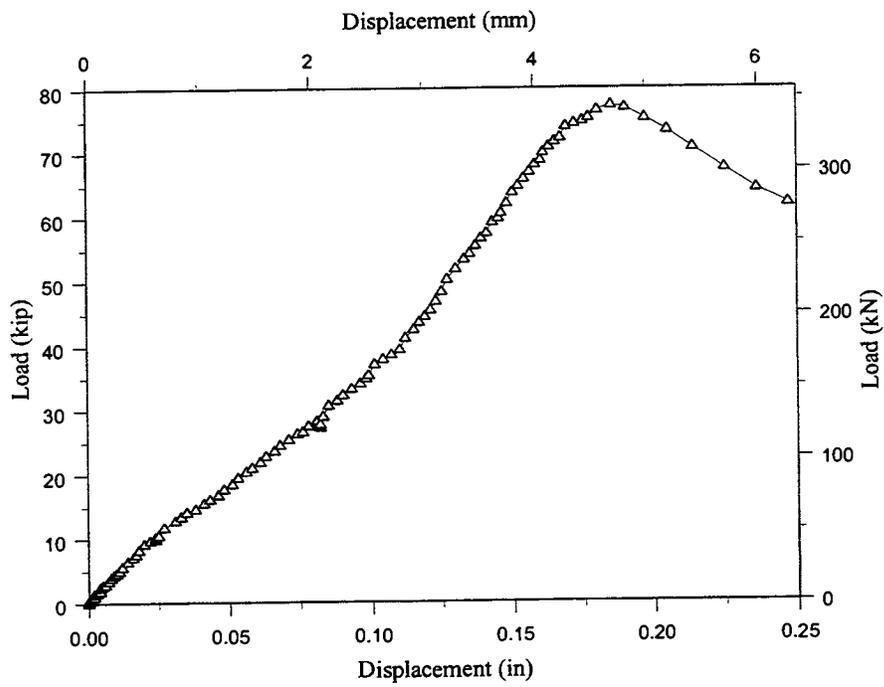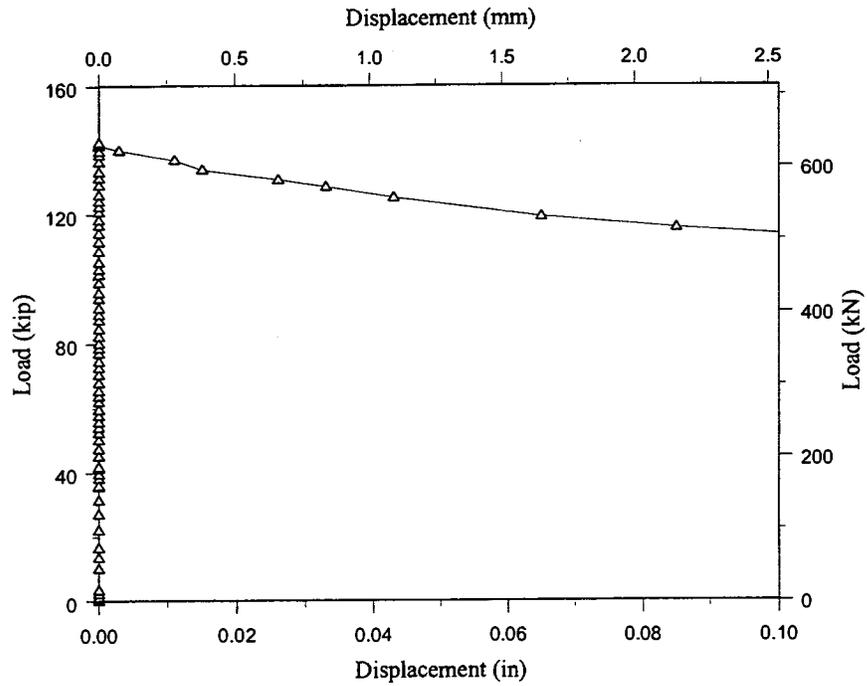

Figure I-30 Load vs. displacement - specimen H11 (steel, 2d, bentonite).
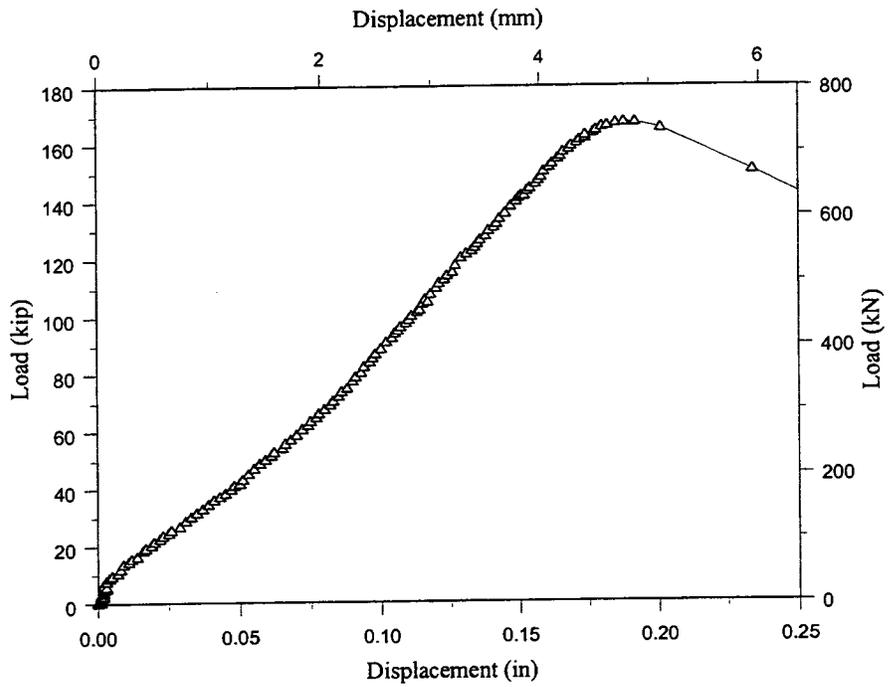
Figure I-31 Load vs. displacement - specimen H21 (steel, 1.5d, salt water).
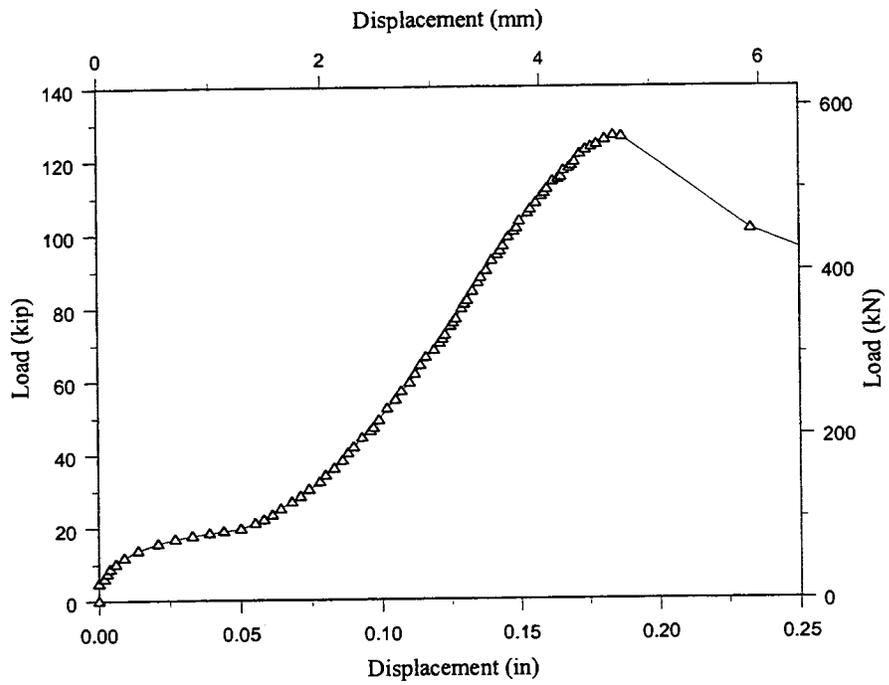
Figure I-32 Load vs. displacement - specimen H22 (steel, 2d, salt water).
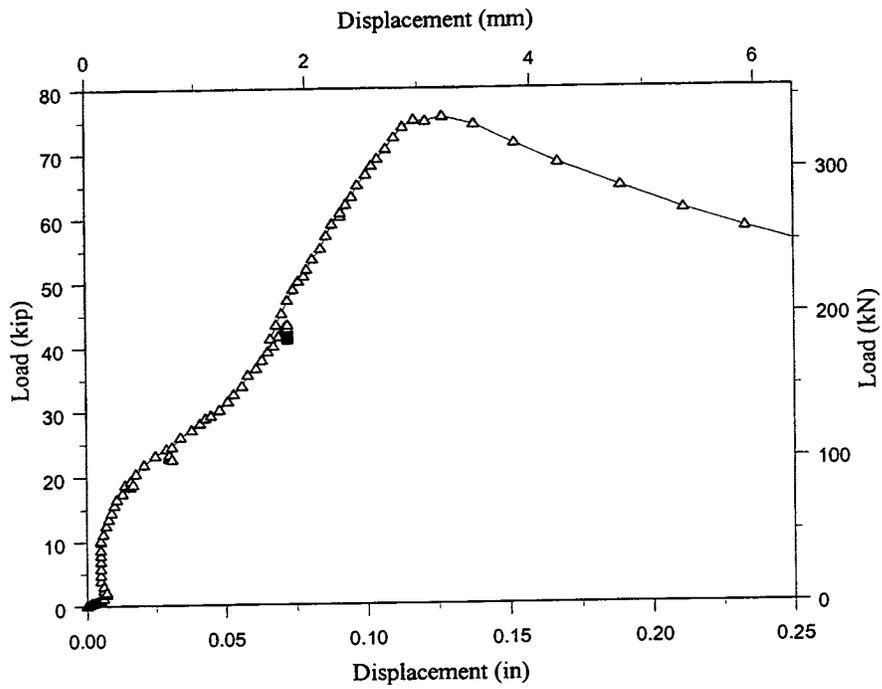
Figure I-33 Load vs. displacement - specimen H31 (steel, 1.5d, fresh water).
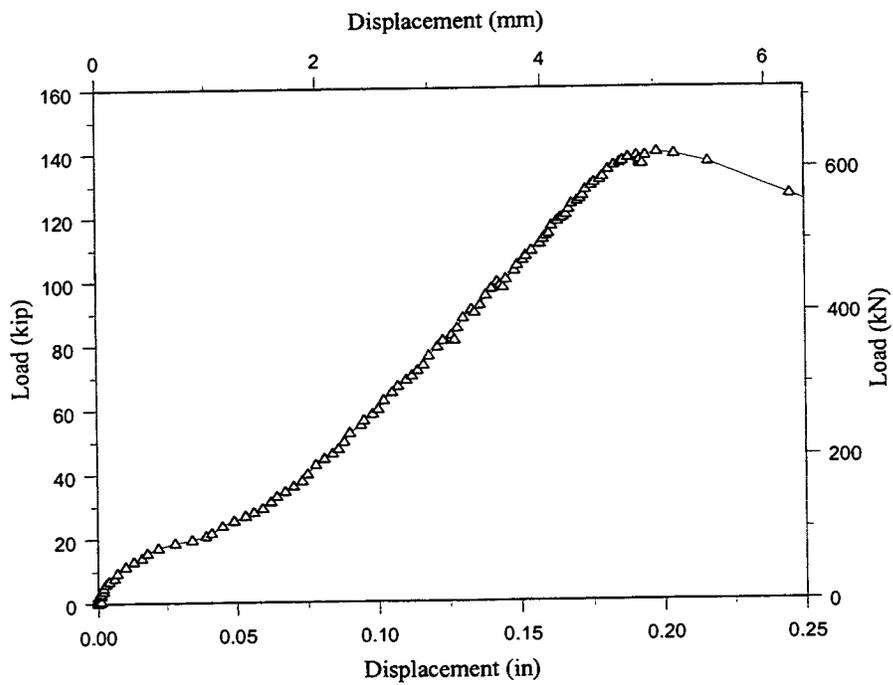
Figure I-34 Load vs. displacement - specimen H32 (steel, 2d, fresh water).

134
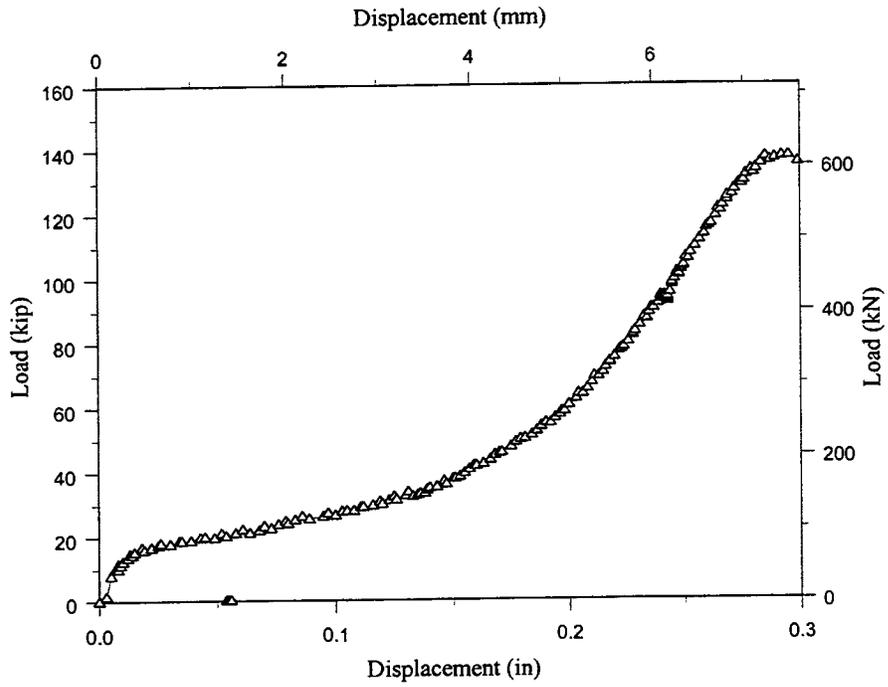
Figure I-35 Load vs. displacement - specimen H41 (steel, 1.5d, control).
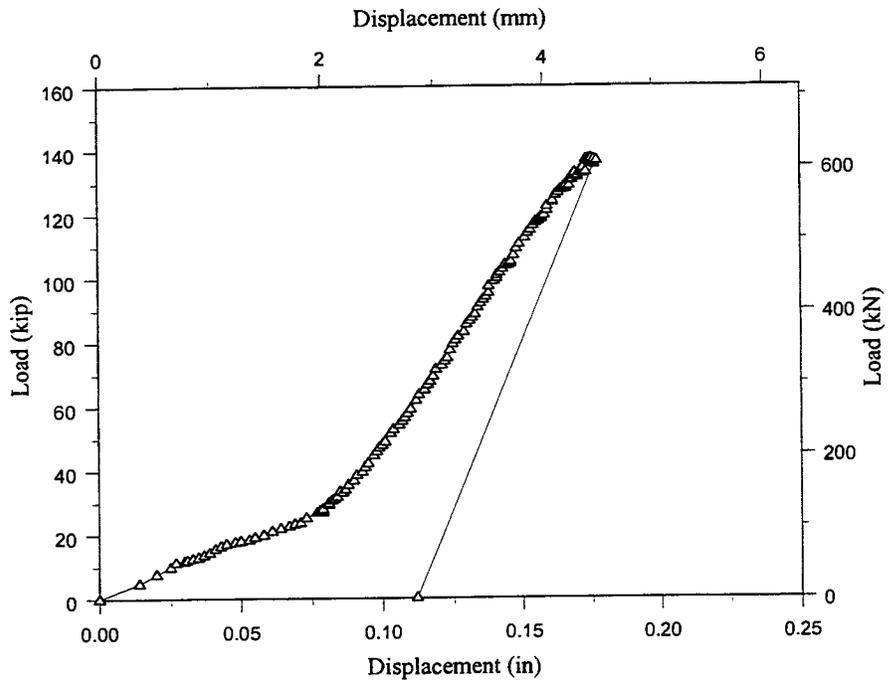
Figure I-36 Load vs. displacement - specimen H42 (steel, 2d, control).

Appendix II Full-Scale Test Data

Figure II-1 Load vs. displacement - specimen B1A (concrete, 1d, bentonite, soil-caked).

Figure II-2 Load vs. displacement - specimen B1B (concrete, 1d, bentonite).

Figure II-3 Load vs. displacement - specimen B1C (concrete, 1d, bentonite, soil-caked).

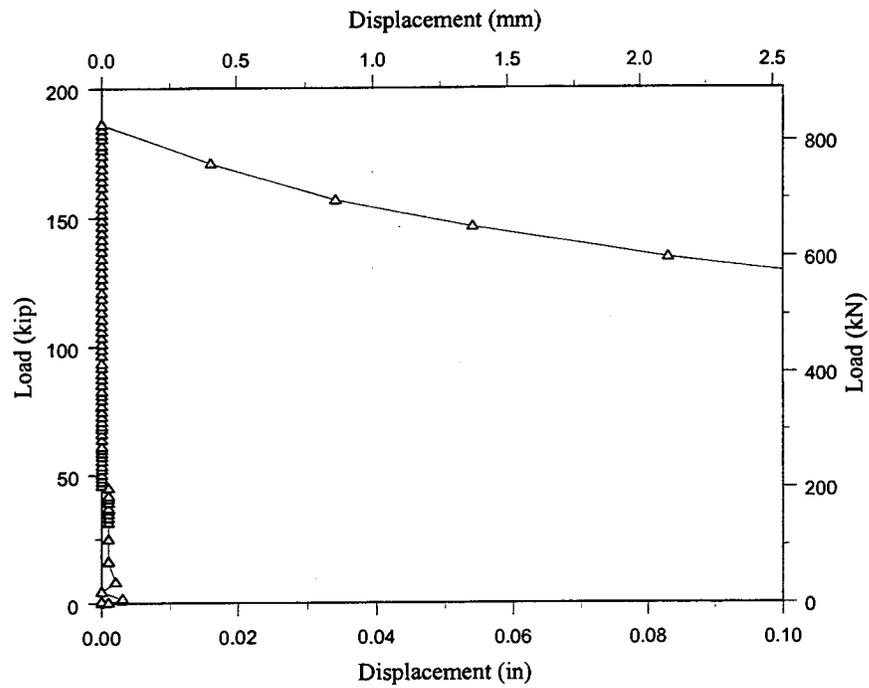Figure II-4 Load vs. displacement - specimen B1D (concrete, 1d, bentonite).

Figure II-5 Load vs. displacement - specimen B2A (concrete, 2d, bentonite).
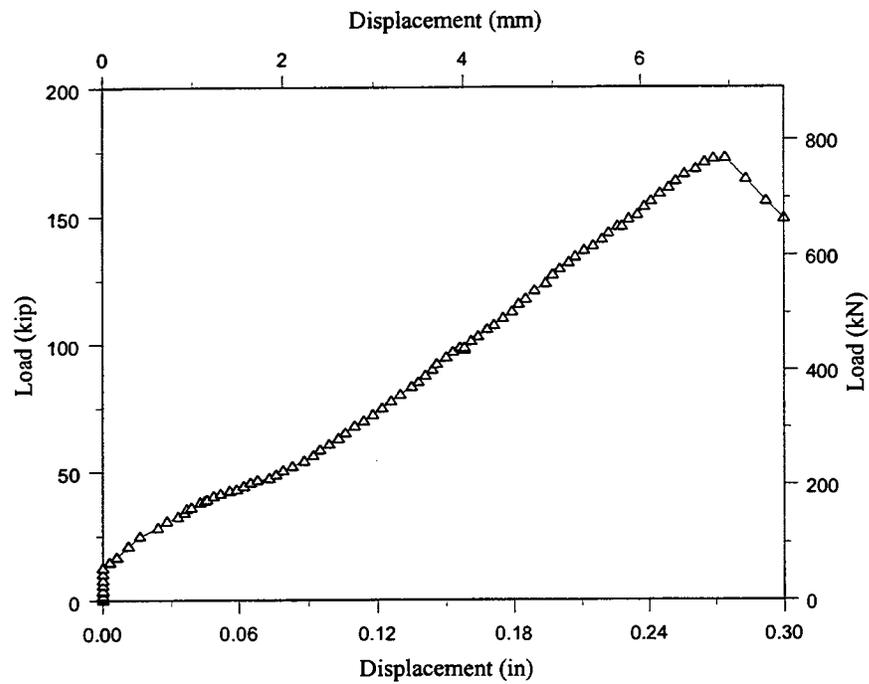

Figure II-6 Load vs. displacement - specimen B2B (concrete, 2d, bentonite).
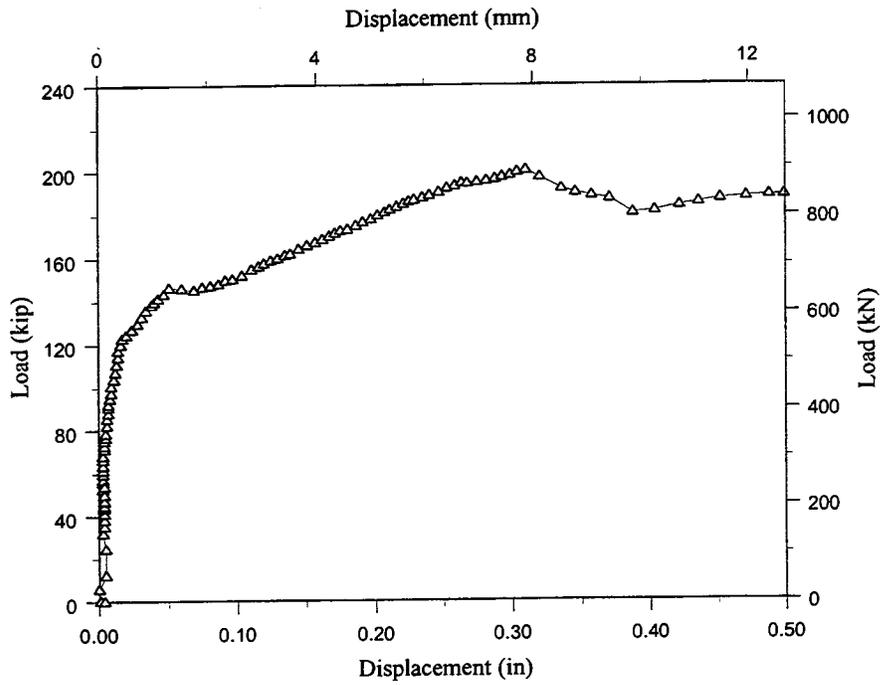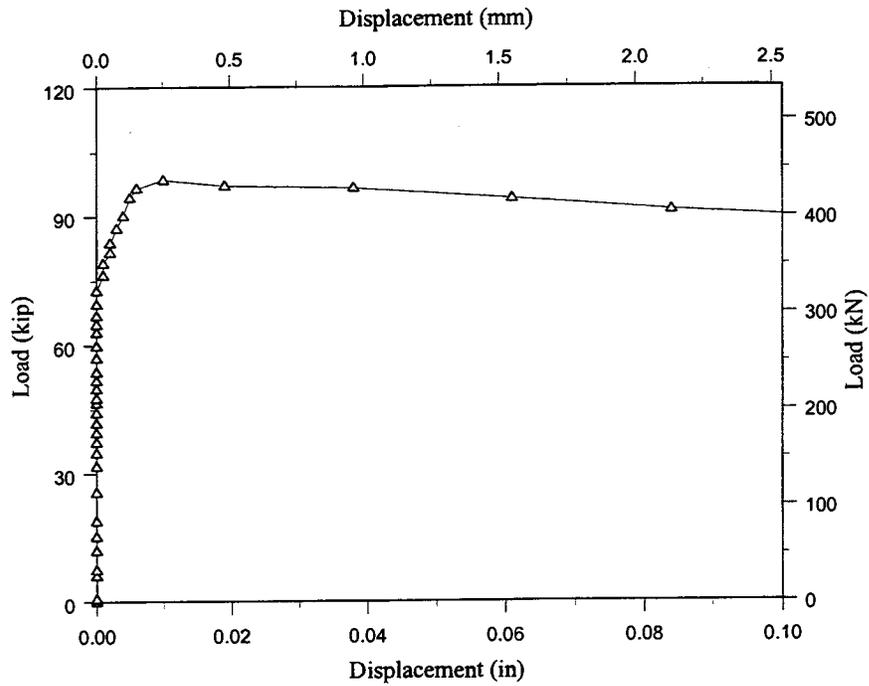
Figure II-7 Load vs. displacement - specimen W0.5 (concrete, 0.5d, water).

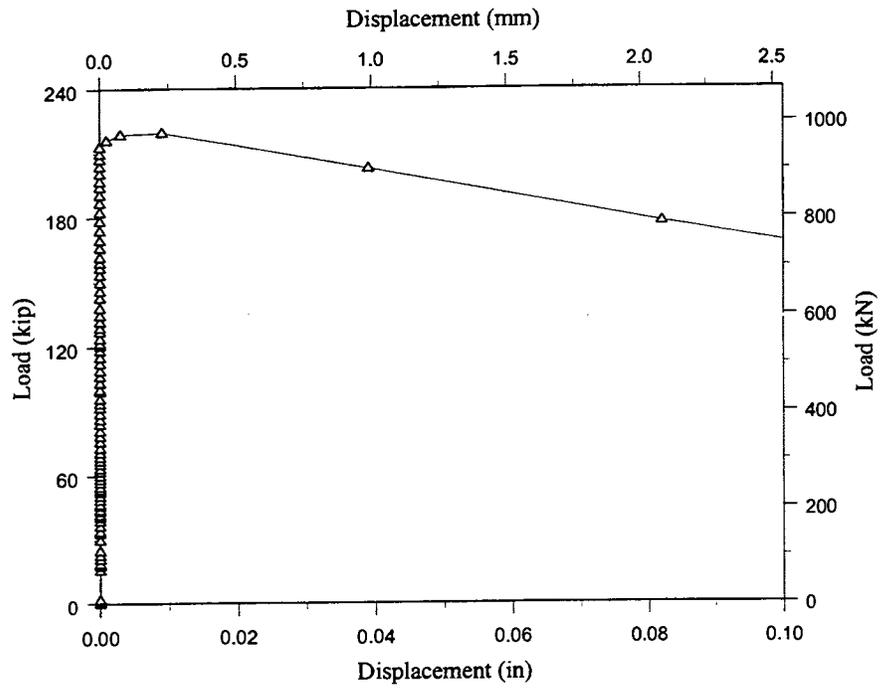Figure II-8 Load vs. displacement - specimen W1.0A (concrete, 1d, water).
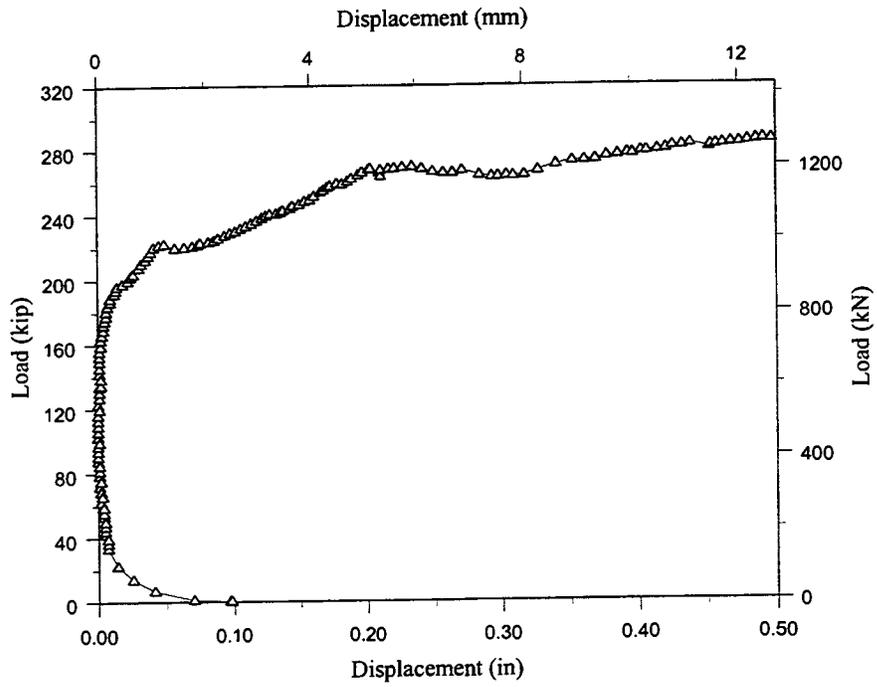
Figure II-9 Load vs. displacement - specimen W1.0B (concrete, 1d, water).
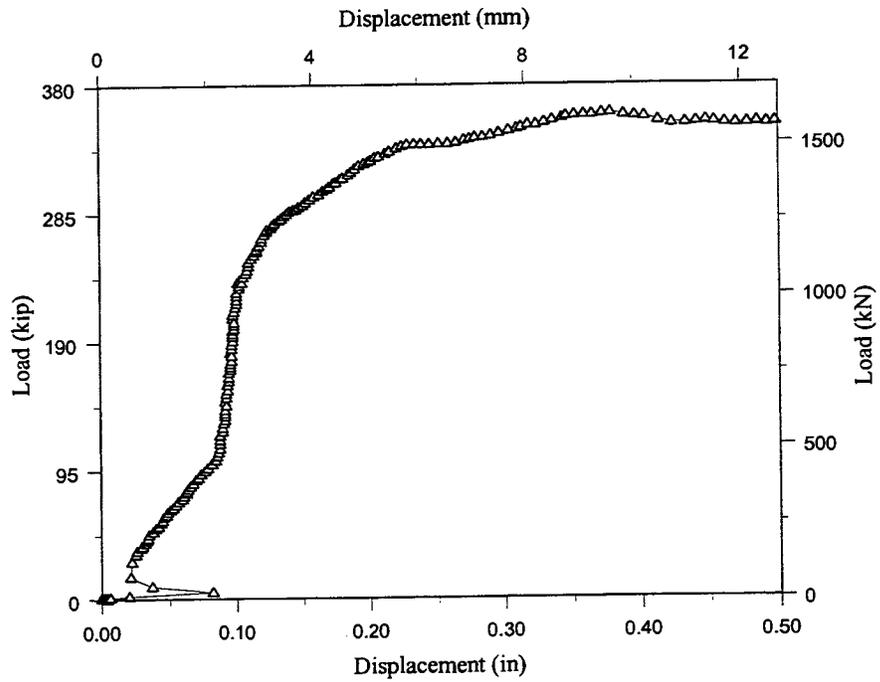
Figure II-10 Load vs. displacement - specimen W1.5A (concrete, 1.5d, water).

Figure II-11 Load vs. displacement - specimen W1.5B (concrete, 1.5d, water).
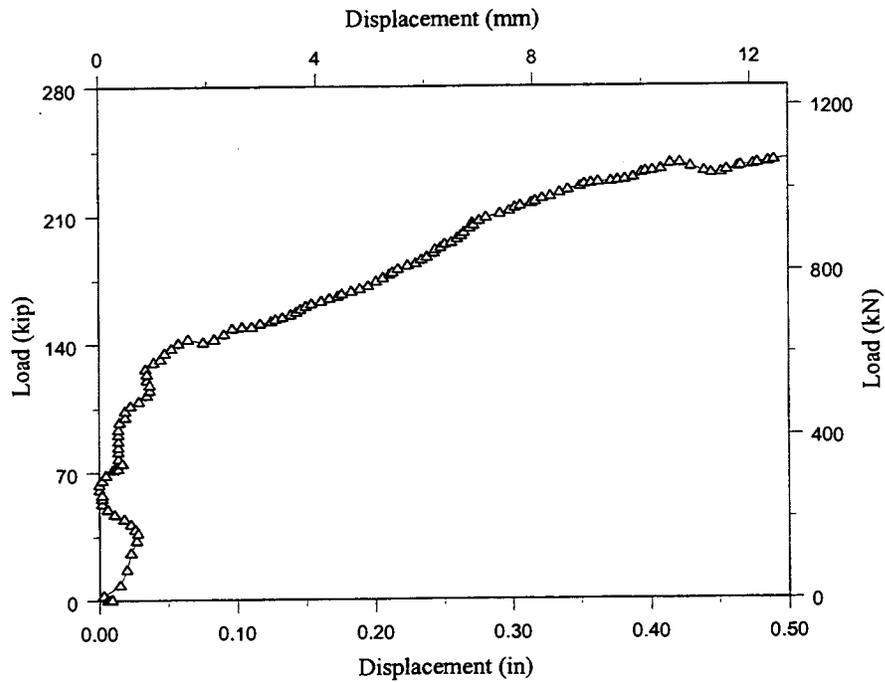
Figure II-12 Load vs. displacement - specimen C0.5 (concrete, 0.5d, control).

141

Figure II-13 Load vs. displacement - specimen C1.0A (concrete, 1d, control).
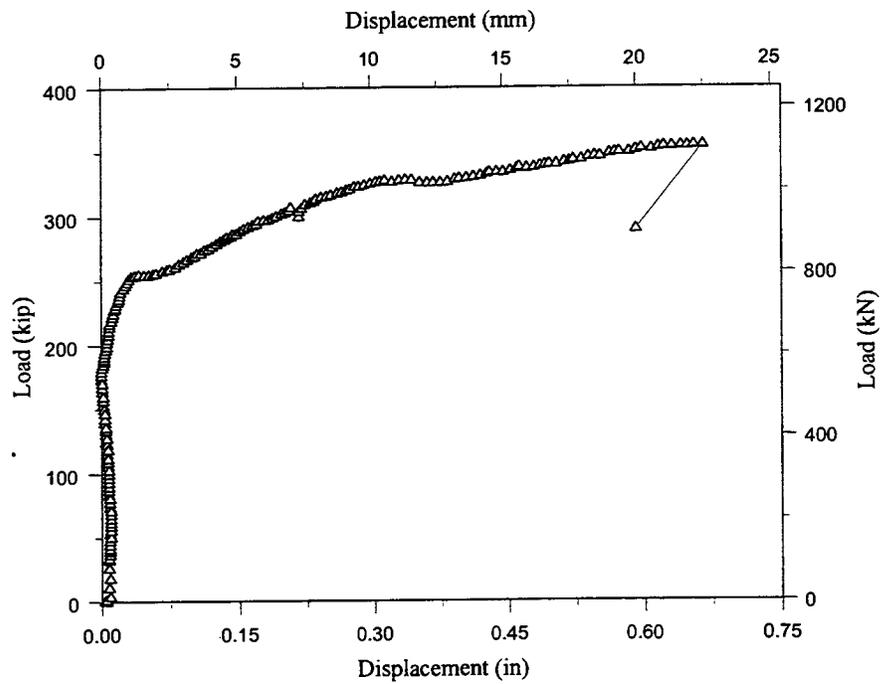
Figure II-14 Load vs. displacement - specimen C1.0B (concrete, 1d, control).

Figure II-15 Load vs. displacement - specimen C1.5A (concrete, 1.5d, control).

Figure II-16 Load vs. displacement - specimen C1.5B (concrete, 1.5d, control).

143

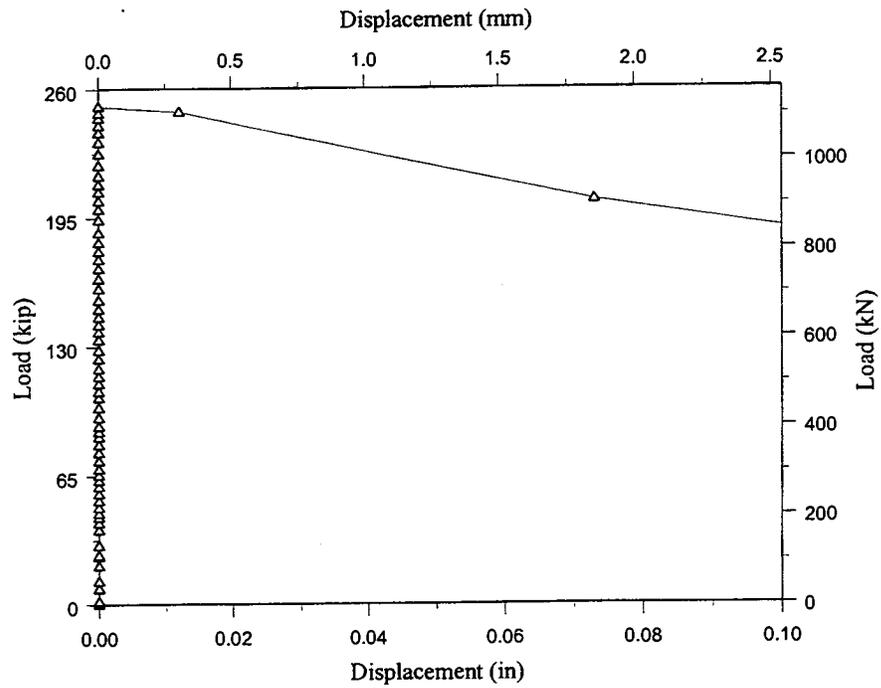Figure II-17 Load vs. displacement - specimen SB1A (steel, 1d, bentonite, soil-caked).
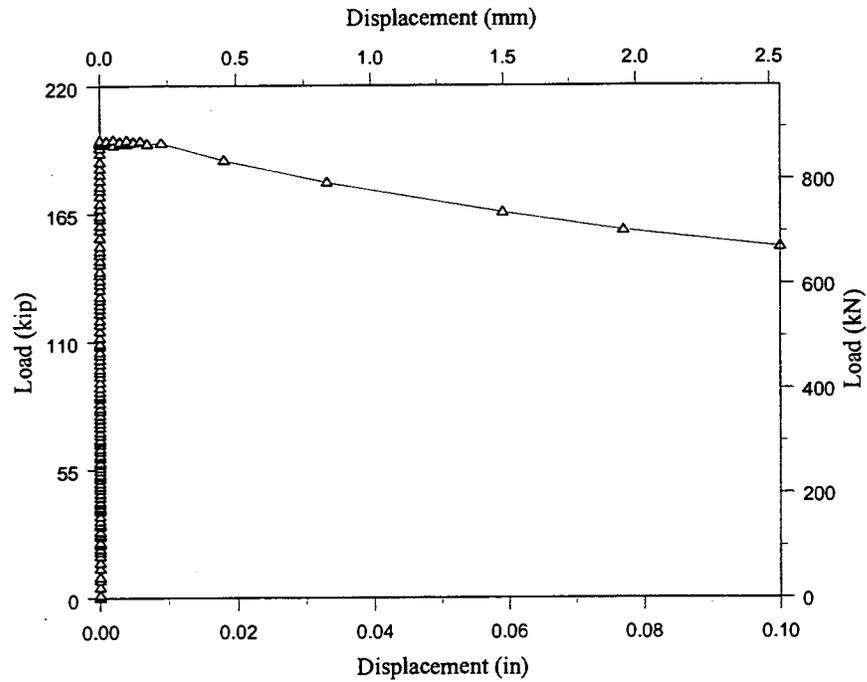
Figure II-18 Load vs. displacement - specimen SB1B (steel, 1d, bentonite).
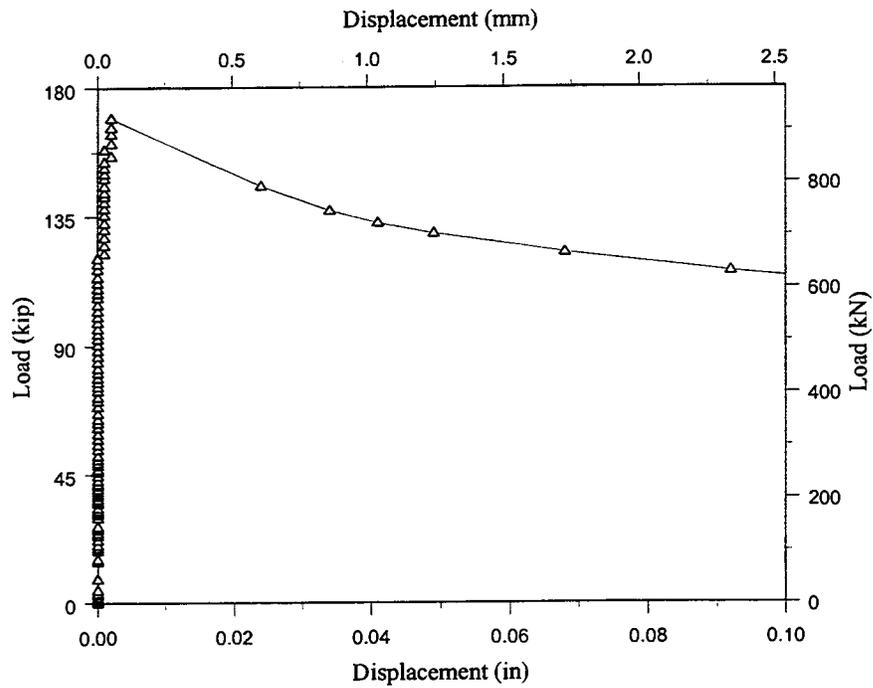
Figure II-19 Load vs. displacement - specimen SB1C (steel, 1d, bentonite, soil-caked).
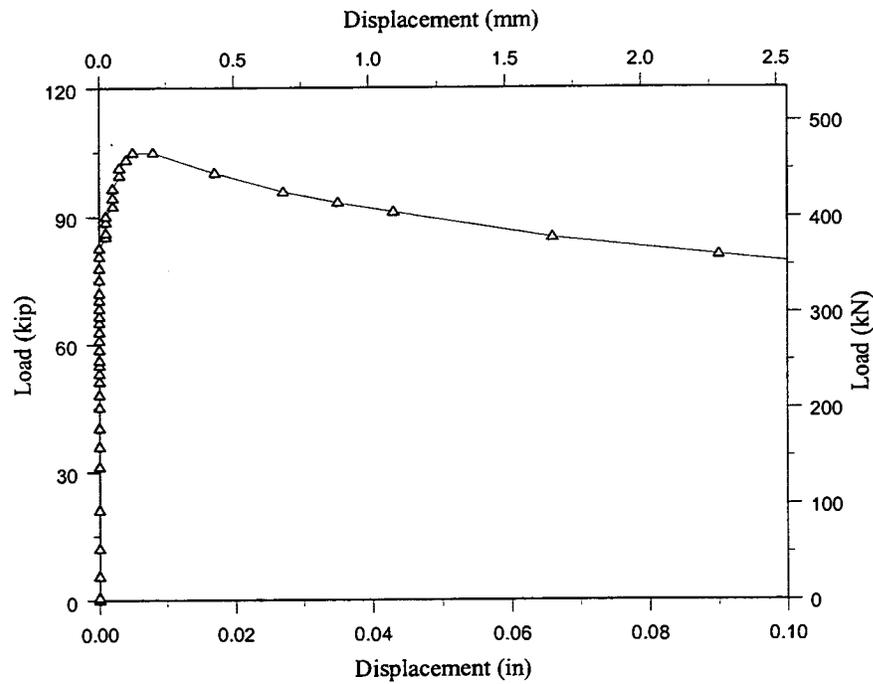
Figure II-20 Load vs. displacement - specimen SB1D (steel, 1d, bentonite).

145

Figure II-21 Load vs. displacement - specimen SB2A (steel, 2d, bentonite).

Figure II-22 Load vs. displacement - specimen SB2B (steel, 2d, bentonite).

Figure II-23 Load vs. displacement - specimen SW0.5 (steel, 0.5d, water).
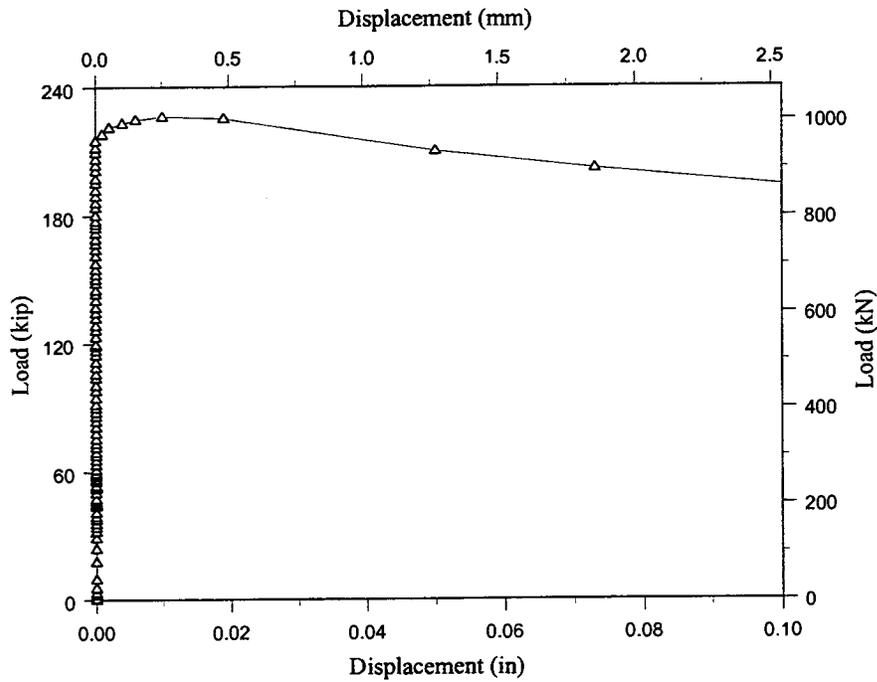
Figure II-24 Load vs. displacement - specimen SW1.0A (steel, 1d, water).

147

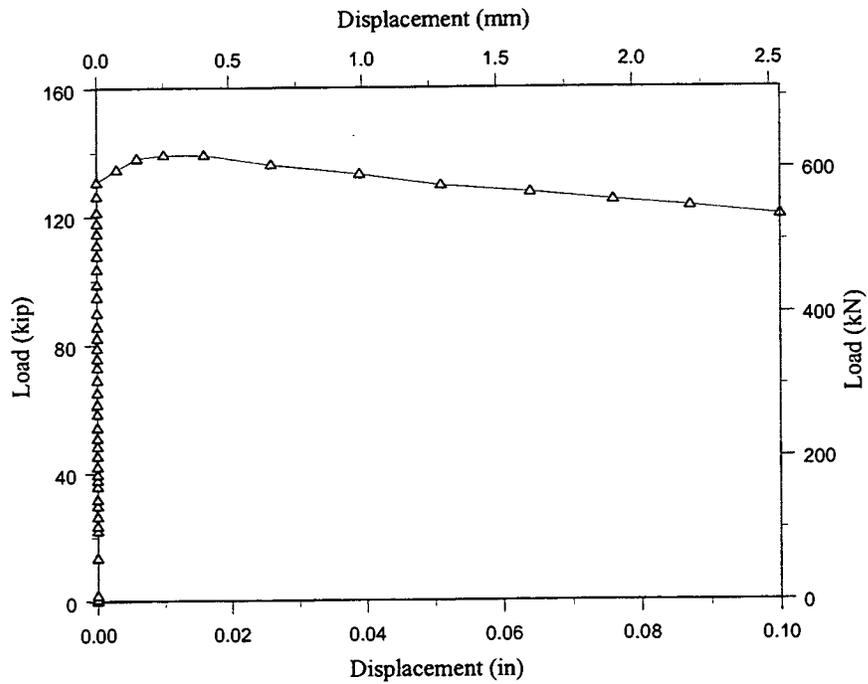Figure II-25 Load vs. displacement - specimen SW1.0B (steel, 1d, water).
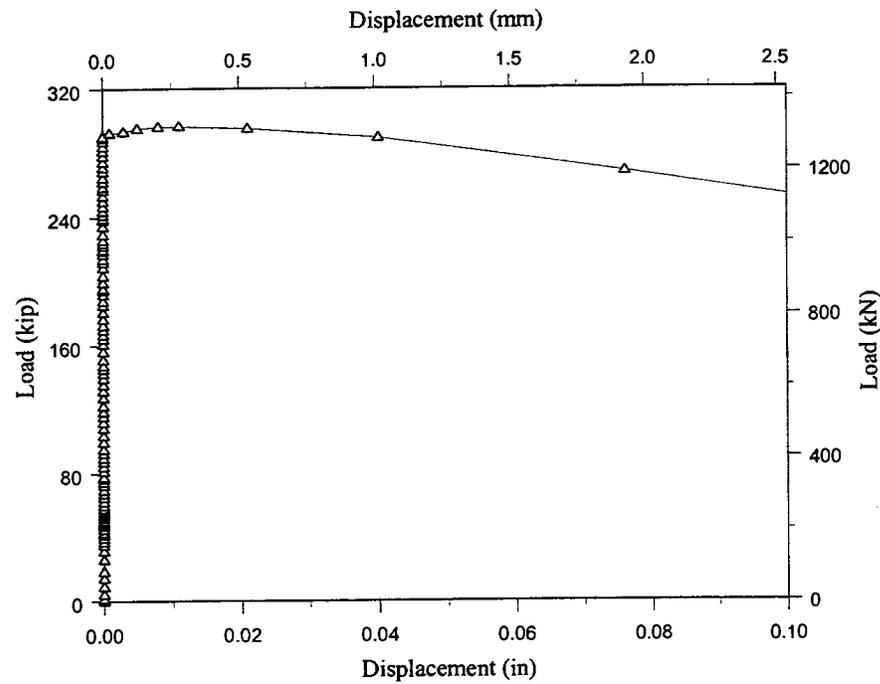
Figure II-26 Load vs. displacement - specimen SW1.5A (steel, 1.5d, water).

148

Figure II-27 Load vs. displacement - specimen SW1.5B (steel, 1.5d, water).

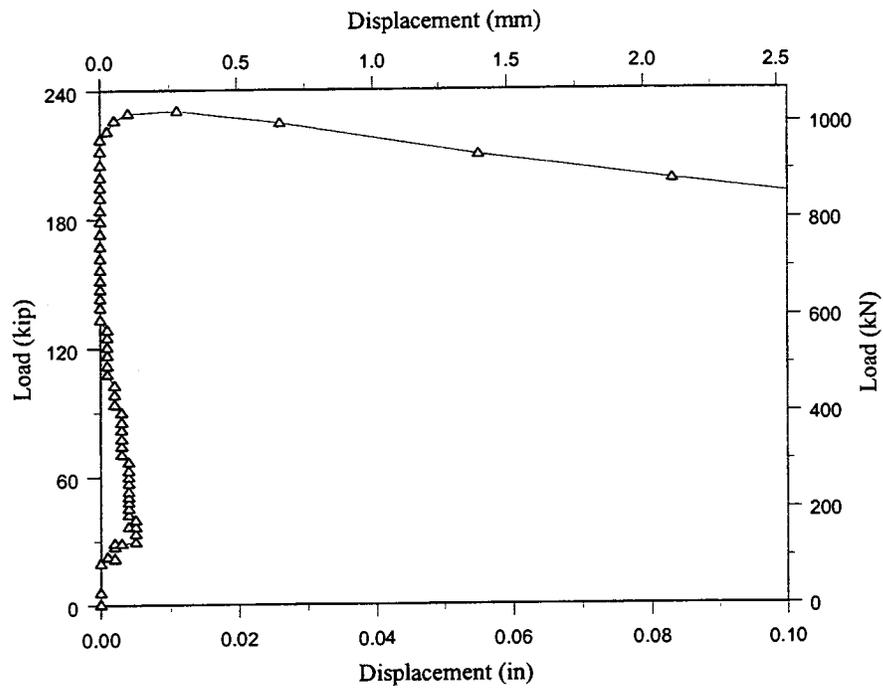Figure II-28 Load vs. displacement - specimen SC0.5 (steel, 0.5d, control).

149

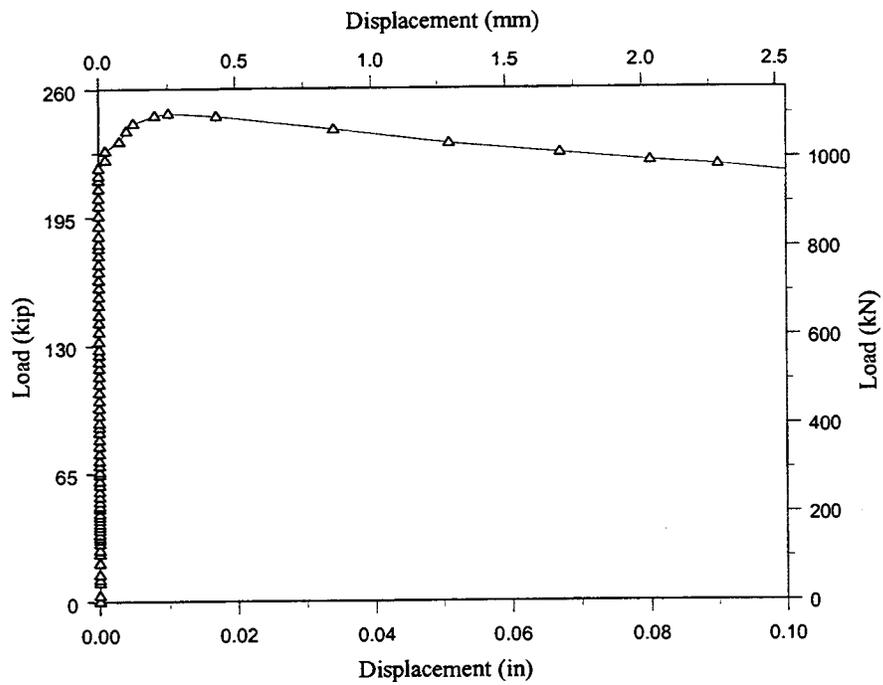Figure II-29 Load vs. displacement - specimen SC1.0A (steel, 1d, control).

Figure II-30 Load vs. displacement - specimen SC1.0B (steel, 1d, control).
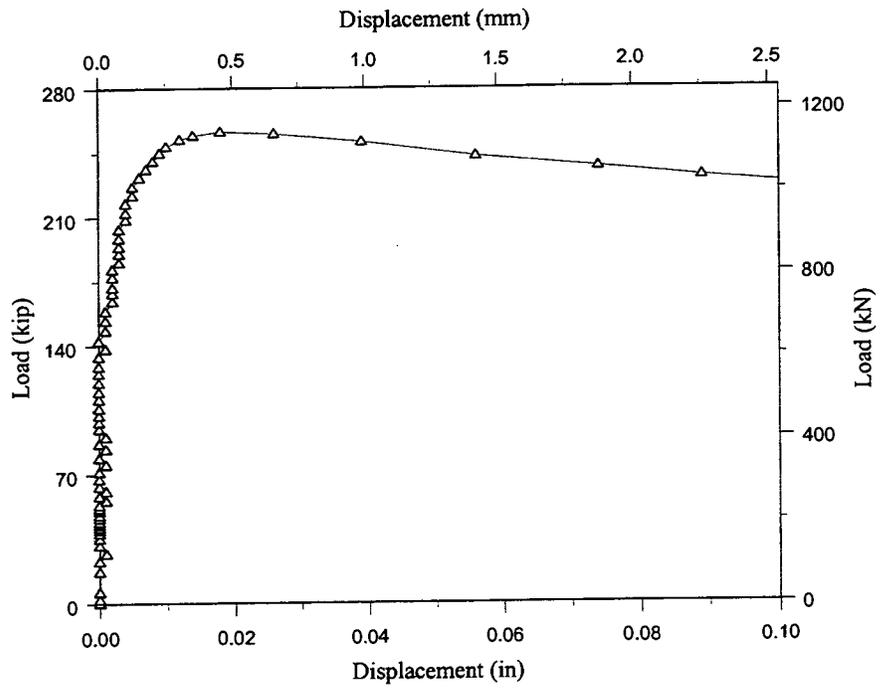
150

Figure II-31 Load vs. displacement - specimen SC1.5A (steel, 1.5d, control).
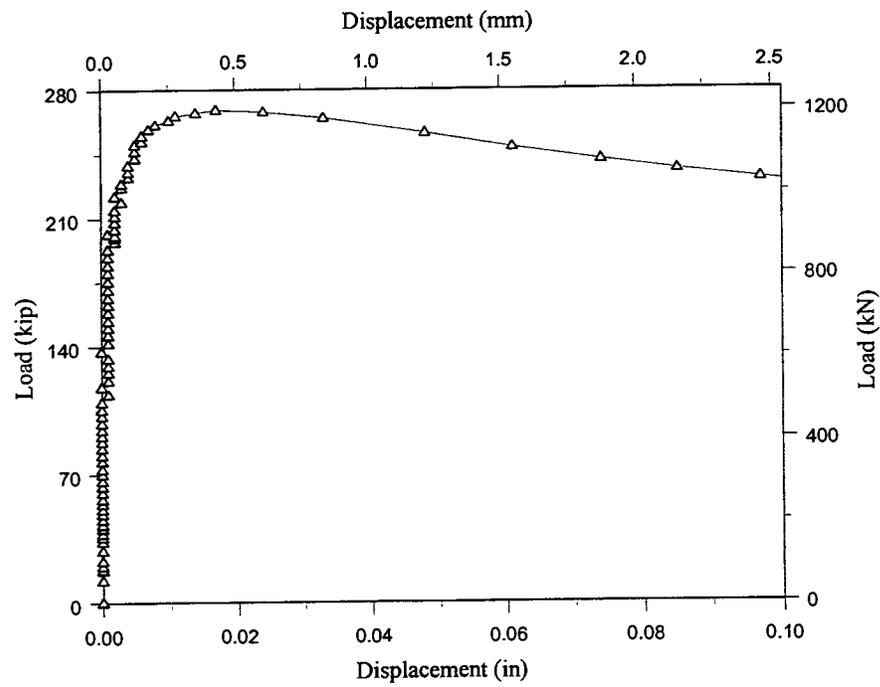

Figure II-32 Load vs. displacement - specimen SC1.5B (steel, 1.5d, control).